ABSTRACT

Title of Dissertation:	IMPROVING STORMWATER QUALITY USING A NOVEL PERMEABLE PAVEMENT BASE MATERIAL
	Travis Ostrom Doctor of Philosophy, 2019
Dissertation directed by:	Dr. Allen P. Davis Professor and Charles A. Irish, Sr. Chair in Civil Engineering Department of Civil and Environmental Engineering

A novel stormwater treatment media has been developed using expanded shale aggregate, Al-based water treatment residual (WTR), and psyllium-based binder. The media (HPMM) has sufficient structural capacity and hydraulic conductivity to serve as a permeable pavement base material and demonstrated effective phosphorus (P) retention in lab- and field-scale studies. Long-term adsorption capacity is projected to exceed 600 years of useful life before P saturation under conditions typical of urban stormwater in Maryland (i.e., 0.20 mg/L dissolved P (DP) influent and 100 cm of direct rainfall per year). A dynamic model was developed to describe DP adsorption onto the media based on lab testing and verified under field monitoring. The model predicted 62% DP concentration reduction and

65% DP mass load reduction. Actual reductions from 17 months of monitoring in a field pilot study were 67% for DP concentration and 69% DP mass load.

Total Cu and Zn were also removed from stormwater in lab and field studies. Percent concentration reductions of 59-69% for Cu and 78-90% for Zn were shown in lab studies using synthetic stormwater. Mass load was reduced in field monitoring by 32 and 21% for Cu and Zn, respectively.

WTR in the media was shown to be a potential source of nitrogen (N). An internal water storage (IWS) zone was established in a 5-cm permeable pavement base layer to mitigate N export by promoting denitrification. The IWS was shown to effectively lower N concentrations in simulated stormwater when carbon (C) was available in excess (~10 mg/L total C as C). Elevated Al concentrations were found in some filtrate samples from the field study, resulting from washout of fines from the media. Improved HPMM mix preparation methods have been developed and are critical to prevent Al washout and export.

This research resulted in development of the first known enhanced stormwater treatment media to retain DP in a permeable pavement base layer. With appropriate N and Al control, the novel media can be an effective tool and can enhance permeable pavements to improve urban stormwater quality.

IMPROVING STORMWATER QUALITY USING A NOVEL PERMEABLE PAVEMENT BASE MATERIAL

by

Travis Kyle Ostrom

Dissertation submitted to the Faculty of the Graduate School of the
University of Maryland, College Park, in partial fulfillment
of the requirements for the degree of
Doctor of Philosophy
2019

Advisory Committee:
Professor Allen P. Davis, Chair
Professor Ahmet Aydilek
Professor Alba Torrents
Assistant Professor Birthe V. Kjellerup
Professor Frank J. Coale

Dedication

To Candace McConnell

Acknowledgements

I acknowledge the support of the Maryland Technology Enterprise Institute (Mtech) and its Maryland Industrial Partnerships (MIPS) program, Maryland Department of Natural Resources, and PaverGuide, Inc. (Worton, MD). I also acknowledge the support of the Maryland NanoCenter and its AIMLab for assistance with SEM-EDS and the U.S. Army Corps of Engineers Washington Aqueduct (Washington, DC) for providing WTR.

Table of Contents

List of Tables

List of Figures

Chapter 1: Introduction

As society places increased value on maintaining high-quality water resources in and around urban areas, the impetus to protect these surface waters from pollution likewise increases. Urbanization, however, generally results in increased impermeable surface coverage and increased polluted runoff (NRC 2008). Stormwater runoff is an important avenue for pollutant transport from impermeable surfaces to surface waters. Key pollutants of concern in stormwater include nutrients, nitrogen (N) and phosphorus (P), and toxic metals, Al, Cu, Fe, Pb, and Zn. Reducing P loadings is particularly critical to improving many impaired freshwater systems and estuarine environments, such as the Chesapeake Bay (Ator et al. 2011; Schindler et al. 2016). While wastewater treatment plant upgrades and phasing out P-based detergents have decreased loads to impacted surface waters, urban runoff remains a persistent P source in many watersheds (Schindler 1974; NRC 1992; Howarth et al. 2002; Conley et al. 2009). The annual P load to the Chesapeake Bay due to urban runoff, for example, is estimated to have decreased only 7% from 1985 to 2015 (CBP 2016).

To address the challenge of water quality degradation, stormwater control measures (SCMs) are increasingly designed to manage flood risk and to reduce pollutant loadings (NRC 2008). New approaches to urban land development, including low impact development (LID), are being pursued to meet water quality requirements such as the Chesapeake Bay Total Maximum Daily Load (TMDL), which sets pollution load targets for the contributing watershed (Conley et al. 2009; USEPA 2010; Schueler and Lane 2015). LID typically integrates distributed SCMs into site designs in an attempt to mimic

predevelopment hydrology and reduce pollutant loadings (Davis and McCuen 2005). In developed urban areas, SCMs with small spatial footprints and those which can provide multiple co-benefits (e.g., runoff volume reduction and water quality improvement) are particularly useful. Permeable pavements – including porous asphalt, pervious concrete, and interlocking concrete pavers – are one of the primary stormwater best management practices (BMPs) that have been implemented and researched over the past two decades to mitigate hydrologic and water quality impacts of urbanization (Weiss et al. 2017).

Waterborne pollutants can be removed by permeable pavements via several mechanisms. One principle method is through volume reduction. Permeable pavements can reduce runoff volume via infiltration, from 60 to nearly 100% (Gilbert and Clausen 2006; Dietz 2007; Hunt 2010). To ensure adequate drainage, however, particularly in urban areas with compacted soils, infiltrated water is captured in underdrains and directed to the storm drainage system and ultimately to water bodies (VADEQ 2013; ASCE 2015). It is necessary to ensure infiltrated water is treated prior to discharge. Permeable pavements effectively retain several stormwater constituents through sedimentation and filtration. These mechanisms are effective for particulate matter, and pollutants affiliated with these solids, such as include bacteria, particulate phosphorus (PP), ammonium (NH_4) and organic nitrogen (N_{org}), metals, and toxic organic compounds (Li and Davis 2008; Clark and Pitt 2012; Pitt et al. 1994). Several studies have shown removal efficiencies for permeable pavements consistently above 90% for these pollutants and effluent event mean concentrations (EMCs) below water quality targets (Day et al. 1981; Legret et al. 1996; Gilbert and Clausen 2006; Bean et al. 2007; Boving et al. 2008; Roseen et al. 2012; Drake et al. 2014; Winston et al. 2016).

Particulate-bound pollutants can be treated via filtration, but limited retention or remobilization of dissolved nutrients and metals may be responsible for inconsistent removal in past studies. Performance data from the International Stormwater BMP Database (Clary et al. 2017) showed increases or no significant change in concentrations of dissolved phosphorus (DP), orthophosphate, nitrate (NO_3) plus nitrite (NO_2), and certain dissolved metals including dissolved Cd, Cu, Fe, and Pb. DP removal, often reported as orthophosphate (OP), ranged from negative (i.e., export) to +80% across a range of studies and permeable pavement types. Likewise, nitrate export was encountered in nearly all studies analyzed (Day et al. 1981; Pitt et al. 1994; Legret et al. 1999; Collins et al. 2010a,b; Roseen et al. 2012; Drake et al. 2014; Winston et al. 2016).

DP in stormwater can be retained in SCMs via adsorption processes, depending on surface characteristics of the treatment media (Li and Davis 2016). In permeable paving, however, stormwater infiltrates through a permeable pavement surface layer into crushed granite stone base layers, which serve as structural support and for temporary water storage, but have low capacity for P adsorption (CWP and MDE 2000; Smith and Hunt 2010; VADEQ 2013; ASCE 2015). Consequently, typical permeable pavement materials have failed to demonstrate long-term P retention because their adsorption capacity is rapidly exceeded (Bean et al. 2007; Roseen et al. 2012). As P adsorbs to the media surface, active adsorption sites become occupied until the point at which effluent concentration nears influent concentration, defined as saturation. This highlights a need for base materials with greater long-term P retention capacity. Several studies have investigated the potential for enhanced treatment media to improve DP retention in SCMs (Erickson et al. 2007; O'Neill and Davis 2011; Penn at al. 2017).

Nitrate can be removed through the microbially-mediated process of denitrification. To achieve denitrification, reducing conditions must be present to convert NO_3 into nitrous oxide (N_2O) and nitrogen gas (N_2). Previous studies have implemented an internal water storage (IWS) zone to create reducing conditions and advance denitrification in SCMs (Kim et al. 2003; Winston et al. 2016). Dissolved metals can complex with organic matter (OM) or other adsorbents, including WTR (Brown et al. 2007; Li and Davis 2008a; Castaldi et al. 2015).

Research Goal

The overall goal of this research was to develop and demonstrate the performance characteristics of a permeable pavement base material that can consistently improve stormwater quality over the long term. This work describes the development of a novel permeable pavement base material, dubbed High Permeability Media Mixture (HPMM)

High Permeability Media Mixture

HPMM utilizes aluminum-based water treatment residual (WTR) in combination with expanded shale lightweight aggregate (expanded shale) bound with a psyllium-based soil binder (psyllium). This unique combination of inexpensive and recycled materials results in an affordable water treatment solution to enhance the capability of permeable pavements to improve water quality, in addition to existing stormwater control benefits provided by permeable pavements (Drake et al. 2013).

Aluminum-based WTR is generated during drinking water treatment through addition of aluminum sulfate (alum) to enhance the process of coagulation, flocculation, and sedimentation. The resulting sludge is rich in Al-oxides and organic matter (Babatunde et al. 2009) and has a high proportion of amorphous Al and high oxalate ratio

(OR). OR is strongly correlated with P adsorption capacity and previous research has demonstrated the capacity of WTR for removing dissolved pollutants, particularly P, in a variety of contexts (Ippolito et al. 2011; Lucas and Greenway 2011; O'Neill and Davis 2012b; Liu and Davis 2014). WTR, as received, is a clay-like material that would be inappropriate as a permeable pavement base. Therefore, it was combined with expanded shale, as described below, to provide the required geotechnical characteristics.

Expanded shale is a lightweight, clay-based aggregate with an irregular and angular surface. The irregular surface has been shown to support microbial attachment and growth and thus may enhance N removal via denitrification under saturated, anaerobic conditions (Calheiros et al. 2009). Expanded shale confers structural capacity to the mixture and enables HPMM to be used as a load-bearing aggregate. It also serves as a matrix to physically support the WTR and overcomes the low permeability of WTR when used alone.

Psyllium is a fibrous substance produced from the seeds of the *Plantago ovata* plant. It is used in commercially-available soil binders due to its sticky consistency when moistened. Psyllium binds WTR to the shale, resulting in a WTR-coated expanded shale (Figure 2-1). This prevents washout of WTR and expands its applicability to situations where a powdered or clay-like material would be inappropriate (e.g., high flow treatment applications such as a permeable pavement base).

Research Objectives

Assessing HPMM performance characteristics was carried out in three phases including lab-, mesocosm-, and field-scale studies. The goal of the lab study was to evaluate HPMM geotechnical properties and P treatment effectiveness under laboratory

conditions and to gain an understanding of the mechanism(s) of removal. Mesocosm study assessed HPMM treatment performance under more realistic conditions (rainfall simulations) and sought to determine the potential of the material to leach or retain N and metals. The objective of the field study was to assess HPMM performance under field conditions with respect to target inorganic pollutants, including nutrients and metals.

Specific research objectives were pursued and hypotheses tested to achieve the project goal. These were to:

1) Assess the geotechnical suitability of HPMM for use as a permeable pavement base, testing the hypothesis that HPMM will not limit infiltration and can provide sufficient structural support.
2) Evaluate the P treatment and long-term sorption capacity of HPMM, to support the hypothesis that HPMM can enhance P removal compared to unmodified substrate and achieve acceptable effluent concentrations for at least a 20-year pavement design lifetime.
3) Investigate the kinetics of DP sorption onto HPMM, with the hypothesis that retention is driven by adsorption to Al-oxides in HPMM and is negatively correlated to flowrate.
4) Evaluate P, N, and metals retention onto HPMM in rainfall simulations, with the hypothesis that HPMM will achieve effective P and metals removal but will not significantly retain N.
5) Analyze the influence of simulated rainfall intensity and pH on DP treatment, with the hypothesis that DP retention is negatively correlated with rainfall intensity and pH.

6) Compare pollutant removal for HPMM prepared using two different WTR sources, testing the hypothesis that WTR containing activated carbon will achieve greater N retention.
7) Investigate the potential for an IWS zone to enhance N removal via denitrification, to support the hypothesis that reducing conditions can be created in an IWS to advance denitrification and remove N.
8) Verify expected treatment performance under field conditions with actual stormwater by quantifying percent load reduction and effluent concentrations of total phosphorus (TP), total dissolved phosphorus (TDP), total nitrogen (TN), NH_4, NO_x, and total Al, Cu, Fe, Pb, and Zn, with the hypothesis that performance under field conditions will be as effective as treatment predicted under lab and mesocosm conditions.

Chapter 2: Lab-Scale Studies

High-flow Structural Media for Removing Stormwater Dissolved Phosphorous in Permeable Paving

Abstract

Phosphorus (P) loadings from urban runoff is a persistent contributor to waterbody impairment. Dissolved phosphorus (DP), however, is not well-retained by many stormwater control measures (SCMs), including permeable pavements. This study seeks to evaluate a novel base material developed to enhance P removal in permeable paving. The media has high hydraulic conductivity, $9.0 \times 10^{-4} \pm 1.9 \times 10^{-5}$ m/s (324 ± 6.8 cm/h), and is structurally suitable as a permeable pavement base. It demonstrated long-term DP adsorption capacity and achieved treatment above 90% total DP removal for the first 50 m of applied water, well beyond the typical 20-year pavement design lifetime with no contributing area. This indicates potential application of permeable pavement to treat run-on at loading rates of 5:1 or possibly higher. Adsorption to aluminum (hydr)oxides is thought to be the primary mechanism for DP retention. DP uptake is described by a first-order steady-state plug flow model developed and fit to experimental data. This novel media has the potential to improve P retention in permeable pavement and enable run-on treatment.

Keywords: stormwater, phosphorus, permeable paving, enhanced media

This chapter has been accepted for publication as:

Ostrom, T., Aydilek, A., and Davis, A. P. (2019). "High-flow Structural Media for Removing Stormwater Dissolved Phosphorus in Permeable Paving." *Journal of Sustainable Water in the Built Environment*, 5(1).

Introduction

Reducing phosphorus (P) loadings is critical to improving many impaired freshwater systems and estuarine environments, such as the Chesapeake Bay (Ator et al. 2011; Schindler et al. 2016). While wastewater treatment plant upgrades and phasing out P-based detergents have decreased loads to impacted surface waters, urban runoff remains a persistent P source in many watersheds (Schindler 1974; NRC 1992; Howarth et al. 2002; Conley et al. 2009). The annual P load to the Chesapeake Bay due to urban runoff, for example, is estimated to have decreased only 7% from 1985 to 2015 (CBP 2016). Failure to achieve water quality improvements has spurred more stringent regulatory requirements, notably the Chesapeake Bay Total Maximum Daily Load (TMDL), which sets P targets for the contributing watershed (Conley et al. 2009; USEPA 2010). To meet water quality requirements, new approaches to urban land development, including low impact development (LID), are being pursued (Schueler and Lane 2015).

LID typically integrates stormwater control measures (SCMs), including permeable paving, into site designs in an attempt to mimic predevelopment hydrology and reduce pollutant loadings (Davis and McCuen 2005). Permeable pavements can reduce runoff volume via infiltration, from 60 to nearly 100% (Gilbert and Clausen 2006; Dietz 2007; Hunt 2010). To ensure adequate drainage, however, particularly in urban areas with compacted soils, infiltrated water is captured in underdrains and directed to the storm drainage system and ultimately to water bodies (VADEQ 2013; ASCE 2015). It is necessary to ensure infiltrated water is treated prior to discharge.

Permeable pavements effectively retain several stormwater constituents, including particulate matter, and pollutants affiliated with these solids, such as toxic organics and metals. A number of studies have shown removal efficiencies consistently above 90%

199 for these pollutants and effluent event mean concentrations (EMCs) below water quality
200 targets (Day et al. 1981; Legret et al. 1996; Gilbert and Clausen 2006; Bean et al. 2007;
201 Boving et al. 2008; Roseen et al. 2012; Drake et al. 2014; Winston et al. 2016). This
202 treatment is largely achieved through sedimentation and filtration of particulate matter
203 (Pitt et al. 1994; Gilbert and Clausen 2006). Particulate-bound P and nitrogen (N) can
204 also be treated via these mechanisms, but limited retention or remobilization of dissolved
205 nutrients may be responsible for inconsistent removal in past studies. Dissolved
206 phosphorus (DP) removal, often reported as orthophosphate (OP), ranged from negative
207 (i.e., export) to +80% across a range of studies and permeable pavement types. Likewise,
208 nitrate export was encountered in nearly all studies analyzed (Day et al. 1981; Pitt et al.
209 1994; Legret et al. 1999; Collins et al. 2010a,b; Roseen et al. 2012; Drake et al. 2014;
210 Winston et al. 2016).
211 DP has been reported to account for an average 36-44% of total phosphorus (TP)
212 in urban runoff (Pitt and Maestre 2005). Selbig (2016) noted higher dissolved
213 percentages, greater than 85%, in the fall season from leaf litter degradation. DP in
214 stormwater can be retained in SCMs via adsorption processes, depending on surface
215 characteristics of the treatment media (Li and Davis 2016). In permeable paving,
216 however, stormwater infiltrates through a permeable pavement surface layer into crushed
217 granite stone base layers, which serve as structural support and for temporary water
218 storage, but have low capacity for P adsorption (CWP and MDE 2000; Smith and Hunt
219 2010; VADEQ 2013; ASCE 2015). Consequently, typical permeable pavement materials
220 have failed to demonstrate long-term P retention because their adsorption capacity is
221 rapidly exceeded (Bean et al. 2007; Roseen et al. 2012). As P adsorbs to the media

surface, active adsorption sites become occupied until the point at which effluent concentration nears influent concentration, defined as saturation. This condition is reached after only a few years or possibly months for traditional permeable pavement materials, highlighting a need for base materials with greater long-term P retention capacity.

High Permeability Media Mixture

This work describes the development of a novel permeable pavement base material, referred to as high permeability media mixture (HPMM), to address this need. HPMM utilizes aluminum-based water treatment residual (WTR) in combination with expanded shale lightweight aggregate (expanded shale) bound with a psyllium-based soil binder (psyllium). This unique combination of inexpensive and recycled materials results in an affordable water treatment solution.

Aluminum-based WTR is generated during drinking water treatment through addition of aluminum sulfate (alum) to enhance the process of coagulation, flocculation, and sedimentation. The resulting sludge is rich in Al-oxides and natural organic matter (Babatunde et al. 2009) and has a high proportion of amorphous Al and high oxalate ratio (OR). OR is strongly correlated with P adsorption capacity and previous research has demonstrated the capacity of WTR for removing dissolved pollutants, particularly P, in a variety of contexts (Ippolito et al. 2011; Lucas and Greenway 2011; O'Neill and Davis 2012b; Liu and Davis 2014). WTR, as received, is a clay-like material that would be inappropriate as a permeable pavement base. Therefore, it was coated over expanded shale to provide the required geotechnical characteristics.

Expanded shale is a lightweight, clay-based aggregate with an irregular and angular surface. The irregular surface has been shown to support microbial attachment and growth and thus may enhance N removal via denitrification under saturated, anaerobic conditions (Calheiros et al. 2009). Expanded shale confers structural capacity to the mixture and enables HPMM to be used as a load-bearing aggregate. It also serves as a matrix to physically support the WTR.

Psyllium is a fibrous substance produced from the seeds of the *Plantago ovata* plant. It is used in commercially available soil binders due to its sticky consistency when moistened. Psyllium binds WTR to the shale, resulting in a WTR-coated expanded shale (Fig. 1). This prevents washout of WTR and expands its applicability to situations where a powdered or clay-like material would be inappropriate (e.g., high flow treatment applications such as a permeable pavement base).

Research Objectives

The overall goal of this research was to develop and demonstrate the performance characteristics of a permeable pavement base material, as described above, that can consistently retain DP over the long term. The goal of the present study was to evaluate HPMM geotechnical properties and P treatment effectiveness under laboratory conditions and to gain an understanding of the mechanism(s) of removal. Three specific research objectives were pursued to achieve this goal:

1) Assess the geotechnical suitability of HPMM for use as a permeable pavement base, testing the hypothesis that HPMM will not limit infiltration and can provide sufficient structural support.

2) Evaluate the P treatment and long-term sorption capacity of HPMM, to support the hypothesis that HPMM can enhance P removal compared to unmodified substrate and achieve acceptable effluent concentrations for at least a 20-year pavement design lifetime.
3) Investigate the kinetics of DP sorption onto HPMM, with the hypothesis that retention is driven by adsorption to Al-oxides in HPMM and is negatively correlated to flowrate.

Methods and Materials

High Permeability Media Mixture

WTR used in this study was collected at a moisture content (MC) of 3.22 ± 0.17 g wet/g dry (69 ± 2 %) from the Dalecarlia drinking water treatment plant (Washington, D.C.). It was first sieved through a 2.00 mm sieve, then air dried for at least one week to MC = 1.21 ± 0.02 g wet/g dry (17 ± 1 %) and powdered by hand to a bulk density of 0.56 g/cm^3. Haydite "H" size expanded shale (DiGeronimo Aggregates, Cleveland, OH), graded by the supplier to between 1.59 mm (1/16 in) and 4.76 mm (3/16 in) was used in this application. The shale was further sieved through a 2.00 mm sieve with a resulting bulk density of 0.84 g/cm^3. Two HPMM mixtures, designated HPMM-1 and HPMM-2, were prepared using different sources of psyllium. HPMM-1 included Psyllium Husks Powder (Yerba Prima, Ashland, OR) and HPMM-2 utilized *Stabilizer* (Stabilizer Solutions, Phoenix, AZ). HPMM-1 and -2 had bulk densities of 0.76 g/cm^3 and 0.63 g/cm^3, respectively.

Geotechnical Analysis

A series of constant-head hydraulic conductivity tests were conducted on HPMM following the procedures outlined in ASTM Standard Method D2434. A 10-cm diameter fixed-wall permeameter was used to measure flow at three different hydraulic gradients (defined as h/L): 2.3, 2.8, and 3.2. For hydraulic conductivity calculations, stabilized flow rates were used and the tests were terminated when the average of the last three consecutive flow rates for each hydraulic gradient fell within ±10% of the mean value. Duplicate specimens were tested as quality control and the average of these two tests were reported as results. Hydraulic conductivity, k, was calculated as follows at each hydraulic gradient and the three values were averaged to obtain the reported hydraulic conductivity value:

$$k = QL/Ah \tag{2-1}$$

where Q = volumetric flowrate, L = length of specimen, A = cross-sectional area of specimen, and h = change in head.

The California bearing ratio (CBR) test is a penetration test for evaluating the bearing capacity of road subgrades and base courses. It relates the loading force or stress required to penetrate a piston a specified depth (2.54 mm) into a test material to the stress required to penetrate a standard reference material (6.9 MPa). To perform the CBR test, optimum moisture content and maximum dry unit weight were first determined using the Standard Proctor Test according to ASTM Standard Method D698 Method B and Maryland State Highway Administration Standard Method MSMT 321. The latter method was employed because water began to seep from the compaction mold at 23% moisture content before achieving maximum dry unit weight. Moisture content was measured following ASTM Standard Method D2216

313 using approximately 50 g samples oven-dried at 45 °C to prevent loss of organic
314 material. Compaction was achieved in a 101.6-mm diameter mold using a 24.5-N
315 weight rammer to deliver 25 blows at a drop distance of 305 mm to each of 3 layers.
316 The appropriate amount of water was added to new 1000 g samples to increase
317 moisture by approximately 4% for each compaction.

318 All HPMM specimens for the CBR tests were compacted at their optimum
319 moisture content of 24% and maximum dry unit weight of 10.1 kN/m^3. Penetration
320 with a 50 mm diameter piston proceeded at 1.27 mm/min in an S5840 Multi-Loader
321 compression machine (Geotest Instrument Corporation, Burr Ridge, IL). Duplicate
322 specimens were tested for CBR tests as quality control, and the averages of these two
323 tests were reported as results.

324 The direct shear test is a method used to determine the shear strength of a
325 material. It indicates the capacity of a material to resist force parallel to an internal
326 plane that would cause the material to slide against itself. The test is performed by
327 placing a test material in a shear box, applying a normal force, and displacing one
328 half of the shear box laterally, producing a shearing force along a plane. Direct shear
329 tests were performed according to ASTM Method D3080 with a digital shear machine
330 (ELE International, Bedfordshire, UK) and 10 cm wide shear box. Shearing was
331 performed at a rate of 0.5 mm/min under normal loads of 168, 266, and 364 N.
332 Specimens were compacted at 23% moisture content to 8.6 kN/m^3 dry unit weight.
333 The resulting shear stress and normal stress were plotted to determine peak friction
334 angle (angle of internal friction) and cohesion using the Coulomb failure criterion
335 (Burland et al. 2012).

Material Characterization

Amorphous Al, Fe, and P were extracted from HPMM and WTR using an oxalate extraction procedure from McKeague and Day (1966). Triplicate samples of 1.0 and 0.4 g for HPMM and WTR, respectively, were placed in 40 mL of oxalate extraction solution. A 1:100 mass:volume ratio was used for the WTR per Dayton and Basta (2005) because of its elevated Al concentration. Oxalate extraction solution was prepared by combining 227 mL of 0.2 M ammonium oxalate with 200 mL of 0.2 M oxalic acid to achieve a pH of 3. Samples were shaken for 24 h, centrifuged at 1600 x g for 13 min, and then filtered through 0.22 µm ceramic filters. Total Al and Fe concentrations were analyzed as described below. P concentrations were measured by a method modified from Wolf and Baker (1990) using a 0.126 M molybdate solution. This method mitigates interference by oxalate complexes formed with molybdate which prevents use of the traditional ascorbic acid molybdenum blue colorimetric method from Standard Method 4500-P (APHA et al. 2012). Oxalate ratio (OR) was calculated as a measure of P adsorption potential as follows:

$$OR = \frac{Al+Fe}{P} \quad (2\text{-}2)$$

where Al, Fe, and P represent oxalate-extractable content in mmol/kg of media.

Scanning Electron Microscope (SEM) and Energy Dispersive Spectroscopy (EDS) analyses were conducted using a SU-70 field emission gun scanning electron microscope (Hitachi High-Technologies in America, Clarksburg, MD) using 10kV accelerating voltage. Samples were first coated with Au and Pd.

Batch Equilibrium Study

P isotherms were determined using a batch equilibrium method modified from Nair et al. (1984). Depending on the material, 0.1-1.0 g was added to 50 mL solutions in plastic centrifuge tubes and shaken end-over-end for 24 h. Solutions were prepared using deionized (DI) water with a background electrolyte concentration of 0.01 M NaCl and P concentrations between 0.0 and 10.0 mg/L diluted from a 1000 ppm as P KH_2PO_4 standard (Table 2-1). After shaking, samples were centrifuged for 10 minutes at 2800 x g and the supernatant was decanted. Samples were analyzed for initial and final pH and total dissolved phosphorus (TDP) as described below. P adsorption capacity q was calculated as

$$q = \frac{V(C_{in} - C_{out})}{M} \quad (2\text{-}3)$$

where C = TDP concentration, V = solution volume, and M = mass of adsorbent. HPMM is composed of 8.5% WTR by oven-dry mass. Therefore, to compare batch results directly, q values obtained for WTR were normalized by multiplying by 0.085 and labeled "WTR-8.5%."

Long-term Continuous Loading Column Study

P removal and long-term P saturation under continuous loading were assessed using glass columns packed with either HPMM or unmodified expanded shale for comparison. The 20 cm tall, 2.5 cm inner diameter columns were run in triplicate using material sieved to between 0.15 and 2.0 mm to ensure a column:media diameter ratio > 12.5, similar to the approach used by O'Neill and Davis (2012a). Synthetic stormwater influent was continuously pumped in an upflow direction to control contact time. Influent and effluent samples were analyzed for pH and TDP as described below.

Synthetic stormwater influent for HPMM-1 contained 500 mg/L NaCl, typical of background electrolyte concentration in stormwater (USEPA 1983), and 0.2 mg/L P KH_2PO_4 in DI water and adjusting the pH to 7.0 with 0.1 M NaOH. For HPMM-2, 1 mg/L N $NaNO_3$, 80 mg/L $CaCl_2$, 2 mg/L N glycine, and 2.6 mg/L C sodium acetate were also included. Due to cloudiness, likely caused by precipitation or microbial growth, the acetate concentration was decreased to 1.3 mg/L C and $CaCl_2$ addition was discontinued (Table 2-1) after 0.17 mg P/kg applied. The measured influent TDP concentration averaged 0.19 mg/L except for some variation during the startup and a period of 11 days in which only 0.10 mg/L P was inadvertently added. The flow rate was maintained at 1.2 mL/min (15 cm/h) for 10 weeks, after which it was increased to 2.1 mL/min (25 cm/h) for 3 weeks, then to 2.8 mL/min (35 cm/h) for 1 week for HPMM-1 and 4 weeks for HPMM-2, respectively.

Removal efficiency in the columns was calculated as:

$$Removal = \frac{C_{in} - C_{out}}{C_{in}} \times 100\% \quad (2\text{-}4)$$

P adsorption capacity q was calculated as:

$$q = \frac{T_{P,in} - T_{P,out}}{M} \quad (2\text{-}5)$$

where T_P = total mass of P entering or exiting the system and M = mass of adsorbent. T_P was calculated as:

$$T_P = \int_0^{t_i} C \cdot Q dt \quad (2\text{-}6)$$

where C = TDP concentration and Q = flow rate.

Flow-modified Column Study

The relationship between P adsorption and flow rate was investigated by testing effluent TDP concentrations at various flow rates using a second set of columns containing either shale or HPMM. Glass columns, 15 cm height and 2.5 cm diameter, were partially filled with 25 cm^3 of media. Influent, composed of DI water, 0.01 M NaCl, 0.19 mg/L P as KH_2PO_4, at pH ≈ 7.0 was pumped through the columns in an upflow direction (Table 2-1). Flow rate was increased stepwise from 0 to 22.2 mL/min (0 to 272 cm/h), allowing approximately 3 bed volumes, 90 mL, to pass at each new flow rate before taking a sample. Flow was then decreased stepwise to investigate potential P saturation effects. Effluent was analyzed for TDP as described below.

Analytical Procedures

Sample pH was measured using a glass electrode probe with Ag/AgCl reference to an accuracy of 0.01 units (Mettler Toledo MA235, Greifensee, Switzerland). TP and TDP concentrations were determined by potassium persulfate digestion and the ascorbic acid molybdenum blue colorimetric method from Standard Method 4500-P (APHA et al. 2012). TDP samples were first filtered through a 0.22 μm ceramic filter. Absorbance was measured using a 5 cm path-length cuvette in a UV-Visible spectrophotometer (UV160U, Shimadzu, Kyoto, Japan) at 880 nm to yield a detection limit of 0.01 mg/L P. Exceptions to this were samples from oxalate extractions, which were analyzed for TDP using a method modified from Wolf and Baker (1990) and analyzed at 660 nm to a detection limit of 0.01 mg/L P. Total metals were analyzed using inductively coupled plasma atomic emission spectroscopy (ICP-AES) (ICPE-9000 Plasma Atomic Emission Spectrometer, Shimazdu, Kyoto, Japan) at 394.403 and 259.940 nm for Al and Fe,

424 respectively, with a detection limit of 25 µg/L. Values below detection limits have been
425 assigned following the probability plot method from Helsel and Hirsch (2002).

426 *Results and Discussion*

427 Suitability as a Permeable Pavement Base

428 To assess the suitability of HPMM as a permeable pavement base material,
429 hydraulic conductivity, CBR, and direct shear testing were conducted. Hydraulic
430 conductivity for HPMM was found to be $9.0 \times 10^{-4} \pm 1.9 \times 10^{-5}$ m/s (324 ± 6.8 cm/h).
431 Burland et al. (2012) provide typical hydraulic conductivity ranges for clean gravels, > 1
432 x 10^{-3} m/s (360 cm/h), and sand/gravel mixtures, 1 x 10^{-5} to 1 x 10^{-3} m/s (3.6-360 cm/h).
433 The observed value falls within the expected range for sand and gravel mixtures. It was
434 anticipated that HPMM would have a hydraulic conductivity similar to that of gravel
435 because of the use of 9.5 mm shale. Addition of WTR and psyllium to the mix blocks
436 some pores, thus reducing the permeability slightly. High permeability native soils
437 classified as hydrologic soil group (HSG) A soils by the Natural Resources Conservation
438 Service (NRCS) must have hydraulic conductivity greater than 4.0×10^{-5} m/s (14.4 cm/h)
439 (NRCS 2009). Because HPMM hydraulic conductivity exceeds this value, it is unlikely
440 to limit infiltration into the subsurface.

441 Optimum moisture content and maximum dry unit weight for HPMM were found
442 to be 21% and 9.58 kN/m^3, respectively. Maximum dry unit weight of 8.44 kN/m^3 at
443 21% moisture has been specified for expanded shale in industry documents (DiGeronimo
444 Aggregates 2016). Testing by aggregate suppliers, however, has found little to no
445 correlation between moisture content and dry unit weight for expanded shale alone
446 (Papadopoulos 2008; Saint-Gobain Weber 2016). Mechleb (2013) related dry density to

moisture content in clay soils amended with expanded shale and found a range of maximum dry unit weight between 14.91 and 16.28 kN/m^3 at 24 and 19% moisture content, respectively. It is not surprising that HPMM maximum dry unit weight was found to be higher than expanded shale alone, but lower than shale-amended clays. Optimum moisture content was also in the range found by Mechleb (2013) for shale-amended clays. This information was used to conduct CBR and shear testing at appropriate moisture content and dry weights.

The HPMM CBR number was calculated to be 35. This falls in the range of a "good" rating for use as a base or sub-base (Asphalt Institute 2007). Peak friction angle of 55 degrees was determined from shear testing. This is a high value, indicating high strength, but not unreasonable because many gravels and natural granular soils have angles of friction in this elevated range (Holtz et al. 2011). HPMM was also found to be relatively cohesionless, with a cohesion of 5.8 kPa. These results taken together indicate the structural suitability of HPMM for use as a permeable pavement base material.

Phosphorus Treatment Capacity

Aluminum Content and Oxalate Ratio

The amorphous (oxalate-extractable) Al content of HPMM was determined to be 10,700 ± 1500 mg Al/kg dry sample (398 ± 55.6 mmol Al/kg dry sample). Because HPMM was prepared using 8.5% WTR by oven-dry mass, this equates to 126,000 mg Al/kg WTR. This falls in the concentration range of 42,000 – 146,000 mg Al/kg WTR found for Al-WTRs from literature as summarized by Komlos et al. (2013). SEM-EDS analysis also confirmed the material to be dominated by Al and O (Fig. 2). HPMM was found to contain 925 ± 213 mg Fe/kg dry sample (16.6 ± 3.82 mmol Fe/kg dry sample) and 47.5 ± 8.50 mg P/kg dry sample (1.53 ± 0.274 mmol P/kg dry sample) of oxalate-

extractable Fe and P, respectively. Because an Al-based WTR was used, the amorphous Fe content was an order of magnitude smaller than the Al content. The resulting OR for HPMM is 270. O'Neill and Davis (2012a) found similar oxalate-extractable Al and Fe content for WTR-amended bioretention soil media (BSM), 396 mmol/kg and 22.1 mmol/kg, respectively. The resulting OR of 56.6 calculated for WTR-amended BSM was lower than that of HPMM due to relatively higher oxalate-extractable P content, 7.39 mmol P/kg in the WTR-amended BSM. The combination of high Al content and low P content results in a high OR and indicates good potential for HPMM as a DP treatment media.

Batch Equilibrium

Relationships between adsorbed P per mass of adsorbent, q (mg/kg), and residual TDP concentrations, C (mg/L), were determined by fitting Langmuir and Freundlich isotherm models to batch equilibrium data using non-linear regression. These models have been found to describe phosphate adsorption to soil media (Nair et al. 1984). The two models were similar for all materials, therefore only Freundlich isotherms are presented to simplify comparison between materials tested (Fig. 3). The Freundlich model takes the form:

$$q = K \cdot C^{\frac{1}{n}} \tag{2-7}$$

HPMM demonstrated greater P adsorption capacity than shale alone. At a TDP concentration of 0.2 mg/L, representative of urban stormwater (Pitt 2011), HPMM-1 and -2 had Freundlich modeled q values of 256 and 235 mg/kg, respectively, compared to 9 mg/kg for shale. It should be noted that WTR only contributes 8.5% of the total HPMM mass. Therefore, a P capacity of 235 mg/kg HPMM is equivalent to 2765 mg/kg WTR

495 (i.e., 235 divided by 0.085). HPMM also performed better than the Ca-containing
496 materials aragonite and crushed oyster shell (not shown). This can be explained by the
497 fact that precipitation of Ca complexes is generally a slower process than the relatively
498 more rapid adsorption of PO_4(-III) to Al(+III) surface groups (Snoeyink and Jenkins
499 1980). Both processes raise pH by liberating OH^- ions (Brattebo and Odegaard 1986).
500 This was found to be true for all materials tested, though the increase was greatest for
501 those materials not containing WTR, which may provide some buffering capacity. From
502 an average initial pH of 4.92 ± 0.17 across all samples, aragonite, oyster shell, shale, and
503 shale-steel wool reached equilibrium pH values of 9.22 ± 0.20, 9.15 ± 0.26, 8.17 ± 0.72,
504 and 8.99 ± 0.55, respectively. WTR-8.5% and HPMM pH at equilibrium were 6.63 ±
505 0.10 and 6.56 ± 0.21, respectively. The more moderate pH increase may be due to
506 hydrolysis of Al complexes in the WTR. Yang et al. (2006) demonstrated that hydrolysis
507 reactions result in H^+ ion release along with increases in Cl^-, SO_4^{2-}, and other ions when
508 WTR is added to water.
509 Freundlich parameters K and 1/n were found to be 385 and 0.246 for HPMM-1
510 and 427 and 0.371 for HPMM-2, respectively. These values are comparable to those
511 from previous studies using WTR in media mixtures (O'Neill and Davis 2012a; Yan et al.
512 2016). The modeled isotherms for HPMM and WTR, when normalized by WTR content
513 (i.e., WTR q values are multiplied by 0.085), do not differ greatly, particularly at lower
514 equilibrium concentrations. The modeled q value for WTR-8.5% at 0.2 mg/L is 192
515 mg/kg, which is 18% lower than HPMM-1 (q = 256 mg/kg) and 25% lower than HPMM-
516 2 (q = 235 mg/kg) at that concentration. This supports the hypothesis that DP adsorption
517 onto HPMM is primarily controlled by the Al content of the WTR. Based on these

results and what is known of the adsorptive properties of Al from previous studies, it was determined that HPMM holds potential as a treatment media and further study is warranted.

Long-term Continuous Loading

Adsorption capacity reaches a limit as surface sites become saturated with solute, but the adsorption process can also be limited by the mass transfer rate of P from solution onto an adsorbent (Weber et al. 1991; Howe et al. 2012). Packed columns were subjected to continuous loading with synthetic stormwater (Table 2-1) over four months to determine the P saturation point of the media. The flowing conditions also provided insight into mass transfer limitations. Effluent TDP concentrations asymptotically increased with continued P loading as adsorption sites became occupied (Fig. 4). HPMM (HPMM-1 and -2) treated over 600 m of influent before reaching P saturation compared to 6 m for un-amended shale. This corresponds to an adsorption capacity of 1068 mg/kg for HPMM-2, compared to 10 mg/kg for shale alone. By comparison, Yan et al. (2018) found an adsorption capacity of 134 mg/kg when subjecting WTR-amended high flow media (sand) to similar continuously loaded column conditions (e.g., flow rate, inorganic P concentration, proportionate mass of WTR amendment, and column diameter to media particle size ratio). Higher adsorption capacity found in the present study may be attributable to a difference in WTR source. Yan et al. (2018) sourced WTR with a lower OR, 59, than the WTR in the present study, 270. The column adsorption capacity of 1068 mg/kg is also higher than the isotherm-modeled capacity of 281 mg/kg from the batch study. Experimental conditions, including flow, mixing, and background matrix

conditions, differed between column and batch studies complicating determination of the specific cause for the difference.

Assuming an average annual rainfall typical for College Park, Maryland of 1 m (40 inches) per year and no contributing area, 600 m of flow represents a useful lifetime of 600 years as a permeable pavement base before reaching P saturation at 0.19 mg/L P. HPMM achieved a removal efficiency above 90% for the first 50 m of applied water (years of service) and removal remained above 40% for the initial 450 m of runoff treated. The expanded shale removal efficiency dropped below 40% after just 3 m of water (3 years of service), yet the typical permeable pavement is designed for a 20-year lifetime. A more practical benefit of the enhanced P adsorption capacity is to enable permeable pavements to receive run-on flow from other areas such as roofs. At a loading rate of 5:1, HPMM could potentially maintain above 90% removal efficiency for 10 years of service, 40% removal for 90 years, safely beyond the 20-year pavement lifetime, and last 120 years before reaching saturation at 0.19 mg/L P influent concentration.

P Sorption Model

A simple plug flow model was developed to describe P retention by HPMM. It is similar to models developed by Erickson et al. (2007) and Li and Davis (2016). First-order P adsorption kinetics were assumed and the liquid-phase mass balance was written as:

$$\frac{dM}{dt} = Q \cdot C - Q(C + dC) - k(C - C_{eq})dA_r \quad (2\text{-}8)$$

where Q = flow rate, C = TDP in the water, k = adsorption rate constant, C_{eq} = TDP concentration in the water in equilibrium with the media surface, and A_r = reactive surface area of the media. The reactive surface area, A_r, relates to the available reactive

surface sites capable of adsorbing P. Because HPMM is a mixture of reactive WTR and less reactive shale, this is different than the total surface area of the media. It can be related to the bulk media volume, V_m, by the specific reactive surface area, SSA_r, which is a constant characteristic of the media, through Equation 2-9.

$$\frac{A_r}{V_m} = SSA_r \tag{2-9}$$

Substituting and rearranging Equation 2-9 into Equation 2-8 and assuming steady state conditions results in

$$\frac{dC}{C-C_{eq}} = -\frac{k \cdot SSA_r}{Q} dV_m \tag{2-10}$$

C_{eq} is expected to increase over the long term as P is adsorbed onto the media surface, thereby diminishing the concentration gradient $C\text{-}C_{eq}$ driving adsorption. Over the short term, however, C_{eq} is essentially constant. Treating C_{eq} as a constant and integrating with boundary conditions dC: C_{in} to C_{out} and dV_m: 0 to V_m yields

$$\frac{C_{out}}{C_{in}} = \frac{C_{eq}}{C_{in}}\left(1 - e^{\frac{-k \cdot SSA_r \cdot V_m}{Q}}\right) + e^{\frac{-k \cdot SSA_r \cdot V_m}{Q}} \tag{2-11}$$

Under long-term continuous loading in columns, effluent TDP (C_{out}) increased with continued loading and asymptotically approached the influent TDP concentration (C_{in}) at media saturation (Fig. 4). In other words, the fraction of TDP retained, (C_{in}-C_{out})/C_{in}, approaches zero at saturation. This trend can be described mathematically with an exponential decay function as follows.

$$\frac{C_{in}-C_{out}}{C_{in}} = e^{-\beta_0 \Sigma M} \tag{2-12}$$

where β_0 is a fitting parameter that describes the rate at which unoccupied adsorption sites are filled and ΣM = cumulative mass of P adsorbed per mass of adsorbent media. At low flow rate, it can be demonstrated from Equation 2-11 that $C_{out} = C_{eq}$. This is

equivalent to assuming effluent TDP is in equilibrium with the media surface. This assumption is supported by the long-term column studies because doubling and tripling the flow rate did not result in a drop in treatment effectiveness. Setting $C_{out} = C_{eq}$ and solving for C_{eq} in Equation 2-12, then substituting the result into Equation 2-11 yields

$$\frac{C_{out}}{C_{in}} = 1 - e^{-\beta_0 \sum M} + e^{-\left(\beta_0 \sum M + \beta_1 \frac{V_m}{Q}\right)} \quad (2\text{-}13)$$

where $\beta_1 = k \cdot SSA_r$. This model was fit to long-term column data and plotted on Fig. 4. The calculated values for β_0 and β_1 are shown in Table 2-2. β_0 is a long-term parameter related to the adsorption capacity of the media. β_1 is a short-term parameter related to the adsorption kinetics and media reactive surface area. Lower values of β_0 and greater values of β_1 indicate greater retention. β_0 was lower for HPMM-1 and -2 than shale by factors of 78 and 132, respectively, indicating lower impact of accumulated P and greater retention by HPMM. β_1 was greater for shale than HPMM-1 and -2, by factors of 2 and 3, respectively. Differences in β_1, however, had little impact on P retention over the long-term study compared to β_0, which controls how rapidly the media approaches P saturation.

Kinetics in Flow-modified Columns

It was hypothesized that P retention is negatively correlated with flow rate. This relationship was not apparent in long-term column studies. Therefore, a column study was conducted in which flow rate was modified more drastically to explore the effect of increasing advective mass transport relative to diffusional. The flowrates tested, 0-272 cm/h, are in the range that could be expected in permeable pavement applications where flow through the base material could occur up to the hydraulic conductivity of the HPMM, 324 cm/h.

611 Effluent TDP increased as flow rate increased for both HPMM and unmodified
612 shale (Fig. 5). Effluent TDP was lower for HPMM than for shale at nearly all flow rates.
613 Normalized effluent TDP (i.e., C_{out}/C_{in}) ranged from 0.04 to 0.28 at flow rates of 14 and
614 28 cm/h, which is in line with expectations based on the beginning of the long-term
615 column study, before significant P loading saturated adsorption sites. As flow rates
616 increased, retention time and P removal decreased, indicating mass transfer limitation on
617 adsorption as advective transport overwhelms adsorption kinetic transfer rates. It should
618 be noted that the flow rates tested exceed expected rainfall intensities for even high
619 intensity storms near College Park, MD (Bonnin et al. 2006).
620 The flow-modified column test reinforced the conclusion from the long-term
621 column study that HPMM has enhanced adsorption capacity. Effluent concentration
622 curves for stepping up and stepping down flow rates were similar for HPMM (Fig. 5).
623 This indicates the media had not reached P saturation and that the change in effluent TDP
624 concentration was a result of changing contact time. In contrast, shale effluent TDP
625 concentration did not decrease as the flow rate was stepped down. This suggests that the
626 shale had become saturated during the time of the test. The original removal efficiency at
627 lower flow rates could not be restored because P adsorption capacity had been reached.
628 The model from Equation 2-13 was fit to this data set and the resulting parameters
629 are given in Table 2-2. β_1 was only 8% greater for HPMM than for unmodified shale.
630 This suggests the adsorption kinetic transfer rates may not differ greatly if open
631 adsorption sites are available. As phosphate occupied adsorption sites on the shale,
632 however, retention was diminished. This can be observed in the higher β_0 value of 129
633 for shale as compared to 26.7 for HPMM. The relative difference in β_0 is substantial

when one considers that the β_0 parameter is in an exponential function in Equation 2-13. This supports the findings from the long-term study that adsorption capacity is rapidly taken up for shale but persists much longer for HPMM.

Conclusions

The results of this study support the hypotheses that HPMM 1) is a structurally suitable permeable pavement base material, 2) can enhance P removal from rainfall/runoff for the duration of a permeable pavement design life, and 3) retains DP primarily through adsorption to Al (hydr)oxide surfaces with more effective retention at lower flowrate.

Geotechnical testing demonstrated that the media has high hydraulic conductivity and would be suitable, with respect to infiltration rate, for use as a permeable pavement base. The structural strength of the media was also shown to be good for use as a base material from analysis of CBR and direct shear test results.

Batch equilibrium testing demonstrated the relatively high capacity of HPMM to adsorb P from aqueous solutions as compared to Ca and Fe-containing materials. Continuous loading with synthetic stormwater containing P, NaCl, N, and a C source in column testing supported the adsorption capacity calculated from batch testing, though the two adsorption capacities were not directly comparable, possibly due to differences in experimental conditions such as flow, mixing, and background matrices. Long-term P adsorption capacity after greater than 600 m of applied water was calculated as 1068 mg/kg at 0.19 mg/L P input. These studies also demonstrate the efficacy of HPMM to reduce P concentrations under flowing conditions, with consistently high P removal

efficiency (90% or above) well beyond the anticipated 20-yr lifetime treatment volume for a permeable pavement receiving no run-on flow. This enhanced P retention capacity could enable permeable pavements to receive run-on flow from other surfaces at loading rates of 5:1 or possibly higher without diminishing P treatment throughout the pavement lifetime.

A steady-state plug-flow model was developed and fit to experimental data. The model describes DP retention as a function of rapid surface transfer rate kinetics and long-term cumulative DP loading effects. The model effectively describes DP removal by the test media. It should be noted that data used to fit the model were obtained under controlled laboratory conditions and may not account for effects of adsorption competition or preferential flowpath development under field conditions. Further validation of the model presented herein could be carried out using additional data, including field data.

There is a need for consistent, long-term P removal from runoff intercepted by stormwater control measures. A novel media mixture has been developed using an aluminum-rich recycled resource. Effective P treatment and geotechnical characteristics demonstrated in this study indicate that HPMM has potential applicability as a base material in permeable pavements and can improve water quality. This new tool to address nonpoint pollution could enable wider applicability of permeable paving due to its capacity to retain P from direct precipitation and in run-on from contributing areas.

678 **List of Figures**

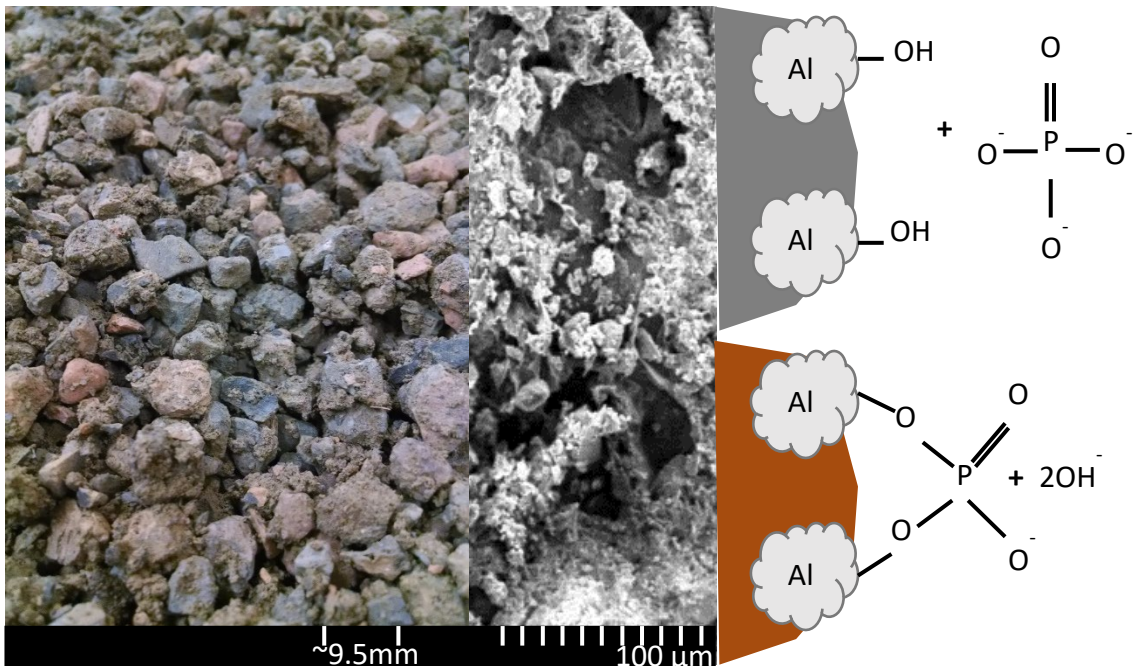

679

680 Figure 2-1. Close-up image of HPMM showing WTR coating expanded shale
681 approximately 9.5 mm in diameter (left). Scanning electron microscope (SEM) image of
682 HPMM showing WTR coating the irregular porous surface of expanded shale (middle).
683 Depiction of ligand exchange mechanism through which phosphate adsorbs to reactive Al
684 surface sites on the HPMM and releases hydroxyl ions (right) (adapted from Li and Davis
685 2015).

686

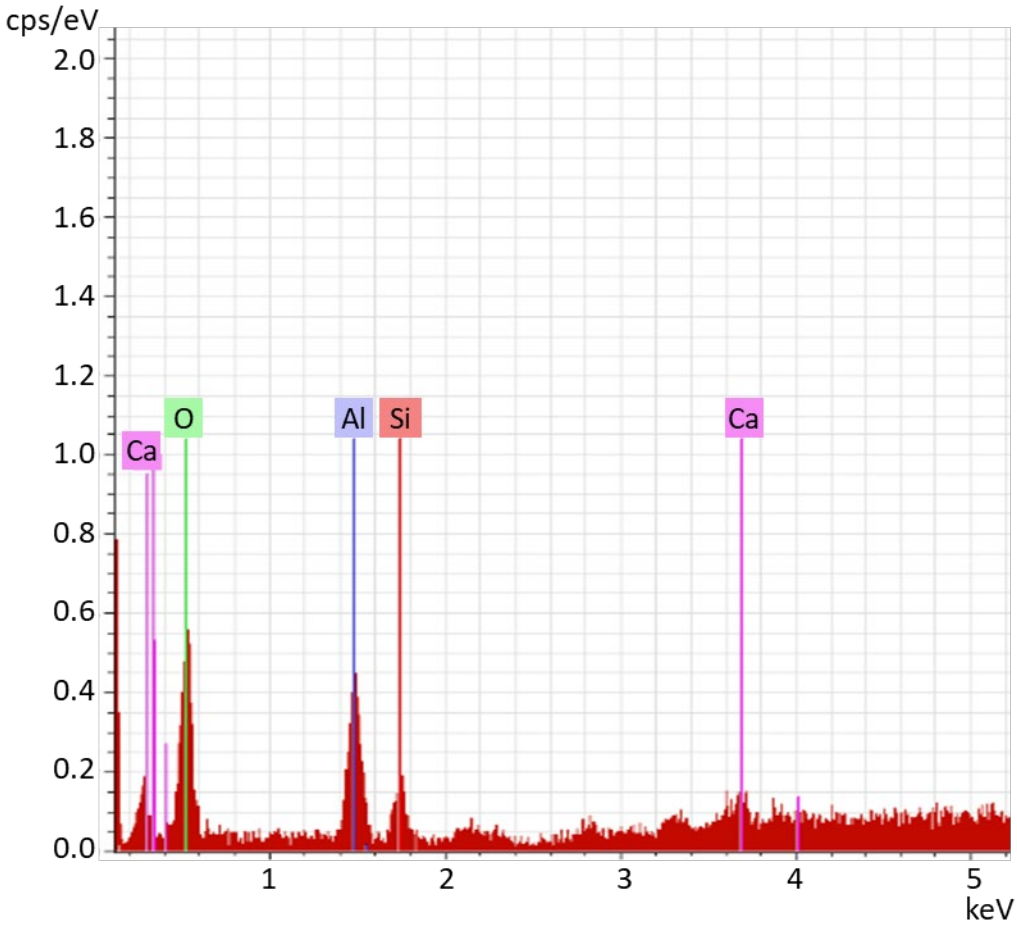

687

688 Figure 2-2. SEM-EDS analysis showing elements present in the HPMM. O (2nd peak
689 from left) and Al (3rd peak from left) are most prevalent.

690

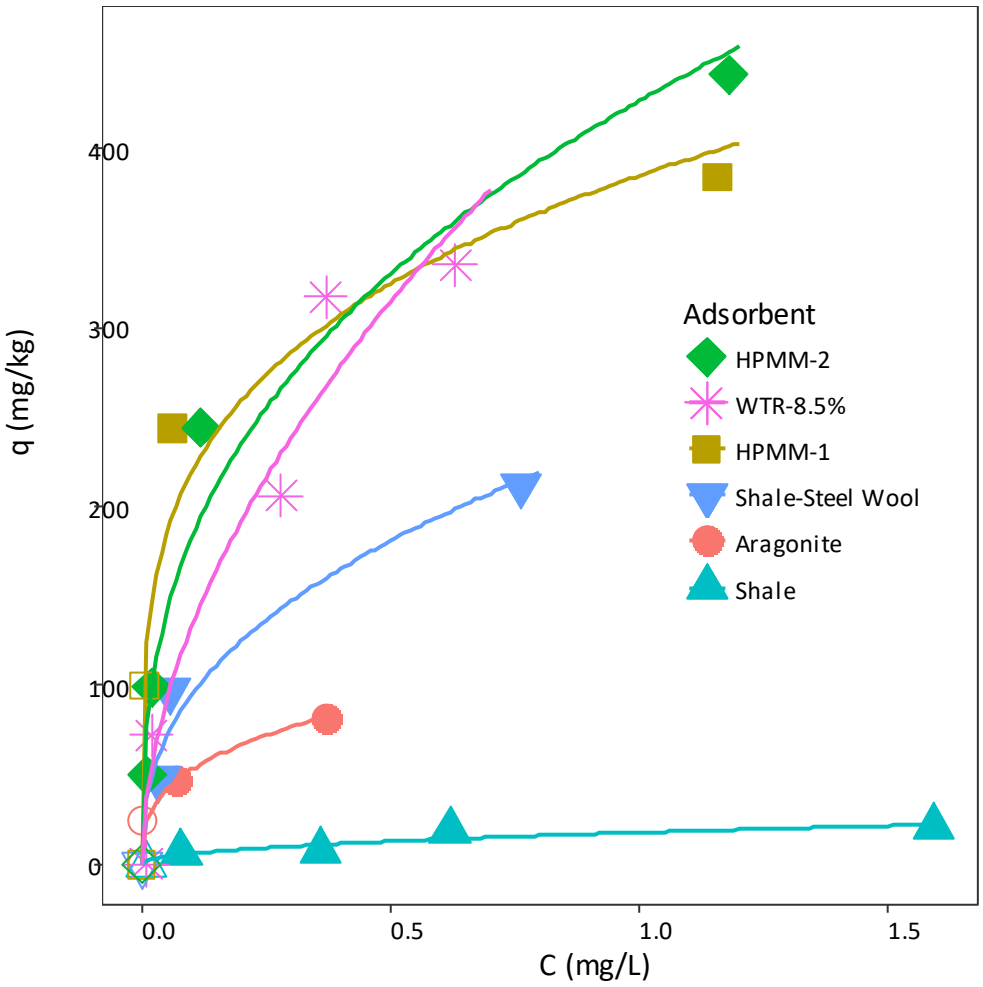

691

692 Figure 2-3. Freundlich isotherms fit to adsorption equilibrium data for various materials.
693 Data points reflect equilibrium after 24 h contact with 0 - 10 mg/L P solutions and a
694 background electrolyte concentration of 0.01 M NaCl. HPMM-1 and -2 were prepared
695 using psyllium binders from different suppliers. The WTR-8.5% data series was obtained
696 by multiplying q values for WTR by 0.085.

697

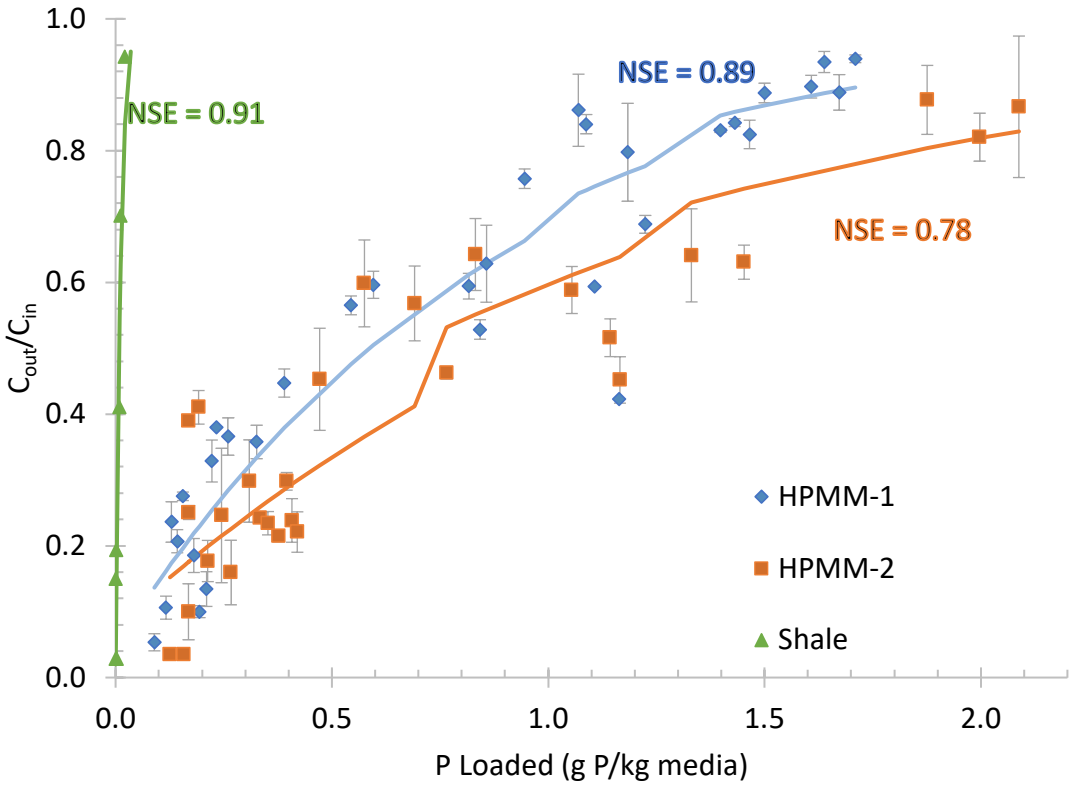

698

699 Figure 2-4. Influent-normalized TDP concentrations in columns continuously fed with
700 synthetic stormwater as specified in Table 2-1. Flow rate was held at 1.2 mL/min (15
701 cm/h) for 10 weeks, increased to 2.1 mL/min (25 cm/h) for 3 weeks, then to 2.8 mL/min
702 (35 cm/h) for 1 week for HPMM-1 and 4 weeks for HPMM-2, respectively. Lines are
703 modeled data (Equation 2-13).

704

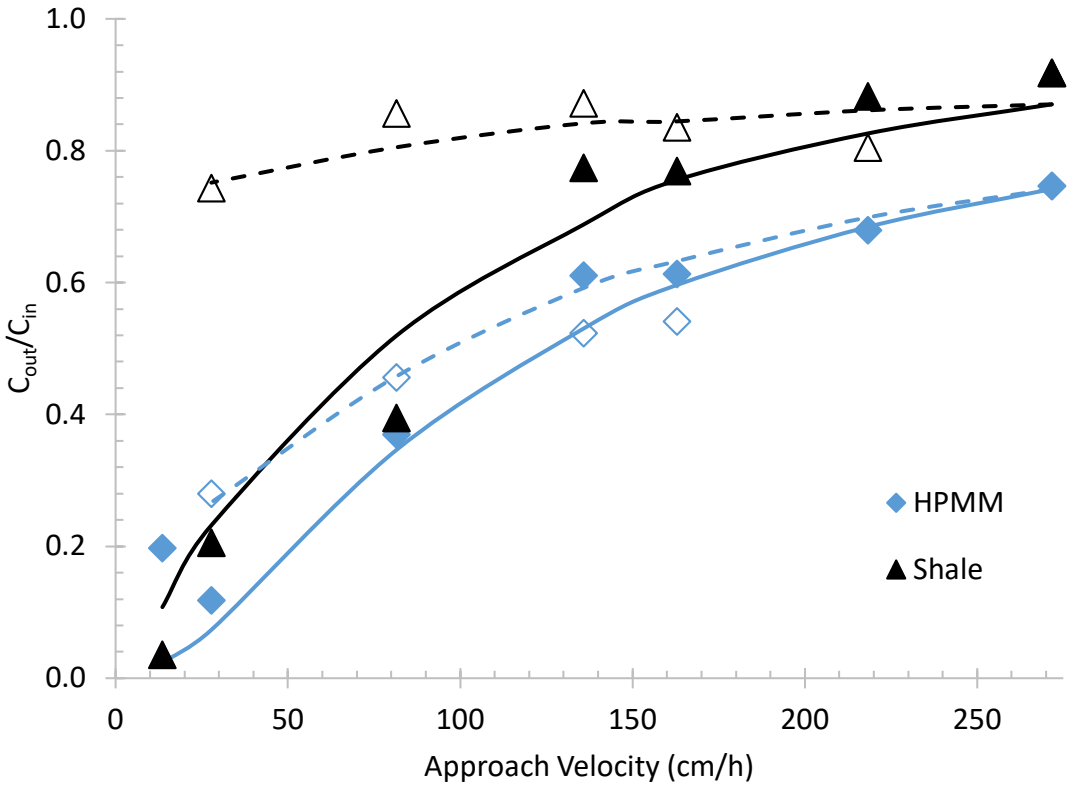

705

706 Figure 2-5. Effect of approach velocity on P removal in mini-columns containing 25 cm^3
707 of media. Synthetic stormwater containing 0.2 mg/L P and 500 mg/L NaCl at pH = 7
708 was applied. Lines are modeled data (Equation 2-13). Solid points and lines indicate
709 forward operation as flow rate was stepped up as the test proceeded. Open points and
710 dashed lines indicate reversed operation as flow rate was stepped down as the test
711 proceeded.

712

713

714 Table 2-1. Synthetic stormwater composition used in batch equilibrium, continuous-flow
715 column, and flow-modified column experiments.

Constituent	Batch Equilibrium	Long-term Column	Flow-modified Column
Solvent	DI water	DI water	DI water
Phosphorus (KH_2PO_4)	0.0-10.0 mg/L as P	0.2 mg/L as P	0.2 mg/L as P
Inorganic Nitrogen ($NaNO_3$)	-	1 mg/L as N	-
Organic Nitrogen (Glycine)	-	2 mg/L as N	-
NaCl	584 mg/L	500 mg/L	500 mg/L
Sodium Acetate	-	1.3 mg/L as C	-
HCl and NaOH	-	As needed to adjust pH to 7	As needed to adjust pH to 7

716

717 Table 2-2. Parameters from Equation 2-13 fit to experimental data for long-term
718 continuous flow columns and flow-modified columns.

Media	Long-term Column		Flow-modified Column	
	β_0 (kg/g)	β_1 (h^{-1})	β_0 (kg/g)	β_1 (h^{-1})
Shale	85.4	14.5	129	3.66
HPMM-1	1.10	7.25		
HPMM-2	0.646	4.97	26.7	3.94

719

720

Chapter 3: Mesocosm-Scale Studies

Evaluation of an Enhanced Stormwater Treatment Media and Permeable Pavement Base under Simulated Rainfall

Introduction

As society places increased value on maintaining high-quality water resources in and around urban areas, the impetus to protect these surface waters from pollution likewise increases. Stormwater runoff is an important avenue for pollutant transport from impermeable surfaces to surface waters. Consequently, stormwater control measures (SCMs) are increasingly designed to manage flood risk and to reduce pollutant loadings (NRC 2008). Permeable pavements – including porous asphalt, pervious concrete, and interlocking concrete pavers – are one of the primary stormwater best management practices (BMPs) that have been implemented and researched over the past two decades to mitigate hydrologic and water quality impacts of urbanization (Weiss et al. 2017).

Waterborne pollutants can be removed by SCMs via several mechanisms. Sedimentation and filtration effectively remove suspended solids and much of the load of particulate-bound pollutants, which can include bacteria, particulate phosphorus (PP), ammonium and organic nitrogen (N_{org}), metals, and toxic organic compounds (Li and Davis 2008; Clark and Pitt 2012). Dissolved constituents often require additional treatment processes to achieve water quality goals (Lefevre et al. 2015). Performance data from the International Stormwater BMP Database (Clary et al. 2017) show effective treatment in permeable pavements of total suspended solids (TSS), total phosphorus (TP), total Kjeldahl nitrogen (TKN) and certain total metals, including total Cd, Cu, and Pb.

744 The same analysis showed increases or no significant change in concentrations of
745 dissolved phosphorus (DP), orthophosphate, nitrate (NO_3) plus nitrite (NO_2), and certain
746 dissolved metals including dissolved Cd, Cu, Fe, and Pb.

747 DP can be removed from stormwater via adsorption to reactive surfaces. Several
748 studies have investigated the potential for enhanced treatment media to improve DP
749 retention in SCMs (Erickson et al. 2007; O'Neill and Davis 2011; Penn at al. 2017).
750 Nitrate can be removed to the atmosphere through the microbially-mediated process of
751 denitrification. To achieve denitrification, reducing conditions and available carbon as an
752 electron donor must be present to convert NO_3 into nitrous oxide (N_2O) and nitrogen gas
753 (N_2). Previous studies have implemented an internal water storage (IWS) zone to create
754 reducing conditions and advance denitrification in SCMs (Kim et al. 2003; Winston et al.
755 2016). Dissolved metals can complex with organic matter (OM) or other adsorbents,
756 including WTR (Brown et al. 2007; Li and Davis 2008a; Castaldi et al. 2015).

757 To improve dissolved pollutant retention in permeable pavements, a novel
758 treatment media was developed as described in Chapter 2. This structural treatment
759 media, dubbed High Permeability Media Mixture (HPMM), was designed as a permeable
760 pavement base material capable of retaining DP in stormwater. Laboratory studies from
761 Chapter 2 showed effective DP retention using HPMM, but further study is required with
762 the goal of assessing HPMM treatment performance under more realistic conditions
763 (rainfall simulations) and to determine the potential of the material to leach or retain N
764 and metals. The following objectives were identified to achieve this goal.

1) Evaluate phosphorus (P), nitrogen (N), and metals retention onto HPMM in rainfall simulations, with the hypothesis that HPMM will achieve effective P and metals removal but will not significantly retain N.
2) Analyze the influence of simulated rainfall intensity and pH on DP treatment, with the hypothesis that DP retention is negatively correlated with rainfall intensity and pH.
3) Compare pollutant removal for HPMM prepared using two different WTR sources, testing the hypothesis that WTR containing activated carbon will achieve greater N retention.
4) Investigate the potential for an IWS zone to enhance N removal via denitrification, to support the hypothesis that reducing conditions can be created in an IWS to advance denitrification and remove N.

Methods and Materials

High Permeability Media Mixture

HPMM comprises aluminum-based water treatment residual (WTR), expanded shale lightweight aggregate (shale), and a psyllium-based soil binder (psyllium). WTR used in this study was collected from two sources. The first WTR was sourced at a moisture content (MC) of 3.22 ± 0.17 g wet/g dry (69 ± 2 %) from the Dalecarlia drinking water treatment plant in Washington, D.C. The second WTR was sourced from an Aqua America drinking water treatment plant in Philadelphia, PA at a MC of 3.51 ± 0.11 g wet/g dry (71 ± 1 %). Both WTRs were sieved through a 2.00 mm sieve, then air dried for at least one week to MC = 1.21 ± 0.01 g wet/g dry (17 ± 1 %) and powdered by

hand. The Dalecarlia (WTR-D) and Aqua America (WTR-AA) WTRs are aluminum-based, resulting from the coagulation and flocculation process using alum addition. The Aqua America treatment plant also adds activated carbon and polymer along with alum, which settle out in the WTR. Haydite "B" size expanded shale (DiGeronimo Aggregates, Cleveland, OH), graded between 2.38 (No. 8 sieve) and 9.5 mm (3/8 in) was used in this application and *Stabilizer* (Stabilizer Solutions, Phoenix, AZ) was used as a psyllium-containing binder.

The mix ratio used to prepare HPMM is such that each kg contains 905 g shale, 85 g WTR, and 10 g psyllium by oven-dry mass. HPMM used in this study was prepared with air-dry WTR at a MC of 1.2 g wet/g dry. Accounting for MC, component quantities per kg of HPMM were measured as 890, 100, and 10 g of shale, WTR, and psyllium, respectively. Different mix preparation methods were tried, but not tested in rainfall simulations, to improve WTR coating and binding to the shale surface. More even coating and effective binding, based on visual inspection, was achieved by mixing components moist, rather than first drying and powdering WTR. This preparation method requires weighing components at as-received MC. For MC = 3.2 g wet/g dry for WTR-D, each kg of HPMM contains 760, 230, and 10 g of shale, WTR, and psyllium, respectively.

Amorphous Al, Fe, and P were extracted from HPMM and WTR using an oxalate extraction procedure from McKeague and Day (1966) as described in Chapter 2. Extraction results for HPMM-D (HPMM prepared with WTR-D), WTR-D, and WTR-AA are shown in Table 3-1. No extraction was performed on HPMM-AA (HPMM

prepared with WTR-AA). Oxalate Ratio (OR) is defined as the ratio of oxalate-extractable (i.e., amorphous) Al + Fe to P (in mmol/kg).

Table 3-1. Amorphous Al, Fe, and P content and OR of HPMM and WTR.

	HPMM-D	WTR-AA	WTR-D
Al (mg/kg dry media)	10700 ± 1500	57100 ± 1250	70900 ± 8430
Fe (mg/kg dry media)	925 ± 213	4410 ± 92.9	3740 ± 382
P (mg/kg dry media)	47.5 ± 8.50	693 ± 20.4	828 ± 199
Al (mmol/kg dry media)	398 ± 55.6	2120 ± 46.3	2630 ± 313
Fe (mmol/kg dry media)	34.3 ± 7.90	163 ± 3.44	138 ± 14.1
P (mmol/kg dry media)	1.53 ± 0.274	22.4 ± 0.657	26.7 ± 6.41
OR	282	102	103

Rainfall Simulation Mesocosm

A mesocosm-scale experiment was established to mimic storm events under representative local rainfall conditions for College Park, MD. Two mesocosms were setup inside 0.31 m^2 water-tight boxes (51 x 61 cm). Three parallel perforated PVC drainage pipes were placed at the bottom of each box for effluent sampling. Approximately 1.5 cm of water-washed pea gravel filled the space around and to the top of the drainage pipes and a 5 cm layer of HPMM was placed on top of the pea gravel layer. HPMM used in mesocosm testing was determined to have bulk density of 0.72 g/cm^3. Each mesocosm, therefore, contained 0.015 m^3 and 11.1 kg of HPMM. HPMM prepared with WTR-D (HPMM-D) was placed in Box 1 and HPMM prepared with WTR-AA (HPMM-AA) was placed in Box 2. A single PaverGuide^{TM} grid was then placed over the HPMM layer. PaverGuide^{TM} is a proprietary geosynthetic product which can replace the typical stone base in permeable pavements (PaverGuide 2018).

828 Rainfall was simulated using misting devices, positioned at the top corners of
829 each box and fed by individual flow lines using peristaltic pumps. Synthetic stormwater
830 was prepared by adding representative urban runoff constituents to tap water (Table 3-2).
831 No additional P was added as the tap water was found to contain levels approximately
832 equal to those reported in stormwater runoff (Pitt and Maestre 2005). This experimental
833 design simulates rainfall applied directly to a pavement surface (i.e., no run-on flow) at
834 different rainfall intensities. Water infiltrated into a permeable pavement from direct
835 rainfall would contain only the pollutants washed from the pavement surface. Past
836 studies have shown pollutant accumulation on pavements to be site-specific and to vary
837 with use (Gilbert and Clausen 2006; Dietz 2007; Hunt 2010). Therefore, the urban runoff
838 constituents used here are a reasonable approximation of expected rainfall infiltrate
839 composition.
840 Three sets of storm simulations were carried out. The first set consisted of 12
841 simulations conducted on Box 1 containing HPMM-D (configuration D). The second set
842 of 12 simulations was conducted on Box 1, containing HPMM-D (configuration D-IWS),
843 and Box 2, containing HPMM-AA (configuration AA), simultaneously. For the second
844 set, the outflow tube in Box 1 was elevated to maintain the water level inside the
845 mesocosm at the top of the HPMM layer, thus creating a 5-cm IWS zone. Each storm
846 was conducted under a unique combination of rainfall intensity, i, (0.66 ± 0.02, $1.34 \pm$
847 0.06, 1.95 ± 0.05, or 2.62 ± 0.10 cm/h) and influent pH (5.97 ± 0.12, 6.96 ± 0.08, or 8.03
848 ± 0.07), both of which were held constant throughout each simulation. In the third set, an
849 additional 5 storm simulations were carried out on Box 1 and 2 simultaneously. This set
850 consisted of storm simulations conducted for the purpose of testing reproducibility of

results and to investigate effects of varying influent P and C concentrations. For all simulations, influent spray from misting devices was captured in a graduated cylinder to measure *i*. Simulations were conducted regularly to maintain an average antecedent dry period of 11 ± 8 days (range 4-46 days).

For each simulation, 4-12 effluent samples were collected at even intervals, apart from Sample 1 which was collected as outflow first occurred. The delay between the start of influent and effluent flow indicates some amount of storage within the mesocosm setup, likely in the bottom of the box and in moisture retained by the HPMM. As noted by the as-received moisture content, WTR can retain significant water, above a 3:1 wet to dry mass ratio. At least 12 L of influent was used in each simulation, resulting in 6-, 4-, and 3-hour storm durations. Samples were analyzed for pH, TP, TDP, TN, NH_4-N, NO_3-N, NO_2-N, and total Al, Cu, Fe, Pb, and Zn as detailed below. Event mean concentration (EMC) is defined as:

$$EMC = \frac{\int_{t_i}^{t_f} Q(t) \cdot C(t) \cdot dt}{\int_{t_i}^{t_f} Q(t) \cdot dt} \quad (3\text{-}1)$$

where C(t) = concentration in sample collected at time t, Q(t) = flow rate at time t, and t_i and t_f represent time at the start and end of flow, respectively. The integral was approximated using the trapezoidal rule. EMC for pH was calculated by converting individual pH measurements to H^+ ion concentration ([H+]), inputting [H^+] into Equation 3-1, and converting the EMC back to pH units.

Table 3-2. Synthetic stormwater composition used in rainfall simulation experiments. Tap water was used as the solvent.

Constituent	Concentration
Phosphorus[1]	0.25 ± 0.035 (0.19-0.30) mg/L as P
Inorganic Nitrogen ($NaNO_3$)	1 mg/L as N
Organic Nitrogen (Glycine)	2 mg/L as N
NaCl	100 mg/L
$CaCl_2$	80 mg/L
Sodium Acetate	1.3 mg/L as C
Copper ($CuCl_2$)	0.06 mg/L as Cu
Zinc ($ZnCl_2$)	0.5 mg/L as Zn
HCl and NaOH	As needed to adjust pH
$NaHSO_3$ (for dechlorination)	2.2 mg/L

[1] Values reflect P concentrations present in tap water with no additional P added.

Analytical Procedures

Sample pH was measured using a glass electrode probe with Ag/AgCl reference to an accuracy of 0.01 units (Mettler Toledo MA235, Greifensee, Switzerland). TP and TDP concentrations were determined by potassium persulfate digestion and the ascorbic acid molybdenum blue colorimetric method from Standard Method 4500-P (APHA et al. 2012). TDP samples were first filtered through a 0.22 μm ceramic filter. Absorbance was measured using a 5 cm path-length cuvette in a UV-Visible spectrophotometer (UV160U, Shimadzu, Kyoto, Japan) at 880 nm to yield a detection limit of 0.01 mg/L P. Exceptions to this were samples from oxalate extractions, which were analyzed for TDP using a method modified from Wolf and Baker (1990) and analyzed at 660 nm to a detection limit of 0.01 mg/L P.

TN was measured using a Total Organic Carbon Analyzer with Total Nitrogen Measuring Unit (TOC analyzer, Shimazdu, Kyoto, Japan) with a detection limit of 0.05 mg/L as N. NH_4-N concentrations were measured using the phenate method from Standard Method 4500-NH_3 (APHA et al. 2012). Absorbance was measure with a 1 cm

path length cuvette at 640 nm in a UV-Visible spectrophotometer to a detection limit of 0.05 mg/L as N. Samples were filtered through a 0.22 µm ceramic filter prior to NO_3 and NO_2 analysis. NO_3-N was measured using ion chromatography (ICS-1100, Dionex, Sunnyvale, CA) following Standard Method 4110. A 4.5 mM Na_sCO_3 and 1.4 mM $NaHCO_3$ eluent solution was run isocratically through an anion-exchange column with 150 mm length, 4 mm ID, and 6.5 µm particle size (IonPac AS22 Fast IC column, Dionex, Sunnyvale, CA) at a flow rate of 1.2 mL/min. The detection limit was 0.1 mg/L as N. NO_2-N was analyzed colorimetrically in a UV-Visible spectrophotometer at 543 nm following Standard Method 4500-NO_2^- (APHA et al. 2012) with a 1 cm path length cuvette to a detection limit of 0.01 mg/L as N. NO_2-N consistently accounted for less than 3% of total N and is excluded from discussion.

Total Al, Cu, Fe, Pb, and Zn concentrations of samples acidified with trace metal grade nitric acid were measured using inductively coupled plasma atomic emission spectroscopy (ICP-AES) (ICPE-9000 Plasma Atomic Emission Spectrometer, Shimazdu, Kyoto, Japan) at wavelengths of 394.403, 324.754, 259.940, 220.353, and 213.856 nm, respectively. The detection limit for Al, Fe, and Pb was 25 µg/L and for Cu and Zn the limit was 10 µg/L. Values below corresponding detection limits for all parameters have been assigned following the probability plot method from Helsel and Hirsch (2002). The Mann-Whitney U test was employed to determine statistically significant difference between summary statistics at 95% confidence level ($\alpha = 0.05$).

Results and Discussion

Phosphorus

Measured influent and effluent TDP concentrations for storm simulations are

913 presented in Figure 2-1. Effluent TDP concentration was lower than influent for all
914 samples. To assess overall performance, TDP EMCs for each set of 12 storms were
915 grouped by configuration and are presented in Figure 2-2. Effluent TDP EMC was
916 observed between 0.01 and 0.15 mg/L P, while event removal efficiency ranged from 48
917 to 98%. The mean TDP EMC for each configuration was significantly lower in effluent
918 compared to influent, while no significant difference in effluent was observed among
919 configurations. Effluent TDP EMC concentrations were below the EPA recommended
920 0.03656 mg/L TP for rivers and streams in ecoregion XIV (USEPA 2000) for all but one
921 storm at i = 0.66 cm/h. This i is just lower than the 1-yr average return interval (ARI)
922 event-averaged storm intensity for a 6 h storm for College Park, MD of 0.8 cm/h (Bonnin
923 et al. 2006). It also exceeds the rainfall intensity of at least 61% of Maryland storms
924 analyzed by Kreeb (2003). The data, therefore, support the hypothesis that HPMM can
925 achieve effective P retention for storm intensities in this range, with respect to DP. TP
926 was measured in a subset of samples and was consistently 10% greater than TDP. If TDP
927 EMC results are increased by 10%, all but one storm event at i = 0.66 cm/h still fall
928 below the EPA-recommended level.

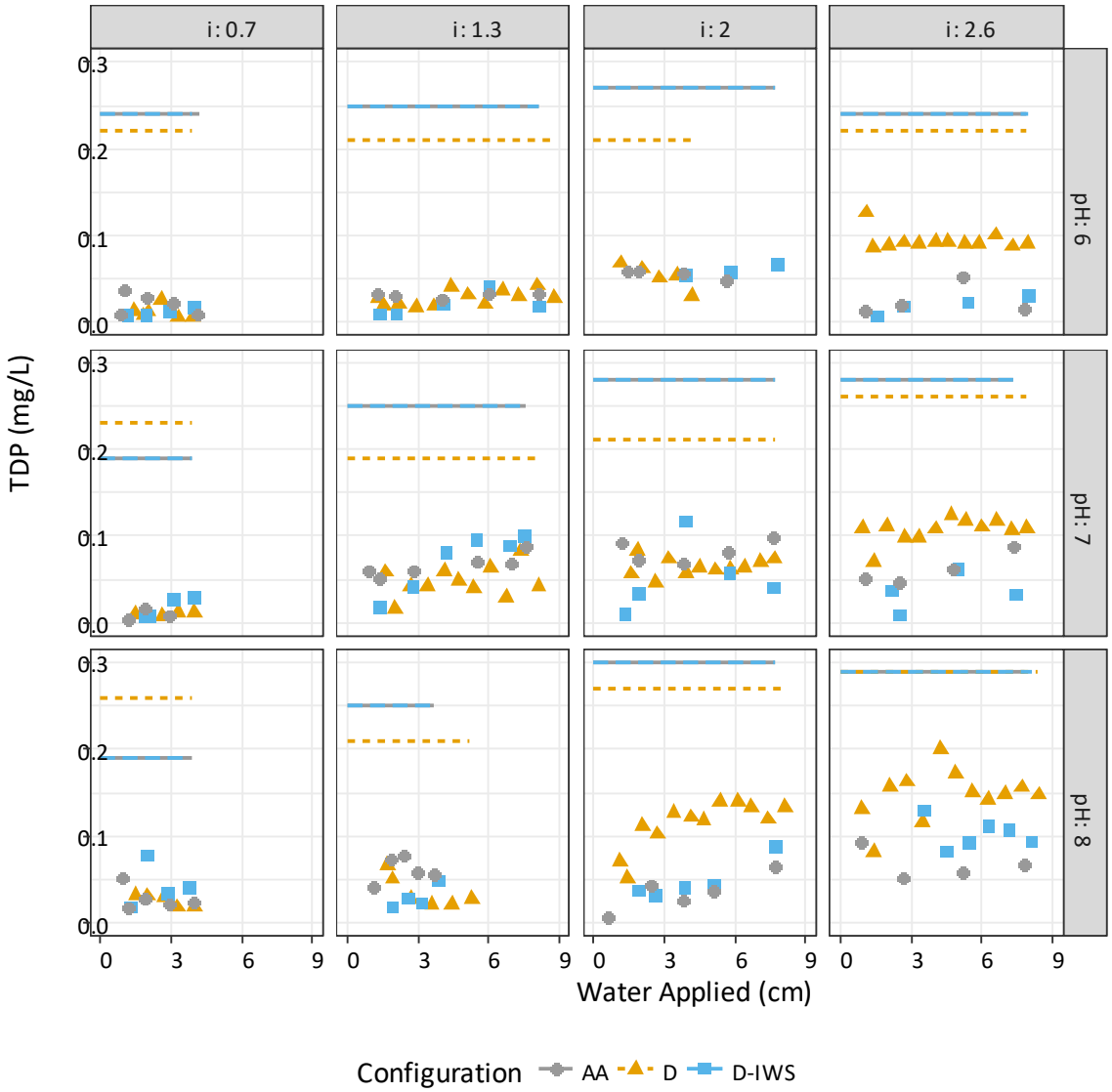

929

930 Figure 3-1. Measured TDP concentrations for 36 storm simulations (12 for each
931 configuration). Synthetic stormwater influent (Table 3-2), indicated by solid lines, at
932 0.25 ± 0.035 mg/L P was applied to a 5-cm base layer of HPMM under one of three
933 different configurations: using HPMM-D (D), HPMM-AA (AA), or HPMM-D with an
934 IWS (D-IWS). Each storm was run at one of four rainfall intensities, *i* (0.7, 1.3, 2.0, or
935 2.6 cm/h), and one of three pH values (6.0, 7.0, or 8.0).
936

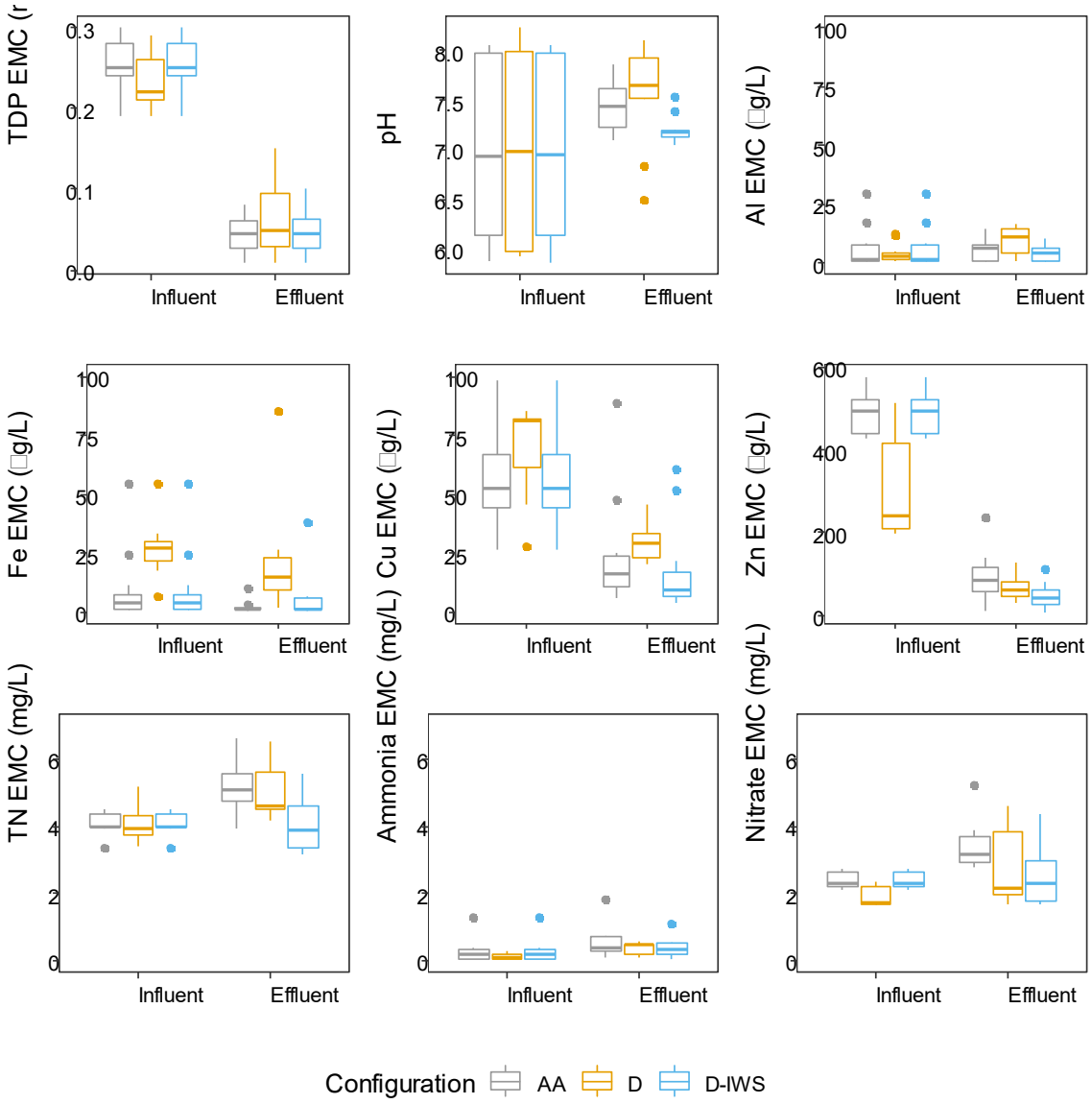

Figure 3-2. Summary of EMC results from 36 storm simulations on a mesocosm containing a 5-cm HPMM layer. Central bars indicate the median of EMCs. Lower and upper extents of the boxes indicate the 1st (Q1) and 3rd (Q3) quartiles, respectively. The interquartile range (IQR) is defined as Q3 – Q1 and the lower and upper extents of the lines indicate Q1 – 1.5·IQR and Q3 + 1.5·IQR, respectively. Points outside the lines are outliers.

A trend toward lower effluent TDP EMC at lower rainfall intensity is apparent for configuration D ($R^2 = 0.772$) (Figure 3-3a). The coefficient of determination (R^2) indicates the percentage of the variation in the variable on the y-axis that can be attributed to variance in the variable on the x-axis. A high R^2 value indicates a strong

950 linear relationship between the two variables (McCuen 2005). A positive linear
951 relationship between TDP EMC and rainfall intensity is also present, but weaker, for
952 configurations AA ($R^2 = 0.356$) and D-IWS ($R^2 = 0.169$). This supports the hypothesis
953 that DP retention will decrease as rainfall intensity increases. Weaker correlation
954 between TDP EMC and rainfall intensity for configuration D-IWS is likely due to
955 differences in the flow regime of this configuration. Because the outlet is elevated, water
956 saturates the media layer following each storm and remains there until the start of the
957 next storm. As new influent is applied, water retained from the previous storm is pushed
958 out of the outlet. Contact time for this "old" water with the media is a function of the
959 time between storms rather than the rainfall intensity of the current storm simulation.
960 Additionally, flow in the D-IWS configuration is under saturated conditions, in contrast
961 to the D and AA configurations for which flow is through unsaturated media. These
962 differences in flow regime appear to result in a damping of the effect of rainfall intensity
963 on DP retention in the D-IWS configuration.
964 The coefficients of determination indicate a weak positive correlation between
965 effluent TDP EMC and flow-weighted event mean effluent pH for configurations AA and
966 D-IWS ($R^2 = 0.070$ and $R^2 = 0.193$, respectively) and a very weak negative correlation
967 for configuration D ($R^2 = 0.002$) (Figure 3-3b). The scatter and distribution in Figure 3-
968 3b indicate that the relationship between effluent TDP EMC and effluent pH EMC is
969 influenced by extreme points in the data set presented or may not be a linear relationship.
970 Phosphate is a triprotic acid and its speciation is pH dependent, with $H_2PO_4^-$ and HPO_4^{2-}
971 being the predominant dissolved species at pH typical of urban runoff, 7.50 ± 0.75
972 (Stumm and Morgan 1996; Pitt et al. 2004). At this pH, electrical double-layer effects

influence phosphate adsorption onto alumina surfaces, as shown by Chen et al. (1973). Higher pH causes the alumina surface to be more negatively charged, increasing the repulsive force acting on negatively charged $H_2PO_4^-$ and HPO_4^{2-}. Adsorption of anions is also a competitive process. Surface complexation (i.e., adsorption) of phosphate species onto metal hydroxides occurs primarily through ligand exchange, where phosphate anions replace hydroxyl (OH^-) ions bound to the adsorptive surface. Greater OH^- ion concentration at higher pH can result in reduced adsorption of phosphate (Brattebo and Odegaard 1986; Stumm and Morgan 1996). Thus, it was expected that P retention would decrease with increased pH. Some of the correlation between effluent TDP and effluent pH may have been masked by the relatively stronger effect of rainfall intensity on effluent TDP, particularly for configuration D, for which TDP and *i* were highly correlated.

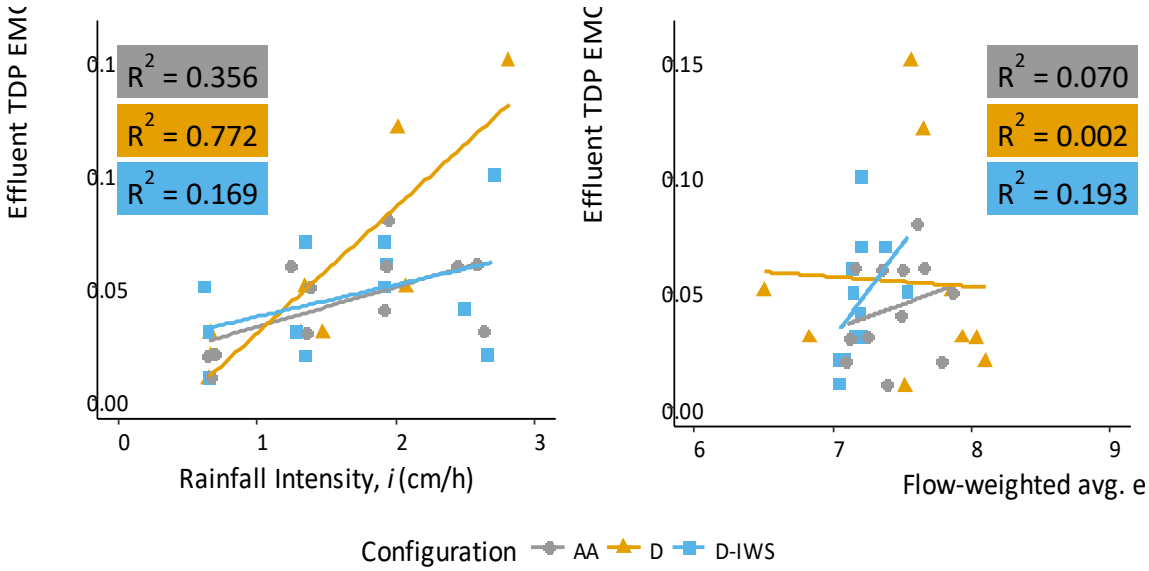

Figure 3-3. Relationship between effluent TDP EMC and (a) rainfall intensity and (b) effluent pH for 36 storm simulations across 3 mesocosm configurations using a 5-cm HPMM base layer.

A model developed in Chapter 2 to describe DP retention by HPMM was employed to mesocosm data from the present study to control for differences in rainfall intensity across storm simulations. The model, shown in Equation 3-2, was developed based on long-term column testing for DP retention in which a scaled-down (shale < 2 mm) version of the HPMM used in the present study was subjected to continuous flow of synthetic stormwater.

$$\frac{C_{out}}{C_{in}} = 1 - e^{-\beta_0 \Sigma M} + e^{-\left(\beta_0 \Sigma M + \beta_1 \frac{V_m}{Q}\right)} \quad (3\text{-}2)$$

β_0 in Equation 3-2 is a long-term parameter related to the adsorption capacity of the media. β_1 is a short-term parameter related to the adsorption kinetics and media reactive surface area. Equation 3-2 can be rewritten by expressing retention time, $\bar{t} = \frac{V_m}{Q}$, in terms of media depth, d, and rainfall intensity, *i*.

$$\frac{C_{out}}{C_{in}} = 1 - e^{-\beta_0 \Sigma M} + e^{-\left(\beta_0 \Sigma M + \beta_1 \frac{d}{i}\right)} \quad (3\text{-}3)$$

This conversion assumes infiltration rate is equal to rainfall intensity, which holds true if there is no ponding and rainfall intensity is less than saturated hydraulic conductivity. HPMM hydraulic conductivity was measured in Chapter 2 to be 324 cm/h, which is an order of magnitude greater than the 1000-year ARI 5-minute duration precipitation intensity estimated for College Park, MD (Bonnin et al. 2006). If infiltration rate is restricted by underlying soil or outlet control in an underdrain, retention time can be expected to increase.

Equation 3-3 was used to calculate β_1 for the specific C_{out}, C_{in}, and *i* of each storm simulation using TDP EMCs. The P loading from the 12 storms was small enough not to significantly influence long-term loading, therefore ΣM was assumed to be zero. The

calculated β_1 values were plotted against flow-weighted event mean effluent pH (Figure 3-4). A stronger correlation between β_1 and pH is observed than was present for TDP EMC and pH for all configurations. β_1 relates to adsorption rates with higher values corresponding to faster adsorption. For all configurations, β_1 increases as pH decreases, indicating faster adsorption at lower pH. This result is consistent with previous studies showing greater phosphate adsorption to aluminum (hydr)oxide surfaces at lower pH (Chen et al. 1973; Goldberg and Sposito 1984; Tanada et al. 2003) and supports the hypothesis that DP retention will be greater at lower pH.

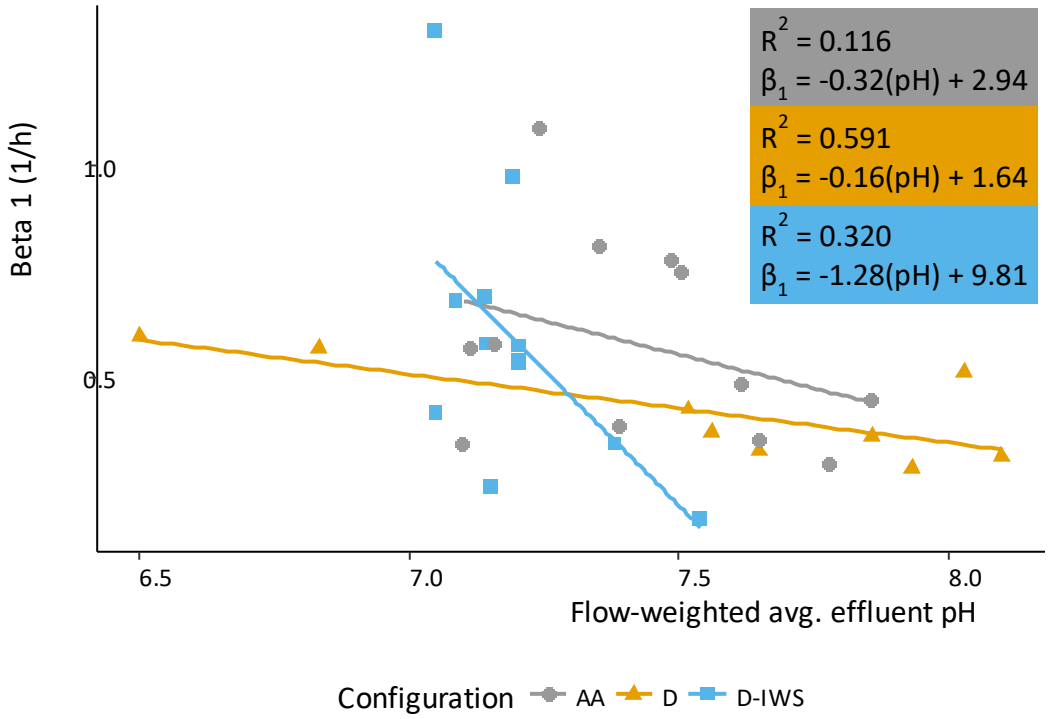

Figure 3-4. Data from 36 storm simulations in mesocosm testing with an 5-cm HPMM layer was input into Equation 3-3 to calculate β_1 values. The relationship between β_1 and effluent pH EMC is expressed by linear regression.

The effect of pH on adsorption kinetics was integrated into the model from Equation 3-3 using the linear equation of best fit from Figure 3-4 to yield Equation 3-4.

$$\frac{C_{out}}{C_{in}} = 1 - e^{-\beta_0 \Sigma M} + e^{-\left(\beta_0 \Sigma M + \beta_1^*(m(pH)+b)\frac{d}{i}\right)} \quad (3\text{-}4)$$

The model can now be fit to experimental data through the fitting parameters β_0 and β_1^*. Operational conditions and measured parameters (i.e., d, *i*, influent TDP EMC, flow-weighted mean effluent pH) for the 12 storm simulations were input into Equation 3-4 to predict effluent TDP EMC. Parameters m and b were taken from the linear best fit for each material as shown in Figure 3-4. Cumulative P loading, ΣM, was set to zero because loading from 12 storm simulations represents less than 1 m of rainfall loading, which is insignificant compared to the projected loading capacity of over 600 m before reaching P saturation of the media reported in Chapter 2 for long-term column studies. Because ΣM was set to zero for the mesocosm study, the value of β_0 is inconsequential. β_1^* was varied to find the best fit and the resulting model predictions are shown in Figure 3-5 with β values summarized in Table 3-3. Lower values of β_0 and greater values of β_1^* (and β_1) indicate greater DP retention.

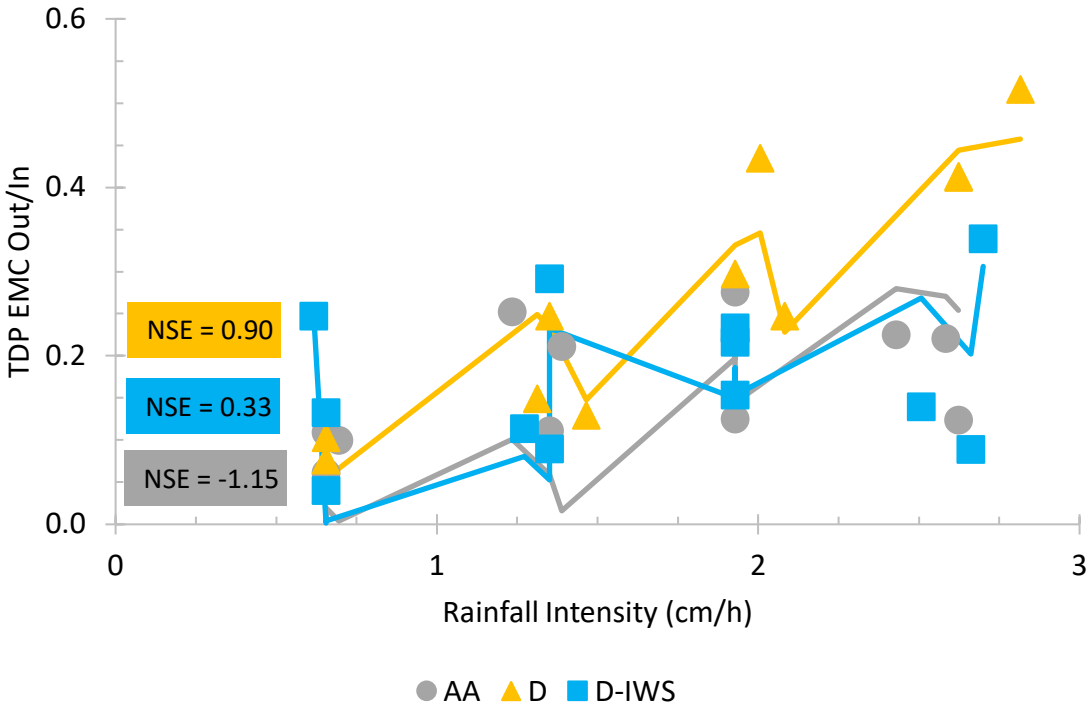

Figure 3-5. TDP retention plotted against rainfall intensity for 36 storm simulations (12 for each configuration) at rainfall intensities ranging 0.66 - 2.9 cm/h and pH ranging 6 - 8 for a mesocosm utilizing 5 cm of HPMM under three configurations. The model from Equation 3-4 was fitted to experimental data by varying β_1^* for each of the three configurations.

To test the ability of the model to predict effluent TDP concentrations, modeled effluent TDP EMCs from Equation 3-4 were compared with observed effluent TDP EMCs for 12 storm simulations at each of three configurations (Figure 3-6). Good agreement is noted between modeled and measured values for configuration D; the relationship was found to be 1 to 1, with an R^2 value of 0.90. The model generally overestimates effluent TDP for configuration AA and D-IWS, with lower correlation and R^2 = 0.25 and 0.52, respectively. This overprediction is particularly pronounced, as shown in Figure 3-5, at higher flow rates while the model underpredicts effluent TDP at lower flow rates for these two configurations. The result is a flatter TDP distribution

with respect to rainfall intensity than predicted by the model. This can be explained for the D-IWS configuration by the damping effect, as describe above, from the IWS zone. The AA configuration is less sensitive to changes in both rainfall intensity and pH than configuration D. This may be due to differences in the WTR source and composition.

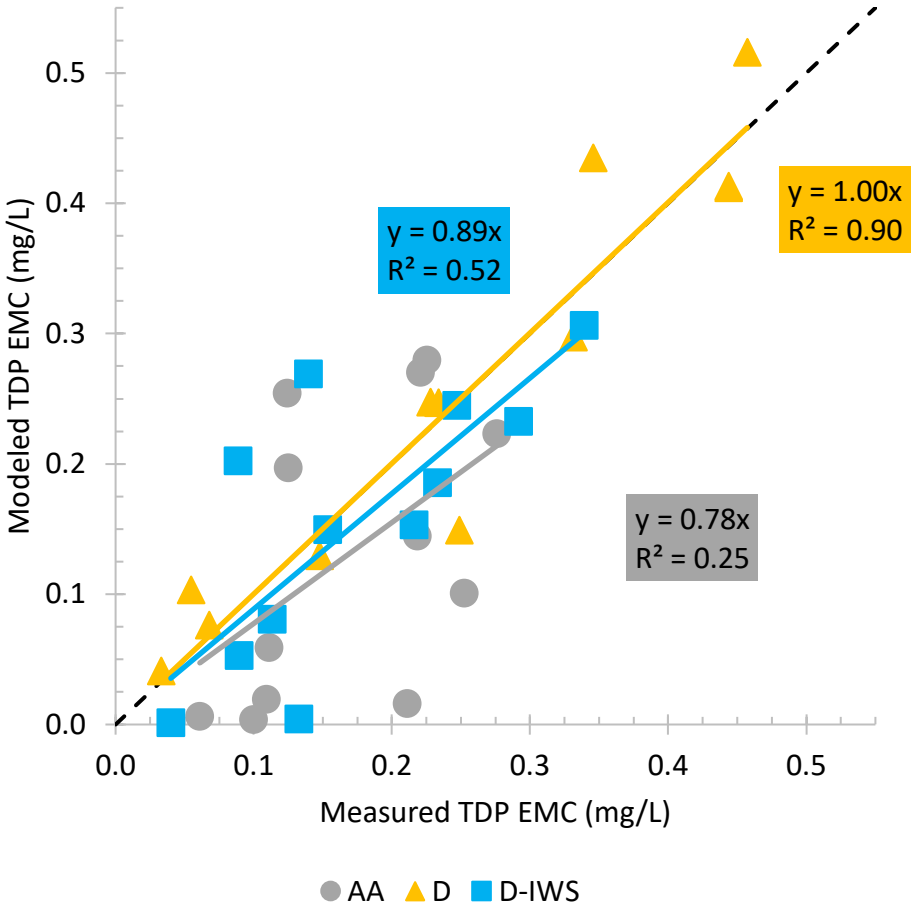

Figure 3-6. Modeled effluent TDP EMC from Equation 3-4 plotted against observed effluent TDP EMC for 12 mesocosm storm simulations. Parameter values used in the model reflected observed values for C_{in} (range 0.19 – 0.30 mg/L as P), *i* (range 0.66 – 2.9 cm/h), d = 5 cm and for influent pH in the range 5.86 – 8.23.

β_1^* and β_1 values in Table 3-3 cannot be compared directly between mesocosm and column testing because of differences in material size and flow conditions. In

column testing, shale measuring 2.0 mm in diameter was used, while the rainfall simulations used full-scale HPMM with 9.5 mm diameter shale. This created different void spacing throughout the media (i.e., different porosity) and transport distances. Additionally, column testing was conducted by pumping water through the media in an upflow direction. This resulted in saturated flow at a constant rate. In rainfall simulations, water was applied to the media surface and percolated by gravity through the media pore space, resulting in unsaturated flow. HPMM hydraulic conductivity is higher than the superficial flow velocities applied, so hydraulic retention time (HRT) or contact time was not limited by infiltration rate. Due to the unsaturated flow, HRT does not fully describe contact between the bulk fluid and the media surface. It was, however, shown above that rainfall intensity has a strong influence on DP removal in this system. It is thought that this influence is due to a combination of changes in advective and diffusional transport. As rainfall intensity increases, more of the void space becomes filled with water increasing transport distance from the bulk fluid to the adsorption surface.

Table 3-3. Parameters from Equations 3-3 and 3-4 fit to experimental data for long-term continuous flow columns (Chapter 2) and mesocosm rainfall simulations.

	Long-term Column	Mesocosm	
	β_0 (kg/g)	β_1 (h^{-1})	β_1^* (h^{-1})
Shale	85.4	14.5	
HPMM-1	1.10	7.25	
HPMM-D	0.646	4.97	1.03
HPMM-D-IWS			1.09
HPMM-AA			1.15

Design Tool - Model Application

The model from Equation 3-4 can inform design decisions for permeable paving installations using HPMM as a base material. Figure 3-7 shows predicted TDP removal

for a 5-cm base layer of HPMM-D at different loading ratios using assumptions representative of conditions in College Park, Maryland. Loading ratio is defined here as the ratio of contributing area to treatment surface area, with 1:1 representing a pavement treating only rainfall falling directly onto the pavement and higher ratios including adjacent areas contributing runoff to permeable pavement. A designer may use the tool to strike the desired balance between loading ratio, removal efficiency, and pavement lifetime. A uniform rainfall intensity of 1.27 cm/h (0.5 in/h) was used for the design tool. This intensity is representative of a 5-yr ARI, 6-h duration precipitation event in College Park, MD and is near the range of most frequently observed storm size and duration in Maryland based on analysis by Kreeb (2003). It is also representative of a storm intensity likely to generate sufficient throughflow. Because homogenous conditions are modeled over a long time period a range is given around the predicted removal efficiency by varying β_1^* ± 10% to account for short term fluctuations in removal resulting from variations in influent DP concentration, pH, rainfall intensity and more parameters that will vary from storm to storm. The model could potentially be expanded, with further data, to include other treatment media. This could enable better-informed decisions and improve estimates from watershed-scale models incorporating SCMs.

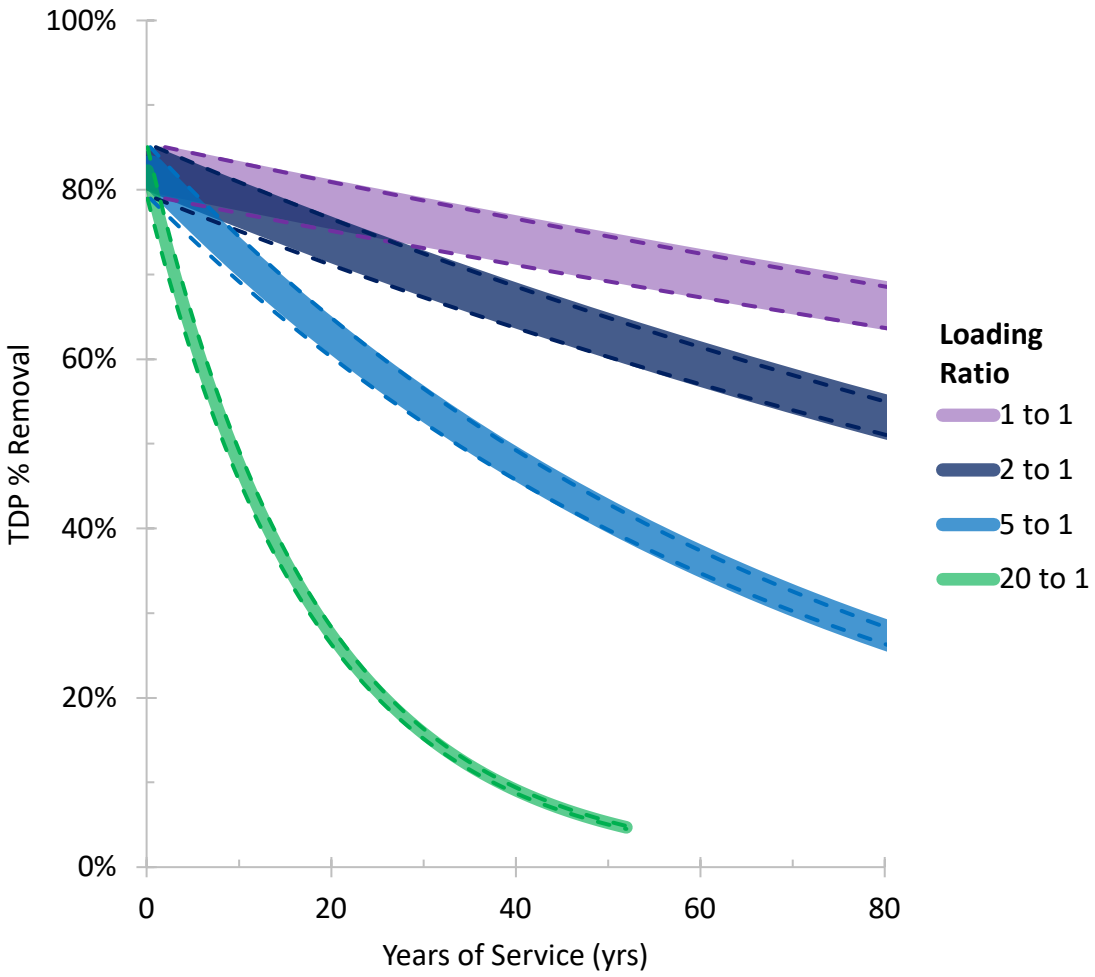

Figure 3-7. TDP removal efficiency by a 5 cm permeable pavement base layer of HPMM-D projected over years of service based on Equation 3-4. Assumptions: C_0 = 0.20 mg/L; rainfall intensity = 1.27 cm/h; pH = 7.5; annual precipitation = 1 m. Width of prediction bands result from varying β_1^* ±10% from best fit to represent a degree of uncertainty in the model prediction.

Nitrogen

Effluent N EMCs were higher than influent for configurations D and AA across all storm events simulated. This was true for TN, NH_4, and NO_3. Comparing a subset of 6 storm events for which N data are available across all three configurations, the mean of EMCs for TN increased from 4.10 to 5.06 mg/L for D, 4.04 to 5.19 mg/L for AA, and

4.04 to 4.09 mg/L for D-IWS (Figure 3-2). This increase was only significant for configuration AA ($p < 0.05$) when the Mann-Whitney U test was applied. The data do not support the hypothesis that configuration AA will improve N retention compared to configuration D. There was no significant difference in the means of effluent EMC TN, NH_4, or NO_3 for these two configurations. As hypothesized, inclusion of an IWS in configuration D-IWS did improve N treatment, but this effect was not consistent across all storm simulations.

Influent N was added as nitrate ($NaNO_3$) and organic N (glycine) in a 1:2 N ratio. Effluent N was dominated by nitrate under configurations D and AA (Figure 3-8). Effluent ammonium concentrations also increased slightly from influent. This indicates mineralization and nitrification likely occurred in these mesocosms, transforming organic N to NH_4 and ultimately to NO_3. Higher effluent TN concentrations are indicative of N leaching from the media. *Stabilizer* may be the source of some of this leached N. *Stabilizer* was dissolved in a 5% acetone solution and analyzed for TN and found to contain 61 ± 4 mg N per kg. WTR, however, is more likely the significant N source. Studies by others found WTR to contain up to 500 mg N/kg WTR (Dayton and Basta 2001; Lei and Davis 2018). At this concentration, HPMM is estimated to contain 42.5 mg N/kg of HPMM and each mesocosm box contains an estimated 472 mg N. This is approximately one third the influent load simulated by 100 cm of water applied, or one year of loading, with the synthetic stormwater containing 4 mg/L TN in the present study.

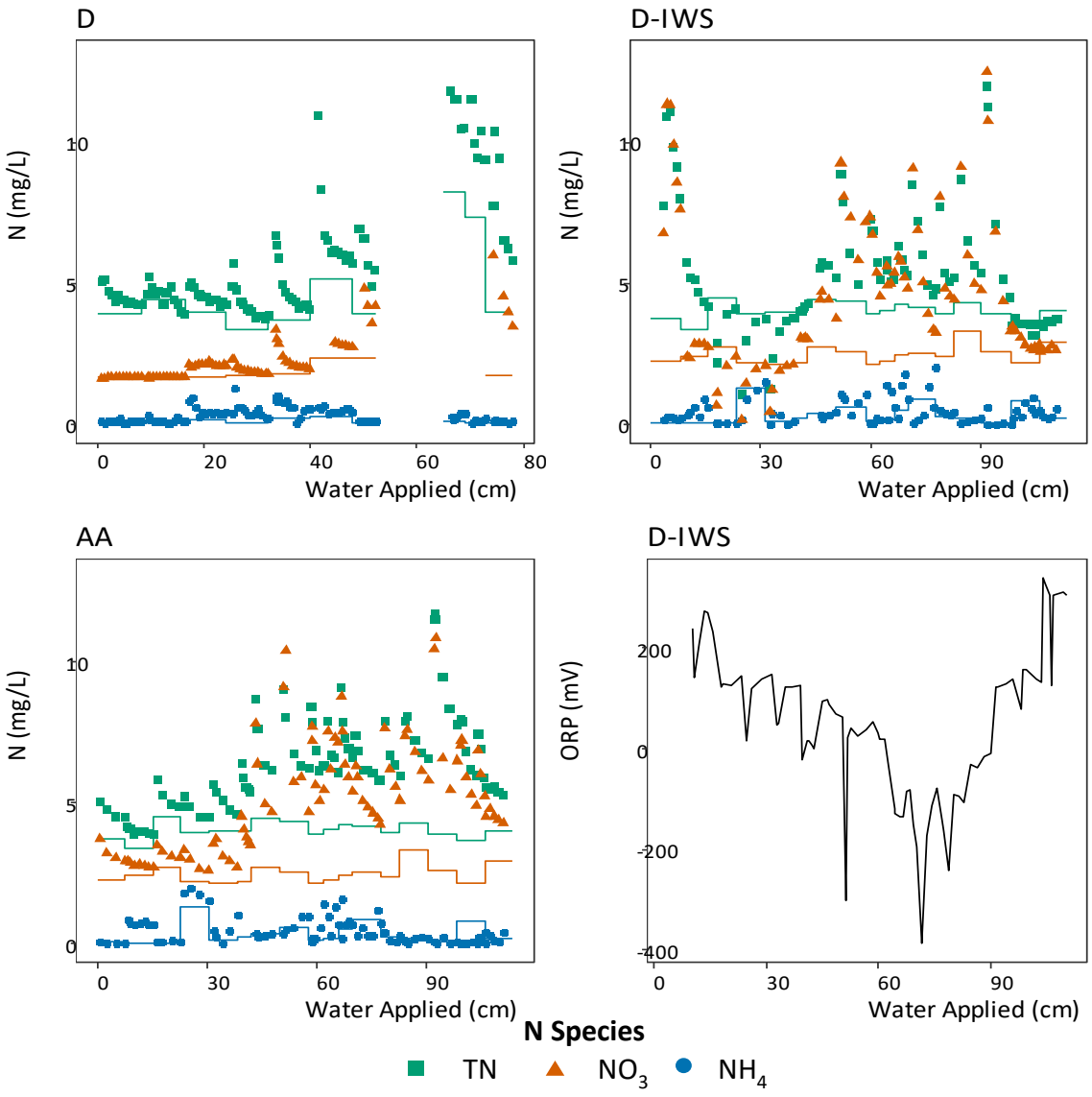

Figure 3-8. N results for configurations D, D-IWS, and AA in mesocosm testing using a 5-cm layer of HPMM. Lines indicate influent concentrations and points indicate effluent. ORP readings from effluent from D-IWS are also presented.

In configuration D-IWS, nitrification and N leaching was evident in 10 of 17 storm simulations (Figure 3-8), resulting in a 12% increase in TN load and 73% increase in NO_3 load over these 10 storms. NH_4 load decreased by 9% and organic N was below detection limit for all samples, represented by complete conversion in Figure 3-9. It is likely that much of this organic N reduction is due to conversion to nitrate. In 4

simulations, effluent TN and NO_3 concentrations were lower than influent (Figure 3-8). This is thought to have resulted from denitrification and been controlled by C availability. An initial period of putative denitrification occurred between the third and fifth storm events. Drift was observed in the oxidation-reduction potential (ORP) instrumentation, making it difficult to conclude whether reducing conditions were present or not in the D-IWS mesocosm. There is, however, a consistent trend on a storm-by-storm basis of ORP dropping between storm events, while the media was saturated, and increasing rapidly at the start of each storm, as oxygenated influent water flushed the old water from the IWS zone. Additional evidence of the presence of reducing conditions comes from metals data. Total Fe concentrations were below detection limit for all samples except those from the second storm simulation in configuration D-IWS, when the mesocosm is thought to have been transitioning from oxidizing to reducing conditions, and the initial denitrification period began. It is hypothesized that this period ended as the OM in the WTR was exhausted as a carbon source and the system became carbon limited. In the final two storms, influent C was increased by a factor of 10, to 13 mg/L as C. This stimulated a second denitrification period for the final storm, in which TN and NO_3 concentrations were again lower for effluent samples compared to influent. The resulting TN load decreased by 33% and NO_3 load decreased by 34% over the 4 storms in which denitrification is thought to have occurred (Figure 3-9). The mean of effluent TN EMCs for these 4 storms was 3.40 mg/L, which was significantly lower ($p \leq 0.05$) than the influent mean TN EMC, 4.11 mg/L, but still exceeds the EPA water quality criteria of 0.69 mg/L.

Figure 3-9 provides a comparative illustration of N transformations during periods with conditions unsuitable to advance denitrification and periods suitable for denitrification. In the former, TN total mass load increased from influent to effluent, with NO_3 constituting the major fraction of N species. In contrast, for the two periods in which denitrification is thought to have occurred, TN mass load decreased from influent to effluent. Organic N was also flushed through the mesocosm without conversion to NH_4 or nitrate during these periods.

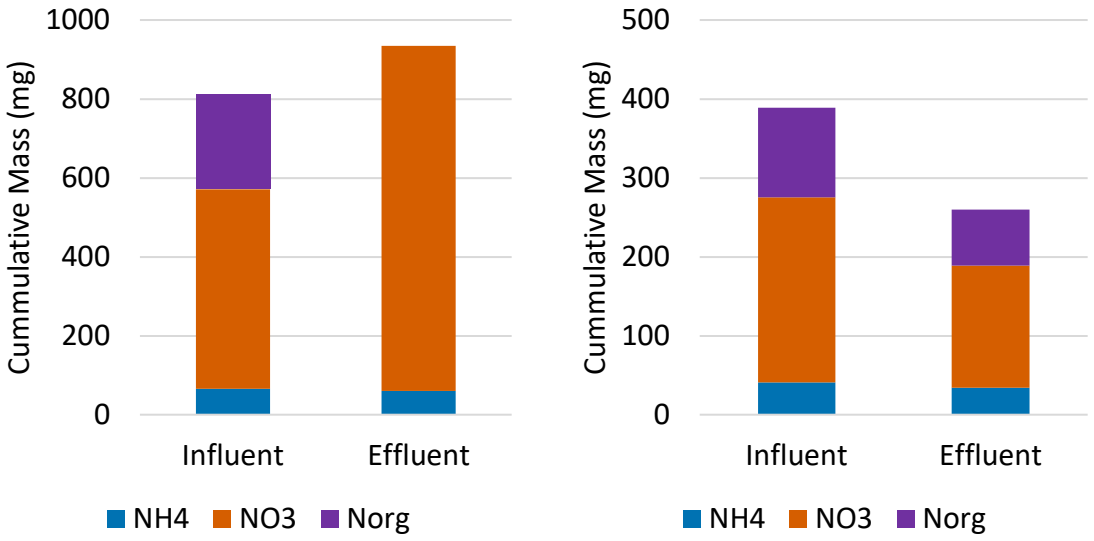

Figure 3-9. N species transformation in mesocosm influent and effluent through a 5-cm HPMM layer under the D-IWS configuration. Storm simulations were divided into those in which denitrification was thought to be (a) absent and (b) present.

Metals

The primary metal of concern for leaching from the test media is Al because HPMM uses Al-based WTR. Oxalate extractable (amorphous) Al content in WTR-D was measured at 70.9 g Al/kg WTR and WTR-AA was shown to contain 57.1 g Al/kg WTR. Mesocosm results indicate low potential for Al leaching under conditions

representative of stormwater runoff. The mean of total Al EMCs increased from 5 to 10 µg/L from influent to effluent in configuration D. This is a significant ($p \leq 0.05$) increase, however these concentrations are well below the EPA ambient water quality criterion for Al, 87 µg/L, for water at pH between 8.5 and 9.0 (EPA 1988). The increase was driven by a few individual effluent samples found in earlier storm events simulated in configuration D. The highest concentration, 123 µg/L, occurred in the first sample collected. All effluent samples from configurations AA and D-IWS had total Al concentrations below the 25 µg/L detection limit. It is likely the few elevated Al concentrations were due to initial wash-out of fines containing powdered WTR or shale from the newly established media rather than from Al being solubilized because pH remained between 6 and 8 for all effluent samples. Al solubility is approximately 9 µg/L ($10^{-6.5}$ M total Al) at pH in this range (Figure 3-10) (Stumm and Morgan 1996; Ippolito et al. 2011). Configuration AA, which was prepared later, did not demonstrate similar washout, possibly indicating the importance of mix preparation in binding fines into the media.

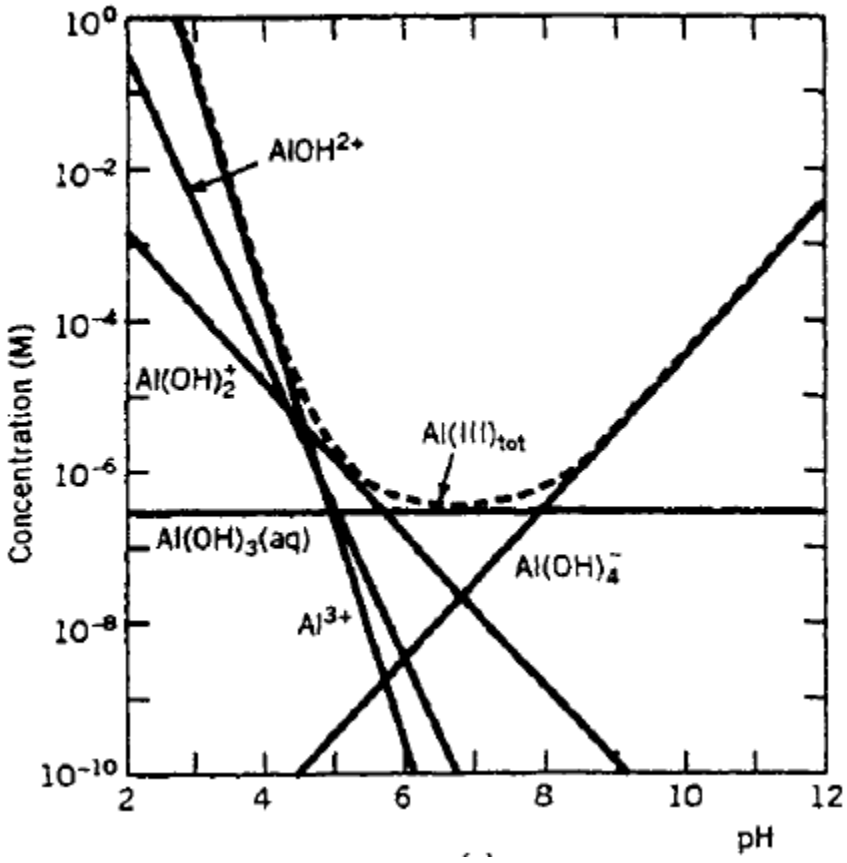

1207

1208 Figure 3-10. Solubility of Al-hydroxides at various pH. Total Al(III) solubility achieves
1209 a minimum in the pH range between 6 and 8. (Figure adapted from Stumm and Morgan
1210 1996)
1211

1212 Effluent total Fe and Pb concentrations were also very low, below 25 µg/L for all
1213 storm simulations and under all configurations. The mean of effluent EMCs was not
1214 significantly different ($p \leq 0.05$) from the mean of influent EMCs for any of the three
1215 configurations. The EPA sets ambient water quality criteria for Fe and Pb at 1000 and
1216 2.5 µg/L, respectively (EPA 1984; EPA 1986). Effluent Fe was far below this level. The
1217 water quality criterion for Pb is below the detection limit used in this study of 25 µg/L.
1218 Therefore, no conclusion can be made regarding attainment of this standard.

Influent was spiked with Cu and Zn to determine if HPMM can remove these potentially toxic water pollutants from stormwater. Results indicate effective and consistent Cu and Zn removal. The mean of EMCs was significantly lower ($p \leq 0.05$) for effluent compared to influent across all configurations for both metals (Figure 3-2). Effluent total Cu EMC averaged 30, 24, and 18 µg/L for configurations D, AA, and D-IWS, respectively. The mean of total Zn EMCs was 67, 92, and 47 µg/L for D, AA, and D-IWS configurations, respectively. The corresponding percent reductions are 59, 59, and 69% for Cu and 78, 81, and 90% for Zn under configurations D, AA, and D-IWS, respectively. The reductions are relative to overall mean influent concentrations of 61, 81, and 73 µg/L Cu and 255, 499, and 458 µg/L Zn for D, AA, and D-IWS, respectively. Water quality criteria for Cu are highly site and species specific, but typically are on the order of a few µg/L (EPA 2016). Zn levels in all three configurations were below the EPA criterion for acute toxicity to freshwater aquatic life of 133 µg/L (EPA 1996).

Metals toxicity can depend on water chemistry of the receiving water, including factors such as pH, hardness, alkalinity, and OM concentrations. The fraction of the metal in dissolved form can also be important as can specific species of concern in the local area. With these complications in mind, tentative conclusions can be made based on the results presented. HPMM does not present a concern for Al or Fe leaching under conditions typical of stormwater runoff. Pb leaching is also low and not likely a concern. HPMM can effectively and consistently reduce Cu and Zn concentrations. This reduction is sufficient to attain water quality standards for Zn, but is likely insufficient to meet very stringent Cu standards.

Conclusions

HPMM was shown effective at reducing DP and total metals concentrations in stormwater under simulated rainfall events. The media also demonstrated potential to reduce N concentrations by including an IWS zone if adequate C is available.

A 5 cm layer of HPMM reduced influent TDP concentrations from 0.25 mg/L to a maximum of 0.05 mg/L P for storm simulations with 0.66 cm/h rainfall intensity at pH between 5.86 and 8.23, typical of stormwater pH. For 9 simulations at this rainfall intensity, 8 fell below the EPA water quality criteria of 0.03656 mg/L for TP. This intensity is slightly lower than the 1-yr ARI for College Park, MD and likely exceeds the intensity of at least 2/3 of Maryland storms (Kreeb 2003).

HPMM did not remove N under aerobic conditions and may be a source of N export. Previous studies have been undertaken using WTR, but typically these have been in contexts with N export from other sources, masking N export from WTR specifically. An IWS zone was successful in decreasing effluent N when sufficient C was present to advance denitrification. WTR source had no impact on N retention.

Metals leaching potential is low based on the findings and under the conditions tested in this study (e.g., pH between 6 and 9). Fe and Pb concentrations were below the 25 µg/L detection limit for all effluent samples from HPMM. The media demonstrated effective and consistent retention of Cu and Zn, with effluent concentrations significantly lower than influent. Percent concentration reductions ranged 59-69% for Cu and 78-90% for Zn. Additional treatment may be necessary to further lower Cu concentrations to avoid toxicity effects if that is a target metal. The mean of effluent EMCs for Al was 10 µg/L, which is below the 25 µg/L detection limit, under configuration D. This was a significant increase from the mean of

influent EMCs, driven by a few samples from early storm simulations with elevated Al concentrations. Initial export of Al is hypothesized to be due to washing out of fines, which can likely be mitigated through careful mix preparation ensuring complete binding of fines to the media.

A model developed in previous work with long-term column studies was extended and fit to mesocosm experimental data with two fitting parameters to predict effluent TDP concentration from HPMM as a function of pH, rainfall intensity, cumulative P loading, and media depth. Using results from rainfall simulations, the model showed good agreement between modeled and measured effluent TDP EMC, with a slope of 1.00 and R^2 of 0.90 for HPMM-D. The model poorly described TDP results for HPMM-AA, prepared with WTR sourced from a different water treatment plant. Inclusion of an IWS zone also decreased model accuracy, likely by damping the effect of rainfall intensity on TDP retention. The model can be used to inform permeable pavement base design decisions including balancing desired removal efficiency with loading ratio and design lifetime.

Chapter 4: Field-Scale Studies

Field Monitoring of an Enhanced Stormwater Treatment Media in a Permeable Pavement Pilot Installation

Introduction

Urbanization generally results in increased impermeable surface coverage and associated issues from increased polluted runoff. This greater volume of stormwater can carry a suite of pollutants including nutrients – nitrogen (N) and phosphorus (P) – and toxic metals (Walsh et al. 2005; Kaushal et al. 2019). Low impact development (LID) approaches or distributed stormwater control measures (SCMs) are employed to mitigate the negative effects of impermeable surfaces. In developed urban areas, SCMs with small spatial footprints and those which can provide multiple co-benefits (e.g., runoff volume reduction and water quality improvement) are particularly useful. Permeable pavements are one such SCM, which directly replace impermeable surfaces with permeable. This can promote infiltration of rainfall leading to decreased runoff volume and delayed timing of runoff peak flows (Dietz 2007). Underdrains are typically installed to ensure drawdown of retained water in the permeable pavement base layer. This results in much of the water infiltrated through permeable pavements being directed to the storm sewer and eventually to surface waters. Water quality in this infiltrate water is generally improved by suspended solids filtration in the surface pavement and base aggregate layers (Drake et al. 2013; Weiss et al. 2017). Field studies across a variety of permeable pavement types, including porous asphalt, pervious concrete, and interlocking concrete pavers, have shown effective retention of total suspended solids (TSS), hydrocarbons,

metals, and total nutrients (Brattebo and Booth 2003; Gilbert and Clausen 2006; Drake et al. 2014; Winston et al. 2016). These pollutants are largely affiliated with solids. There is potential, however, for dissolved pollutants such as nitrate and phosphate to pass through the permeable pavements or remobilize from captured particulates. The study by Drake et al. (2014) illustrates this challenge. In three partial-infiltration (i.e. underdrained) permeable pavement systems, decreases in organic N (N_{org}) and ammonium (NH_4) – relative to impermeable asphalt – were accompanied by increases in NO_3. This was likely due to microbially-mediated nitrification of NH_4 to NO_3 as water drained through the permeable pavements. Phosphate removal was lower than TP removal in all cases and phosphate export was noted in one permeable pavement.

A novel treatment media described in Chapters 2 and 3 was developed to enhance the capability of permeable pavements to improve water quality, particularly with respect to dissolved P and nitrogen. The novel permeable pavement base material, referred to as high permeability media mixture (HPMM), comprises expanded shale lightweight aggregate (expanded shale) coated with aluminum-based water treatment residual (WTR) using a psyllium-based soil binder (psyllium). This unique combination of materials redirects a waste material (WTR) for productive use and overcomes the low permeability of WTR when used alone. The result is an inexpensive stormwater treatment solution. Previous studies, described in Chapters 2 and 3, demonstrated adequate hydraulic conductivity and structural capacity to serve as a permeable pavement base, and long-term P retention capacity to remain in place as a treatment media beyond the expected lifetime of a pavement installation. These studies were conducted under laboratory simulations using synthetic stormwater. The composition of the aqueous matrix can

influence pollutant removal for P and metals undergoing adsorption processes. Competitive adsorption among ions present in the stormwater can alter retention of target pollutants. Formation of complexes between metals and organic matter (OM) or between metals and phosphates can also influence pollutant mobility. These processes can also be pH dependent (Chen et al. 1973a and b; Elliott et al. 1986). Therefore, actual stormwater is necessary to verify expected treatment performance documented under lab conditions. The objective of the present study is to assess performance of this base material under field conditions with respect to a range of inorganic pollutants. The target pollutants to be monitored are total phosphorus (TP), total dissolved phosphorus (TDP), total nitrogen (TN), ammonium (NH_4), nitrate (NO_3), nitrite (NO_2), and total Al, Cu, Fe, Pb, and Zn. Percent reduction in mass load is the primary metric to be used to assess performance because load reduction is one of the primary goals of treating stormwater in SCMs. Effluent concentration can also be important to receiving water body quality, therefore performance will also be assessed by examining effluent concentrations on a storm-by-storm basis and in overall study mean and median values to assess long term effluent trends.

Methods and Materials

High Permeability Media Mixture

HPMM used in this study was blended by Stancills Inc. in Perryville, MD using WTR from the Dalecarlia drinking water treatment plant (Washington, D.C.), Haydite "B" size expanded shale from DiGeronimo Aggregates (Cleveland, OH) graded between 0.094 (No. 8 sieve) and 9.5 mm (3/8 in), and *Stabilizer* from Stabilizer Solutions (Phoenix, AZ). Moist WTR was pressed through a screen with approximately 2 mm gap

space prior to blending without drying. The HPMM was stored overnight and delivered in a cement mixing truck to a field pilot site. During this process, dried clumps of HPMM formed and were broken apart manually for installation in the base layer of a permeable pavement.

Figure 4-1. Field study site in Worton, MD. Direct precipitation onto a 36-m^2 impermeable liner (Control) and 49-m^2 permeable pavement section with 5-cm HPMM base layer (Treatment) was directed into corresponding drainage pipes for flow monitoring and water quality sampling.

Site Description and Monitoring Plan

A field pilot site was installed on November 16, 2016. The site in Worton, MD consisted of a single permeable pavement residential driveway divided into two sections. The 36 m^2 "Control" section was covered with an impermeable plastic liner from which all runoff was directed into an adjacent 6-inch PVC drain pipe (Figure 4-1). The 49 m^2

"Treatment" side consisted of a permeable brick paver surface layer with chipped shale gap fill material (Figure 4-2). A PaverGuide™ base and grid system was used for the reservoir layer. A 5-cm layer of HPMM was placed as the base layer on top of an impermeable plastic liner used to collect infiltrated water. All flow through the permeable layers was directed to a drainage collection pipe at the lower end of the installation, resulting in flow through the HPMM base and PaverGuide™ reservoir layers.

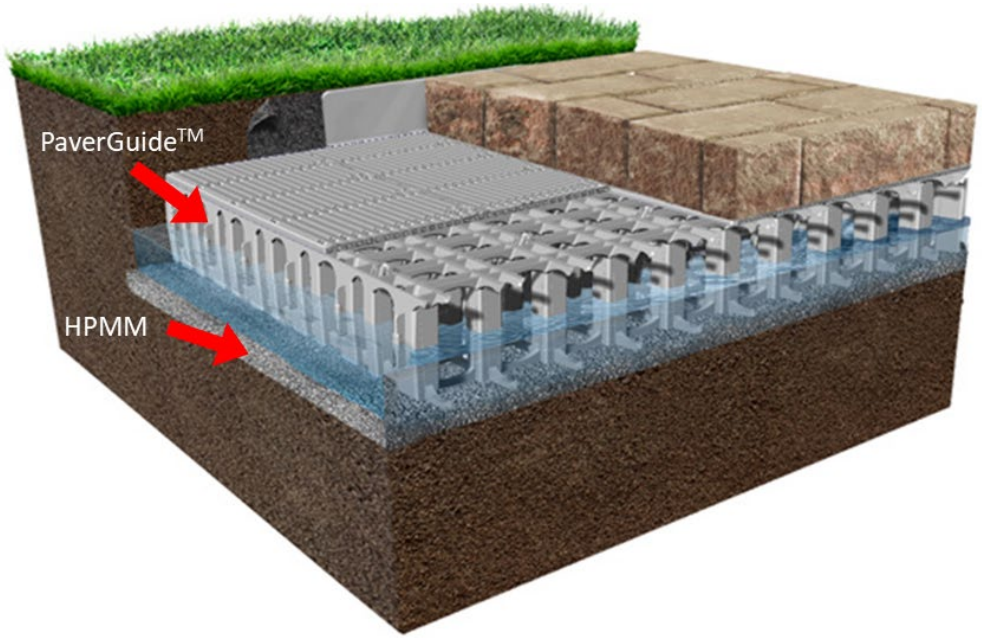

Figure 4-2. Cross section of Treatment permeable pavement construction showing brick paver surface course, PaverGuide™ grid reservoir layer, and HPMM base layer (image provided courtesy of PaverGuide, Inc.).

Monitoring was conducted over the 17-month period from June 7, 2017 through November 2, 2018 (Figure 4-3). 17 paired water samples were collected from Control and Treatment drainage pipes using ISCO Avalanche or 6712 automated sampling

devices and flow was monitored using a 6-inch Thel-Mar V-notch weir pipe insert and ISCO 730 Bubbler Flow Module. An onsite ISCO 674 tipping bucket rain gauge was used to collect localized rainfall data to 0.254-mm sensitivity (Teledyne ISCO, Lincoln, NE). Rainfall and flow data were logged at 2-minute intervals. Composite water samples were collected in 10-liter high density polyethylene (HDPE) bottles by flow-weighted sampler programming. Well-mixed samples were divided into smaller plastic bottles immediately following storm events and temporarily stored at 4°C in a refrigerator onsite, then transferred in iced coolers to the University of Maryland Environmental Engineering Laboratories in College Park, MD. TSS and pH were measured immediately upon delivery to the lab and remaining samples were frozen until analyzed. Sample analysis for all parameters was conducted within 28 days of storm sampling. Samples intended for N analysis were preserved onsite using sample bottles pre-filled with reagent grade sulfuric acid and those intended for metals analysis were preserved onsite using trace metal grade nitric acid (Fisher Chemical, Gaithersburg, MD). All sample bottles and glassware used in collection and analysis were washed with deionized water and 5% hydrochloric acid between uses.

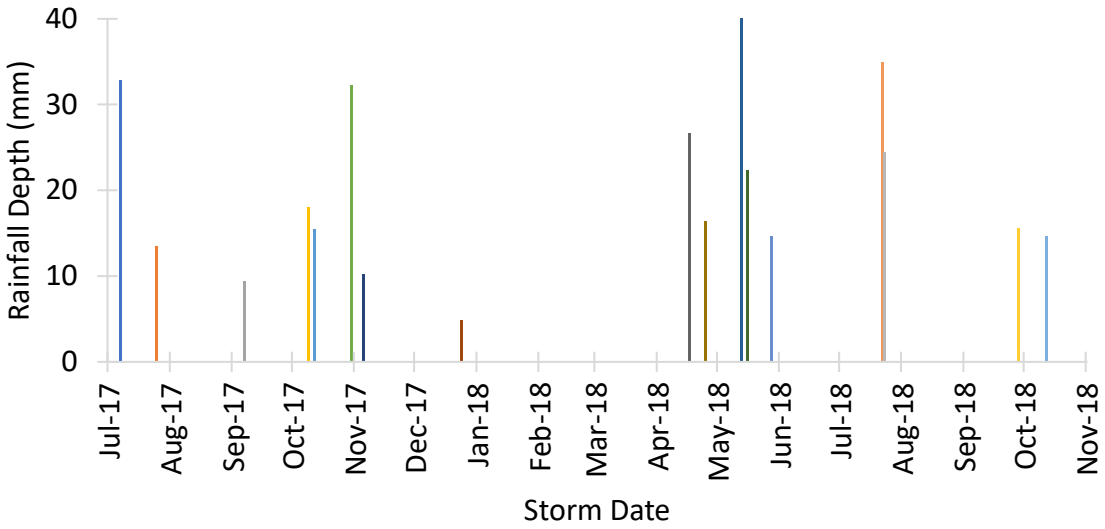

Figure 4-3. Temporal distribution and rainfall depth of storms sampled over a 17-month monitoring period. 17 events for which paired water samples were collected from a Control impermeable pavement section and Treatment permeable pavement section are shown.

Analytical Procedures

Sample analysis was conducted at the University of Maryland Environmental Engineering Laboratories (College Park, MD). Lab pH was measured using a glass electrode probe with Ag/AgCl reference to an accuracy of 0.01 units (Mettler Toledo MA235, Greifensee, Switzerland). Total suspended solids (TSS) was measured following Standard Method 2540-D to a detection limit of 2.5 mg/L TSS. TP and TDP concentrations were determined by potassium persulfate digestion and the ascorbic acid molybdenum blue colorimetric method from Standard Method 4500-P (APHA et al. 2012). TDP samples were first filtered through a 0.22 µm ceramic filter. Absorbance was measured using a 5 cm path-length cuvette in a UV-Visible spectrophotometer (UV160U, Shimadzu, Kyoto, Japan) at 880 nm to yield a detection limit of 0.01 mg/L P. Total Al, Cu, Fe, Pb, and Zn were analyzed using inductively coupled plasma atomic

emission spectroscopy (ICP-AES) (ICPE-9000 Plasma Atomic Emission Spectrometer, Shimazdu, Kyoto, Japan) at 394.403, 324.754, 259.940, 220.353, and 213.856 nm, respectively. The detection limit was 25 µg/L for Pb and Fe, 10 µg/L for Al and Zn, and for 5 µg/L Cu.

TN was measured using a Total Organic Carbon Analyzer with Total Nitrogen Measuring Unit (TOC analyzer, Shimazdu, Kyoto, Japan) with a detection limit of 0.05 mg/L as N. NH_3-N concentrations were measured using the phenate method from Standard Method 4500-NH_3 (APHA et al. 2012). Absorbance was measure with a 1 cm path length cuvette at 640 nm in a UV-Visible spectrophotometer to a detection limit of 0.05 mg/L as N. Samples were filtered through a 0.22 µm ceramic filter prior to nitrate and nitrite analysis. NO_3-N was measured using ion chromatography (ICS-1100, Dionex, Sunnyvale, CA) following Standard Method 4110. A 4.5 mM Na_sCO_3 and 1.4 mM $NaHCO_3$ eluent solution was run isocratically through an anion-exchange column with 150 mm length, 4 mm ID, and 6.5 µm particle size (IonPac AS22 Fast IC column, Dionex, Sunnyvale, CA) at a flow rate of 1.2 mL/min. The detection limit was 0.1 mg/L as N. NO_2-N was analyzed colorimetrically in a UV-Visible spectrophotometer at 543 nm following Standard Method 4500-NO_2^- (APHA et al. 2012) with a 1 cm path length cuvette to a detection limit of 0.01 mg/L as N. NO_2-N consistently accounted for less than 3% of total N and is excluded from discussion. N_{org} was calculated as TN minus the sum of NH_4 and NO_3.

Data Handling

For each storm event, parameter measurements in the flow-weighted composite sample are representative of the flow-weighted mean or event mean concentration

(EMC). The Wilcoxon signed rank test was used to determine statistical difference between the median value of sampled event EMCs for Control and Treatment at a 5% significance level. Annual pollutant mass load, L (kg/ha-year), was calculated according to Equation 4-1.

$$L = \frac{\sum(V_i \cdot EMC_i) \cdot P}{A \cdot \sum D_i} \quad (4\text{-}1)$$

V_i is the total storm event volume from event i, EMC_i is the event mean concentration for event i, P is the average annual precipitation, A is the area of each pavement section, and D_i is the measured rainfall depth for event i. The normal annual precipitation for Chestertown, MD of 112 cm/yr was used (NCEI 2018).

Hydrologic data for 2018 contained numerous gaps and inconsistencies, therefore the NRCS curve number (CN) method was used to calculate a site-specific CN from 2017 data (NRCS 2004). CN was calculated by solving the system of equations, Equations 4-2 and 4-3, for CN given P and Q as the measured rainfall depth and outflow volume, respectively, for each storm event monitored in 2017.

$$Q = \frac{(P - 0.2 \cdot S)^2}{P + 0.8 \cdot S} \quad (4\text{-}2)$$

$$S = \frac{1000}{CN} - 10 \quad (4\text{-}3)$$

The CN was calculated as 91 for Control and 83 for Treatment. These CNs were used to estimate outflow volume for 2018 events based on precipitation data from two stations near Worton, MD (COLEMAN 3 WNW, MD and WORTON 3.9 NW, MD) (NCEI 2018).

For calculating summary statistics (e.g., mean of EMCs), values below corresponding detection limits for all parameters were assigned fill-in values based on probability plot regression lines fit to observed data. This regression on order statistics (ROS) method has been shown by Helsel and Hirsch (2002) and Helsel (2005) to perform well for sample sizes less than 50. The fill-in values can be used collectively to compute summary statistics, however they are not descriptive of individual samples. Where calculations were made on individual concentrations (e.g., storm event mass load), measured values were used for below detection limit (BDL) samples. Based on knowledge of the measurement equipment, these values are considered to be closer to the actual value and are expected to introduce less error into the calculations.

Results and Discussion

The mean and median of EMCs from all 17 storms sampled were lower in the Treatment side than Control for TSS, TP, TDP, NH_4-N, N_{org}, total Cu, and total Fe (Table 4-1 and Figures 4-6). For TN, NO_3, and total Zn, the mean and median of EMCs were higher in Treatment than in Control. Mean and median flow-weighted mean pH was also higher in Treatment than in Control. All Pb results were BDL of 25 µg/L, therefore no determination can be made regarding treatment of this metal and Pb results are not shown. Mass load reduction, comparing Treatment load to Control load, was found for TSS, TP, TDP, N_{org}, Cu, Fe, Pb, and Zn. Treatment drainage had higher mass load than Control for TN, NH_4, NO_3, and Al.

TSS concentrations were below 30 mg/L for all Treatment and Control samples except 2 (Table 4-1 and Figure 4-4). These events, with EMC values of 236 and 389 mg/L, occurred on the Control side and skewed the mean upwards for the Control to 46

mg/L compared to the median EMC of 13 mg/L. Treatment mean and median TSS values were slightly, but not significantly ($p < 0.05$), lower that Control at 10 and 6 mg/L, respectively. Permeable pavements have been shown effective at removing suspended solids from stormwater through filtration through the surface layer and stone aggregate base layers (Balades et al. 1995; Drake et al. 2014; Gilbert and Clausen 2006). The State of Washington established standards for evaluating stormwater treatment technologies, described in the Technology Assessment Protocol-Ecology (TAPE) Guidance Manual (WSDE 2011). The protocol sets water quality treatment goals and target influent concentration ranges to assess novel SCM performance with respect to certain pollutants. TSS concentrations for the Control side fell within the TAPE-specified influent range for 4 events. All 4 met corresponding performance criteria of removal efficiency (RE) greater than 80% or effluent (Treatment) EMC less than 20 mg/L TSS. The resulting mass load reduction for TSS was 39% when comparing Treatment performance to Control.

TP and TDP median EMCs were reduced significantly ($p < 0.05$) from 0.15 and 0.05 mg/L for the Control side to 0.03 and 0.01 mg/L in Treatment for TP and TDP, respectively (Table 4-1 and Figure 4-4). This resulted in overall mass load reduction of 68 and 69% for TP and TDP, respectively. P can be removed through two mechanisms, depending on whether the P is particulate-bound (PP) or in dissolved form (DP). PP is effectively removed along with suspended solids through filtration. DP, however, must be removed from the aqueous phase through sorption or precipitation. In the case of HPMM, DP adsorbs to reactive Al-hydroxide surface sites on the WTR. The capacity of

HPMM to retain DP and kinetics of reaction were explored using a model developed and calibrated in Chapters 2 and 3. The model is discussed in depth in the next section.

N was exported from the Treatment side at a mass load increase of 174, 15, and 316% for TN, NH_4, and NO_3, respectively, as compared to the Control (Table 4-1 and Figure 4-5). As discussed in Chapter 3, the WTR in HPMM contains N which is subject to leaching. N was primarily exported as NO_3, which accounted for 28.7 kg/ha-yr of the 34.1 kg/ha-yr TN mass load in the Treatment section. N_{org} in the WTR is likely converted to NO_3 through nitrification in the thin pavement base layer. This is supported by the data which demonstrate a significant ($p < 0.05$) increase in median TN and NO_3, from 0.86 and 0.28 mg/L for Control to 2.58 and 1.98 mg/L for Treatment TN and NO_3, respectively. These increases were accompanied by a significant ($p<0.05$) decrease in N_{org}, from 0.25 to 0.03 mg/L for Control and Treatment, respectively. The resulting mass load reduction for N_{org} was 48%. Nitrification has been observed in a range of SCMs (Collins et al. 2010). One approach to mitigating this N export is to include an internal water storage (IWS) zone in the base layer. This has been attempted in field studies by Winston et al. (2016) with limited success. Mesocosm experiments with an IWS in an HPMM base layer, described in Chapter 3, indicate conditions can be created in a permeable pavement base layer to advance denitrification and achieve N treatment or at least mitigate N leaching if sufficient C is available.

Natural rainwater pH generally occurs in the range of 4.5 to 5.6, but can vary by location and atmospheric composition, with lower values common in urban areas (Charlson and Rhode 1982; Galloway et al. 1982). As precipitation runs off urban impermeable surfaces, pH generally increases, primarily from weathering of carbonates

in pavements which neutralize acidity (Kaushal et al. 2017). This is the case for permeable pavements as well. Thomle (2010) noted that pervious concrete can raise pH to 8 to 9.5. In the present study, composite sample pH ranged from 5.46 to 7.35 in the Treatment section, with mean and median values of 6.28 and 6.35, respectively. This represents a pH increase compared to Control, which ranged from 4.75 to 6.96 and had mean and median values of 6.01 and 6.08, respectively. It should be noted that pH was measured in the lab after samples had been stored at 4°C for 28 days or less. Despite this limitation, the expected increase in pH was present in the data.

Metals concentrations were generally low, with a high number of EMCs below detection limit. Median Treatment EMC was lower than Control for Cu and Fe, but not significantly different ($p < 0.05$) for any of the five metals monitored (Table 4-1 and Figure 4-6). Al export was apparent from the HPMM in the Treatment section as evidence by 7 of 17 storm EMCs above the EPA ambient water quality criterion for Al of 87 µg/L for water at pH between 8.5 and 9.0 (EPA 1988). The Control section exceeded this limit in 3 events. The difference between median values, however, was not significantly different ($p < 0.05$) between Control (27 µg/L) and Treatment (12 µg/L). The influence of higher Al concentration storm events is evident in the mean EMC and mass loading values. Treatment mean Al EMC was 147 compared to 55 µg/L for Control. Mass load was 331% higher in Treatment than for the Control section. The highest concentration events, including the peak concentration of 1060 µg/L, occurred early in the study. By comparison, mesocosm studies, described in Chapter 3, on HPMM at comparable rainfall intensities produced a maximum individual sample concentration of 123 µg/L. This higher than expected Al flushing was likely a result of poor HPMM

mix preparation. Because HPMM was prepared offsite, stored, and transported to site, clumping of the dried HPMM occurred. Breaking apart the clumps to install the HPMM resulted in loose powdered WTR in the mix. The purpose of the psyllium binder is to adhere the WTR to the surface of the expanded shale to prevent wash-out of free WTR powders. Therefore, it is hypothesized that preparing HPMM onsite and installing while moist will mitigate the need to break apart clumps and will result in Al export in line with storm simulation results from Chapter 3.

Table 4-1. Water quality results from field monitoring of paired Control (C) and Treatment (T) sections of a divided driveway.

Parameter	Range of EMCs (mg/L)[1]		Mean of EMCs (mg/L)[1]		Median of EMCs (mg/L)[1]		L (kg/ha-yr)		Load Reduction (kg/ha-yr)	Load Reduction (%)
	C	T	C	T	C	T	C	T		
pH[1] (n=15)	4.75 - 6.96	5.46 - 7.35	6.01	6.28	6.08	6.35	-	-	-	-
TSS (n=17)	< 2.5 - 389	< 2.5 - 30	46	10	13	6	178	108	70	39
TP (n=17)	0.03 - 0.52	< 0.01 - 0.20	0.16	0.06	0.15	0.03	2.4	0.8	1.7	69
TDP (n=17)	0.01 - 0.24	< 0.01 - 0.17	0.09	0.03	0.05	< 0.01	1.4	0.4	1.0	70
TN (n=17)	0.14 - 2.88	0.66 - 4.56	1.05	2.68	0.86	2.58	12.7	34.4	-21.7	-170
NH_4-N (n=17)	< 0.05 - 0.97	< 0.05 - 1.67	0.29	0.24	0.17	0.08	4.0	4.6	-0.6	-15
NO_3-N (n=17)	0.13 - 1.91	0.54 - 4.53	0.47	2.43	0.28	1.98	7.2	29.0	-21.8	-303
N_{org}-N (n=17)	< 0.05 - 1.46	< 0.05 - 0.44	0.37	0.08	0.25	< 0.05	2.4	1.3	1.2	48
Parameter	**Range of EMCs (µg/L)**		**Mean of EMCs (µg/L)**		**Median of EMCs (µg/L)**		**L (kg/ha-yr)**		**Load Reduction (kg/ha-yr)**	**Load Reduction (%)**
	C	T	C	T	C	T	C	T		
Total Al (n=17)	< 5 - 232	< 5 - 1060	55	147	27	12	0.53	1.54	-1.01	-192
Total Cu (n=17)	< 5 - 16	< 5 - 11	5	< 5	< 5	< 5	0.05	0.03	0.02	33
Total Fe (n=17)	< 25 - 333	< 25 - 184	62	40	33	< 25	0.65	0.32	0.32	50
Total Pb (n=17)	< 25 - 11	< 25 - 47	< 25	< 25	< 25	< 25	0.06	0.04	0.03	44
Total Zn (n=17)	< 10 - 39	< 10 - 33	12	13	< 10	10	0.09	0.07	0.02	24

* indicates significant difference at 95% confidence level using Mann-Whitney U test

[1] pH EMC is expressed as flow-weighted mean in pH units

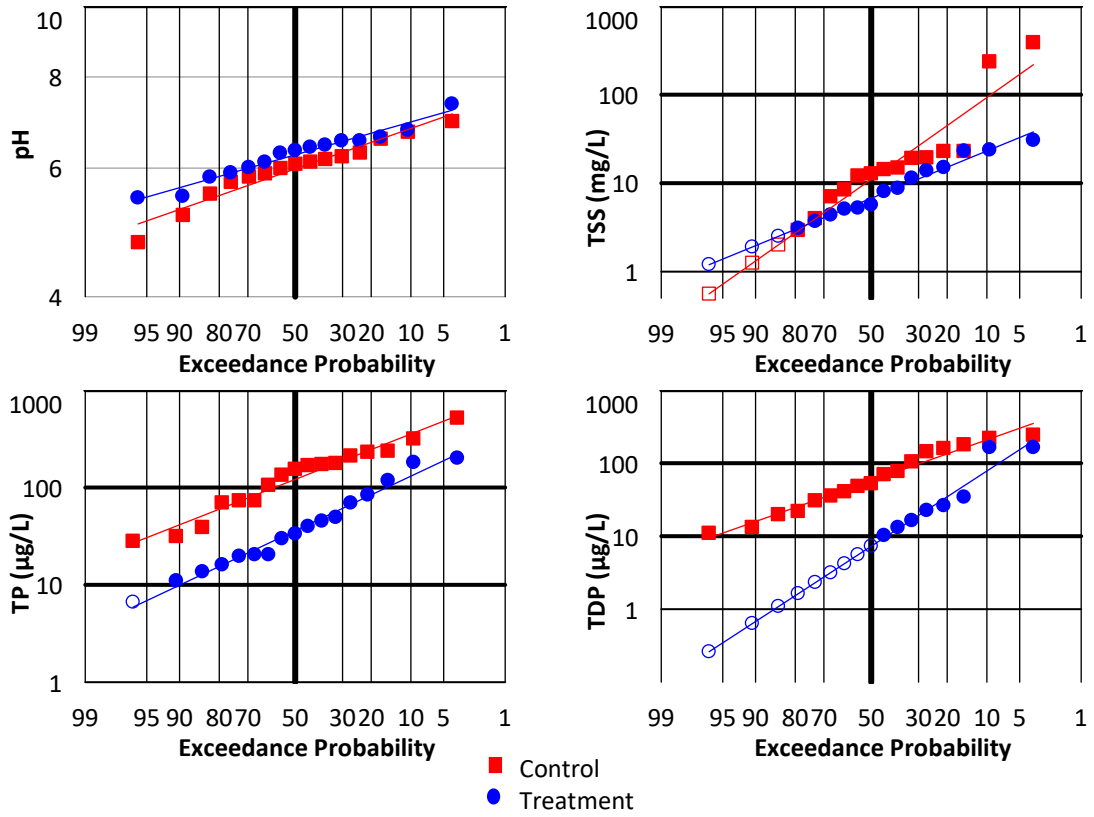

Figure 4-4. Probability plots used to assign fill-in values and calculate summary statistics for pH, TSS, TP, and TDP in a field monitoring study of a paired permeable with HPMM base (Treatment) and impermeable (Control) pavement. Open symbols indicate BDL samples assigned fill-in values extrapolated from regression line.

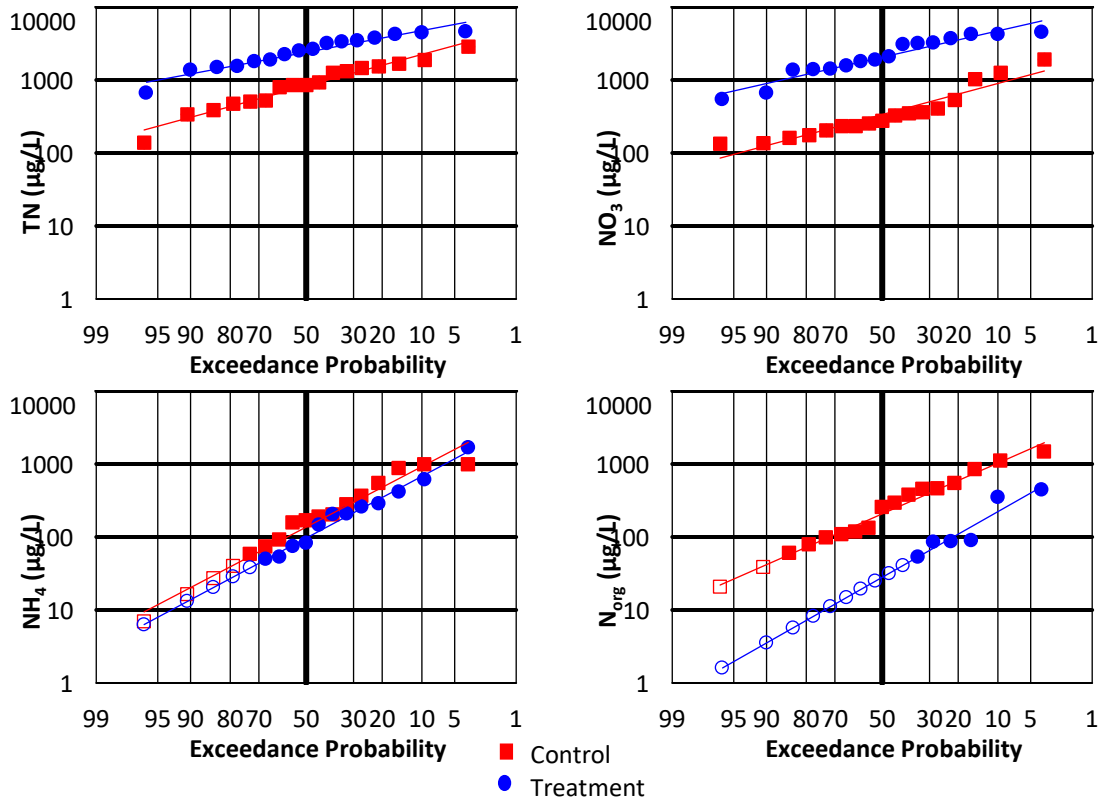

Figure 4-5. Probability plots used to assign fill-in values and calculate summary statistics for N species in a field monitoring study of a paired permeable with HPMM base (Treatment) and impermeable (Control) pavement. Open symbols indicate BDL samples assigned fill-in values extrapolated from regression line.

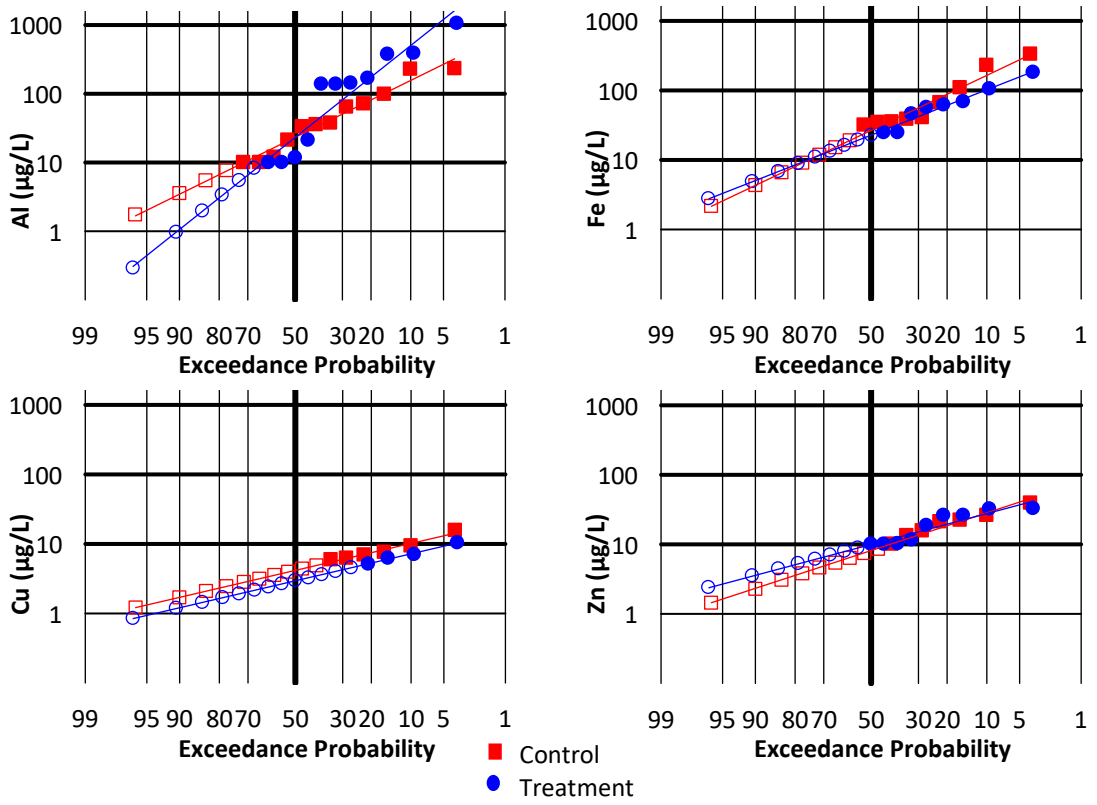

Figure 4-6. Probability plots used to assign fill-in values and calculate summary statistics for four total metals in a field monitoring study of a paired permeable with HPMM base (Treatment) and impermeable (Control) pavement. Open symbols indicate BDL samples assigned fill-in values extrapolated from regression line.

P Adsorption Model

A model describing DP retention by HPMM was developed in Chapter 2 and further improved in Chapter 3. It takes the form of Equation 4-4.

$$\frac{C_{out}}{C_{in}} = 1 - e^{-\beta_0 \Sigma M} + e^{-\left(\beta_0 \Sigma M + \beta_1^* (m(pH)+b)\frac{d}{i}\right)} \quad (4\text{-}4)$$

C_{out} and C_{in} represent TDP concentrations into and out of the media and d and *i* are media depth and rainfall intensity, respectively. ΣM = cumulative mass of DP adsorbed per mass of adsorbent media. The parameters m and b are linear regression parameters fit to the correlation of effluent pH values and another fitting parameter β_1. The fitting

parameter β_0 is a long-term parameter related to media adsorption capacity and β_1^* and β_1 are short-term parameters related to adsorption kinetics. Data from a long-term continuously-loaded column study was fit to the model to determine β_0 in Chapter 2. Mesocosm studies in which rain events were simulated provided data used to establish m, b, and β_1^* for HPMM in Chapter 3. The resulting calibrated parameters are summarized in Table 4-2.

Table 4-3. Parameters from Equations 4-4 and 4-5 fit to experimental data for long-term continuous flow columns (Chapter 2) and mesocosm rainfall simulations (Chapter 3).

	Equation 4-4	Equation 4-5
β_0 (kg/g)	0.646	0.646
m	-0.16	N/A
b	1.64	N/A
β_1^* (h^{-1})	1.025	N/A
β_1 (h^{-1})	N/A	0.446

Data for each monitored storm from the field study was input into Equation 4-4 using the parameters listed in Table 4-2 to obtain expected Treatment TDP EMCs (C_{out}). Peak rainfall intensity for each storm was used for *i*, lab-measured pH for the Treatment side was used as the pH value. The media depth was 5 cm. ΣM was estimated as cumulative DP load (mg P/kg HPMM) on the Control side for all rainfall since the date of installation (November 16, 2016). This calculation was made by multiplying annual TDP mass load (1.4 kg/ha-yr in Table 4-1) by elapsed time from installation and the area of the Treatment section (with appropriate unit conversions). Measured Control TDP EMCs were input as C_{in} values. The predicted Treatment TDP EMCs for each storm were used to calculate storm-by-storm mass loads based on flow data. Comparing predicted

annualized Treatment mass load to measured annualized Control mass load resulted in a 79% predicted mass load reduction. This is a 13% overestimate of the observed 70% load reduction calculated from measurements. The model did not perform as well in describing removal on a storm-by-storm basis. The Nash-Sutcliffe Efficiency (NSE) calculated from modeled and measured Treatment TDP EMCs was negative, indicating no advantage to using the model for predicting these concentrations.

Lower pH values were measured in the field study than were found in mesocosm studies from Chapter 3 on which m, b, and β_1^* are based. Median effluent (Treatment) pH was 6.35 in the field study, which is below the lowest effluent pH value measured in mesocosm studies. Consequently, faster kinetics were predicted in the field study than in the mesocosm studies by extrapolating beyond the model range. To correct this over estimate, Equation 4-4 was simplified to a previous version of the model, Equation 4-5, which bundles pH effects on phosphate adsorption onto Al-hydroxides in HPMM into the fitting parameter β_1.

$$\frac{C_{out}}{C_{in}} = 1 - e^{-\beta_0 \Sigma M} + e^{-\left(\beta_0 \Sigma M + \beta_1 \frac{d}{i}\right)} \quad (4\text{-}5)$$

Table 4-2 lists the parameters used to model TDP removal in the field study using Equation 4-5. The β_1 comes from data fitting using this previous version of the model in Chapter 3. Applying Equation 4-5 to field data yielded a predicted TDP mass load reduction of 66%, which is a 6% underestimate of the observed 70% mass load reduction. The model was still unable to provide valuable predictions on a storm-by-storm basis, however, resulting in a negative NSE.

1636 It is not unusual for field results to differ from predictions based on laboratory
1637 testing. Lab conditions can be closely controlled, while field performance may be
1638 influenced by factors not present in lab testing. For example, mesocosm studies in
1639 Chapter 3 were conducted in a greenhouse using tap water. Consequently, water
1640 temperature was maintained around 21°C throughout the year. Meanwhile, ambient
1641 temperature and presumably pavement and water temperature fluctuated in the present
1642 field study. The effect of temperature changes on TP retention and infiltration capacity in
1643 permeable pavements has been found not to be significant in past studies (Tota-Maharaj
1644 and Scholz 2010; Roseen et al. 2012; Huang et al. 2016). Temperature could have an
1645 impact on water viscosity and adsorption kinetics, however, which may be of greater
1646 importance in the present study where P adsorption onto reactive media is the primary
1647 mechanism of DP retention. Wet and dry periods, driven by weather patterns, can alter
1648 adsorption capacity of the media, though the correlation has not always followed a
1649 consistent pattern (O'Neill and Davis 2012; Hatt et al. 2009).
1650 Water quality and presence of competitive ions can also have an influence on P
1651 removal. Lucas and Greenway (2008) describe three different adsorption mechanisms for
1652 P. The first is electrostatic ion-exchange, which is rapid but easily reversible and
1653 sensitive to competition from other ions in the infiltrate. Specific adsorption through
1654 inner-sphere complexes are much less reversible but can be slower. The final mechanism
1655 involves migration of P from surface sites to interior adsorption sites, thus freeing up
1656 surface sites for additional P retention. The relative influence of these three mechanisms
1657 may have been affected by wetting and drying patterns and water chemistry which
1658 differed from lab studies on which the model was based. Organic matter has also been

shown to negatively influence P sorption and increase P release in soils (Guppy et al. 2005). This is thought to be caused by competition of dissolved organic matter with P for adsorption sites. Degradation of OM can also be a source of organic P, thus increasing the total P within the soil, or in this case, pavement system. Additionally, the organic P fraction of TP may influence sorption onto HPMM. Yan et al. (2018) found WTR demonstrated lower adsorption capacity and slower kinetics for organic P compared to inorganic P.

Conclusions

Based on previous lab and mesocosm studies, HPMM was expected to effectively remove TP, TDP, Cu, and Zn from stormwater in field study. TP and TDP treatment performance were on the order of expected removal with Treatment median EMCs of 0.03 and < 0.01 mg/L for TP and TDP, respectively. Load reduction was also indicative of effective P retention with 69 and 70% of total TP and TDP mass, respectively, retained relative to Control.

The model developed to describe DP adsorption onto HPMM was shown to be a good predictor of overall treatment performance based on percent reduction of annualized mass load and mean and median of all storm event EMCs. Storm-by-storm removal was not well correlated with measured results. This is likely due to differences in experimental conditions from lab to field, such as temperature fluctuations and water constituents. A simplified model is suggested, as a function of median peak rainfall intensity, cumulative DP loading, media depth, and fitting parameters calibrated to lab data. Using the simplified model, load reduction was estimated to be 66%, which is very close to the measured load reduction of 70% for TDP.

N export was observed from the Treatment section. A 174% increase in TN mass load was driven primarily by an increase in NO_3 compared to Control. The 316% NO_3 mass load increase was accompanied by a 48% load decrease in N_{org}. This result, along with previous studies of N dynamics in permeable pavements, indicates nitrification of N_{org} to NO_3 occurred in the HPMM layer and caused N contained in the WTR to be flushed out. It is hypothesized that an IWS zone distributed throughout the pavement base layer can be created through outflow control and may be able to mitigate N leaching, based on results from mesocosm studies.

Cu and Zn mean and median results were not significantly different between Treatment and Control, however load reduction was observed for Cu, Fe, and Zn. Al export may be of concern when implementing HPMM as a permeable pavement base, with load increased by 316% over Control. HPMM mix preparation onsite and installation while moist is hypothesized to mitigate significant flushing out of Al in loose fines. If appropriate measures are taken for N and Al control, HPMM can serve as an effective tool for improving stormwater quality and an enhancement to current permeable pavement design.

Chapter 5: Conclusions

This research resulted in development of a novel stormwater treatment media capable of serving as a permeable pavement base material. The material was developed using expanded shale aggregate, Al-based water treatment residual, and psyllium-based binder. The media (HPMM) has high structural capacity and hydraulic conductivity and demonstrated effective DP and total metals retention in lab-, mesocosm-, and field-scale studies. The media also demonstrated potential to reduce N concentrations by including an IWS zone if adequate C is available.

The results of lab-scale study supported the hypotheses that HPMM is a structurally suitable permeable pavement base material, can enhance P removal from rainfall/runoff for the duration of a permeable pavement design life, and retains DP primarily through adsorption to Al (hydr)oxide surfaces with more effective retention at lower flowrate. Geotechnical testing demonstrated that the media has high hydraulic conductivity and would be suitable, with respect to infiltration rate, for use as a permeable pavement base. The structural strength of the media was also shown to be good for use as a base material from analysis of CBR and direct shear test results. Batch equilibrium testing demonstrated the relatively high capacity of HPMM to adsorb P from aqueous solutions as compared to Ca and Fe-containing materials. Continuous loading with synthetic stormwater containing P, NaCl, N, and a C source in column testing supported the adsorption capacity calculated from batch testing, though the two adsorption capacities were not directly comparable, possibly due to differences in experimental conditions such as flow, mixing, and background matrices. Long-term P

adsorption capacity after greater than 600 m of applied water was calculated as 1068 mg/kg at 0.19 mg/L P input. These studies also demonstrate the efficacy of HPMM to reduce P concentrations under flowing conditions, with consistently high P removal efficiency (90% or above) well beyond the anticipated 20-yr lifetime treatment volume for a permeable pavement receiving no run-on flow. This enhanced P retention capacity could enable permeable pavements to receive run-on flow from other surfaces at loading rates of 5:1 or possibly higher without diminishing P treatment throughout the pavement lifetime.

In mesocosm-scale studies, a 5-cm layer of HPMM reduced influent TDP concentrations from 0.25 mg/L to a maximum of 0.05 mg/L P for storm simulations with 0.66 cm/h rainfall intensity at pH between 5.86 and 8.23, typical of stormwater pH. For 9 simulations at this rainfall intensity, 8 fell below the EPA freshwater ambient water quality criteria of 0.03656 mg/L for TP (EPA 2000). This intensity is slightly lower than the 1-yr ARI for College Park, MD and likely exceeds the intensity of at least 2/3 of Maryland storms (Kreeb 2003). HPMM did not remove N under aerobic conditions and may be a source of N export. An IWS zone, however, was successful in decreasing effluent N when sufficient C was present to advance denitrification. WTR source had no impact on N retention. Heavy metals leaching was not found to be an issue for HPMM. Initial export of Al was observed, which can likely be mitigated through careful mix preparation ensuring complete binding of fines to the media. Cu and Zn concentrations were reduced using HPMM. Additional treatment may be necessary to further lower Cu concentrations to avoid toxicity effects if that is a target metal.

In field-scale study, comparing a control impermeable residential driveway (Control) to a permeable pavement using a 5-cm HPMM base layer (Treatment), TP and TDP treatment performance were on the order of expected removal based on lab- and mesocosm-scale studies. Treatment median EMCs were 0.03 and 0.01 mg/L for TP and TDP, respectively, for 17 storms sampled over a 17-month monitoring period. Load reduction was also indicative of effective P retention with 68 and 69% of total TP and TDP mass, respectively, retained relative to Control. Cu and Zn mean and median results were not significantly different between Treatment and Control, however, load reduction was observed for Cu, Fe, and Zn. Mass load was reduced in field monitoring by 32 and 21% for Cu and Zn, respectively. N and Al export was documented, with load increased by 174 and 316%, respectively. An IWS zone created through outflow control in the permeable pavement base may be able to mitigate N leaching. Elevated Al concentrations likely resulted from washout of fines from the media, due to improper media preparation and installation practices. HPMM mix preparation onsite and installation while moist is likely to mitigate significant flushing out of Al in loose fines.

A dynamic model was developed to describe DP adsorption onto the media based on lab and mesocosm testing and verified under field monitoring. The steady-state plug-flow model describes DP retention as a function of rapid surface transfer rate kinetics and long-term cumulative DP loading effects. Laboratory conditions may not account for effects of adsorption competition or preferential flowpaths. Therefore, model development was extended and fit to mesocosm experimental data with two fitting parameters to predict effluent TDP concentration from HPMM as a function of pH, rainfall intensity, cumulative P loading, and media depth. Using results from rainfall

simulations, the model showed good agreement between modeled and measured effluent TDP EMC, with a slope of 1.00 and R^2 of 0.90 for HPMM-D. The model poorly described TDP results for HPMM-AA, prepared with WTR sourced from a different water treatment plant. Inclusion of an IWS zone also decreased model accuracy, likely by damping the effect of rainfall intensity on TDP retention. Evaluating the model against field monitoring results, it was shown to be a good predictor of overall treatment performance based on percent reduction of annualized mass load and mean and median of all storm event EMCs. The model predicted 62% DP concentration reduction and 65% mass load reduction. Actual reductions from 17 months of monitoring were 67 and 69%, respectively. Storm-by-storm removal was not well correlated with measured results. This is likely due to measured results fluctuating from storm to storm without apparent correlation to available storm parameters. The model can be used to inform permeable pavement base design decisions including balancing desired removal efficiency with loading ratio and design lifetime.

This research resulted in development of the first known enhanced stormwater treatment media to retain DP in a permeable pavement base layer. This new tool to address nonpoint pollution could enable wider applicability of permeable paving due to its capacity to retain P from direct precipitation and in run-on from contributing areas. The studies undertaken also add to body of literature by showing N leaching from WTR. The multi-scale study also demonstrated DP treatment performance in the media under field conditions based on model predictions developed from lab study. This advances the stormwater management field by demonstrating a pathway and improving tools to assess enhanced media with lab testing as a predictor for field performance. With appropriate N

and Al control, the novel media developed and demonstrated in this research can be an effective tool to improve urban stormwater quality.

Appendices

Supplemental Material

Table S1. TSS data from field monitoring of pilot installation

Storm ID	Control TSS EMC (mg/L TSS)	Treatment TSS EMC (mg/L TSS)	RE (%)	Criteria[1]	Meets Criteria (Y/N)
170707	0[2]	6			
170725	0[2]	30			
170907	13	23			
171009	23	11		≤ 20 mg/L TSS	Y
171012	7	14			
171030	236	15	94	> 80% RE	Y
171105	389	5	99	> 80% RE	Y
171224	19	8			
180417	23	9		≤ 20 mg/L TSS	Y
180425	12	1[2]			
180513	8	0[2]			
180516	3	2[2]			
180528	15	24			
180722	2[2]	4			
180723	2[2]	3			
180928	14	0[2]			
181012	19	1[2]			
Mean (mg/L)	46	10			
Median (mg/L)	13	6			
Normalized Annual Mass Load (kg/ha-yr)	178	108	39		

* indicates significant difference using Mann-Whitney U test at 95% confidence level

[1] per TAPE Guidance Manual; empty cells indicate influent concentration was out of influent range (< 20 mg/L)

[2] Below detection limit of 2.5 mg/L TSS

Note: values below detection limit are reported as measured for calculating storm-by-storm RE and mass load. For mean and median calculations, fill-in values were assigned using the probability plot regression on order statistics (ROS) method described by Helsel and Hirsch (2002) and Helsel (2005)

Table S2. TP and TDP data from field monitoring of pilot installation

Storm ID	Control **TP** EMC (mg/L P)	Treatment **TP** EMC (mg/L P)	RE (%)	Criteria[1]	Meets Criteria (Y/N)	Control **TDP** EMC (mg/L P)	Treatment **TDP** EMC (mg/L P)	RE (%)
170707	0.03	0.01	61			0.01	0.005[2]	55
170725	0.03	0.04	-27			0.03	0.01	67
170907	0.07	0.03	57			0.01	0.01	0
171009	0.18	0.12	33	≥ 50% RE	N	0.04	0.03	35
171012	0.07	0.08	-16			0.02	0.02	17
171030	0.32	0.05	86	≥ 50% RE	Y	0.07	0.005[2]	93
171105	0.13	0.02	85	≥ 50% RE	Y	0.04	0.005[2]	86
171224	0.11	0.03	68	≥ 50% RE	Y	0.05	0.005[2]	90
180417	0.07	0.02	72			0.02	0.005[2]	77
180425	0.17	0.01	92	≥ 50% RE	Y	0.10	0.005[2]	95
180513	0.52	0.05	91	≥ 50% RE	Y	0.24	0.02	91
180516	0.24	0.07	70	≥ 50% RE	Y	0.14	0.03	76
180528	0.15	0.02	87	≥ 50% RE	Y	0.08	0.01	93
180722	0.23	0.20	13	≥ 50% RE	N	0.22	0.17	24
180723	0.21	0.18	15	≥ 50% RE	N	0.18	0.16	8
180928	0.04	0.02	59			0.05	0.00	99.8
181012	0.17	0.01	94	≥ 50% RE	Y	0.16	0.00	99.9
Mean (mg/L)	0.16	0.06	65	≥ 50% RE	Y	0.09	0.03	67
Median (mg/L)	0.15*	0.03*	78	≥ 50% RE	Y	0.05*	0.01*	86
Normalized Annual Mass Load (kg/ha-yr)	2.4	0.8	68	≥ 50% RE	Y	1.38	0.42	69

* indicates significant difference using Mann-Whitney U test at 95% confidence level

[1] per TAPE Guidance Manual; empty cells indicate influent concentration was out of influent range (< 0.1 mg/L)

[2] Below detection limit of 0.01 mg/L P

Note: values below detection limit are reported as measured for calculating storm-by-storm RE and mass load. For mean and median calculations, fill-in values were assigned using the probability plot regression on order statistics (ROS) method described by Helsel and Hirsch (2002) and Helsel (2005)

1814 Table S3. Total Cu data from field monitoring of pilot installation

Storm ID	Control Cu EMC (µg/L)	Treatment Cu EMC (µg/L)	RE (%)
170707	0[1]	0[1]	
170725	0[1]	1[1]	
170907	4[1]	5	
171009	7	11	
171012	4[1]	5[1]	
171030	-	4[1]	
171105	6	4[1]	
171224	0[1]	0[1]	
180417	3[1]	6	
180425	4[1]	7	
180513	6	0[1]	
180516	9	0[1]	
180528	8	0[1]	
180722	4[1]	5[1]	
180723	1[1]	2[1]	
180928	0[1]	0[1]	
181012	16	0[1]	
Mean (µg/L)	5	4	29
Median (µg/L)	4	3	29
Normalized Annual Mass Load (kg/ha-yr)	0.05	0.03	32

1815 * indicates significant difference using Mann-Whitney U test at 95% confidence level
1816 [1] Below detection limit of 5 µg/L total Cu
1817 Note: values below detection limit are reported as measured for calculating storm-by-storm RE and mass
1818 load. For mean and median calculations, fill-in values were assigned using the probability plot regression
1819 on order statistics (ROS) method described by Helsel and Hirsch (2002) and Helsel (2005)

1820

Bibliography

American Public Health Association (APHA), American Water Works Association (AWWA), and Water Environment Federation (WEF) (2012). *Standard Methods for the Examination of Water and Wastewater*, American Public Health Association, Washington, D.C.

American Society of Civil Engineers (ASCE) Permeable Pavements Task Committee, Eisenberg, B., Lindow, K. C., and Smith, D. (2015). *Permeable Pavements*, American Society of Civil Engineers, Reston, VA.

Asphalt Institute (2007). The Asphalt Handbook, Asphalt Institute, Lexington, Ky.

Ator, S. W., Brakebill, J. W., and Blomquist, J. D. (2011). "Sources, fate, and transport of nitrogen and phosphorus in the Chesapeake Bay Watershed – An empirical model: U.S. Geological Survey Scientific Investigations Report 2011–5167," 27 p., U.S. Geological Survey, Reston, VA.

Babatunde, A. O., Zhao, Y. Q., Burke, A. M., Morris, M. A., and Hanrahan, J. P. (2009). "Characterization of aluminium-based water treatment residual for potential phosphorus removal in engineered wetlands." Environmental Pollution, 157(10), 2830-2836.

Baladès, J. D., Legret, M., and Madiec, H. (1995). "Permeable pavements: pollution management tools." *Water Science and Technology*, 32(1), 49-56.

Bean, E. Z., Hunt, W. F., and Bidelspach, D. A. (2007). "Evaluation of Four Permeable Pavement Sites in Eastern North Carolina for Runoff Reduction and Water Quality Impacts." Journal of Irrigation and Drainage Engineering, 133(6), 583-592.

Bonnin, G. M., Martin, D., Lin, B., Parzybok, T., Yekta, M., and Riley, D. (2006). "NOAA Atlas 14." U.S. Department of Commerce. National Oceanic and Atmospheric Administration. National Weather Service Silver Spring, MD.

Boving, T., Stolt, M., Augenstern, J., and Brosnan, B. (2008). "Potential for localized groundwater contamination in a porous pavement parking lot setting in Rhode Island." Environmental Geology, 55(3), 571-582.

Brattebø, H., and Ødegaard, H. (1986). "Phosphorus removal by granular activated alumina." Water Research, 20(8), 977-986.

Brattebo, B. O., and Booth, D. B. (2003). "Long-term stormwater quantity and quality performance of permeable pavement systems." *Water Research*, 37(18), 4369-4376.

Brown, S. L., Compton, H., and Basta, N. T. (2007). "Field Test of In Situ Soil Amendments at the Tar Creek National Priorities List Superfund Site." *Journal of Environmental Quality*, 36, 1627-1634.

Burland, J. B., Chapman, T., and Institution of Civil Engineers (Great Britain) (2012). "ICE manual of geotechnical engineering." ICE Publishing, London.

Calheiros, C. S. C., Duque, A. F., Moura, A., Henriques, I. S., Correia, A., Rangel, A. O. S. S., and Castro, P. M. L. (2009). "Substrate effect on bacterial communities from constructed wetlands planted with Typha latifolia treating industrial wastewater." Ecological Engineering, 35(5), 744-753.

Castaldi, P., Silvetti, M., Garau, G., Demurtas, D., and Deiana, S. (2015). "Copper(II) and lead(II) removal from aqueous solution by water treatment residues." *Journal of Hazardous Materials*, 283, 140-147.

1867 Charlson, R. J., and Rodhe, H. (1982). "Factors controlling the acidity of natural
1868 rainwater." *Nature*, 295, 683.
1869 Chen, Y. S. R., Butler, J. N., and Stumm, W. (1973). "Kinetic study of phosphate reaction
1870 with aluminum oxide and kaolinite." *Environmental Science & Technology*, 7(4),
1871 327-332.
1872 Chesapeake Bay Program (CBP) (2016). "Reducing Phosphorus Pollution - Chesapeake
1873 Bay Program."
1874 <http://www.chesapeakebay.net/indicators/indicator/reducing_phosphorus_polluti
1875 on.> (May 31, 2016).
1876 Center for Watershed Protection (CWP) and Maryland Department of the Environment
1877 (MDE) 2000). "Maryland Stormwater Design Manual." Baltimore, MD.
1878 Collins, K. A., Hunt, W. F., and Hathaway, J. M. (2010a). "Side-by-Side Comparison of
1879 Nitrogen Species Removal for Four Types of Permeable Pavement and Standard
1880 Asphalt in Eastern North Carolina." Journal of Hydrologic Engineering, 15(6),
1881 512-521.
1882 Collins, K. A., Lawrence, T. J., Stander, E. K., Jontos, R. J., Kaushal, S. S., Newcomer,
1883 T. A., Grimm, N. B., and Cole Ekberg, M. L. (2010b). "Opportunities and
1884 challenges for managing nitrogen in urban stormwater: A review and synthesis."
1885 Ecological Engineering, 36(11), 1507-1519.
1886 Conley, D. J., Paerl, H. W., Howarth, R. W., Boesch, D. F., Seitzinger, S. P., Havens, K.
1887 E., Lancelot, C., and Likens, G. E. (2009). "Controlling Eutrophication: Nitrogen
1888 and Phosphorus." Science, 323(5917), 1014-1015.
1889 Clark, S. E., and Pitt, R. (2012). "Targeting treatment technologies to address specific

stormwater pollutants and numeric discharge limits." *Water Research*, 46(20), 6715-6730.

Clary, J., Jones, J., Leisenring, M., Hobson, P., and Strecker, E. (2017). "International Stormwater BMP Database 2016 Summary Statistics." Water Environment & Reuse Foundation, Alexandria, VA.

Davis, A. P., and McCuen, R. H. (2005). "Stormwater management for smart growth." Springer Science, New York.

Day, G. E., Smith, D. R., and Powers, J. N. (1981). "Runoff and pollution abatement characteristics of concrete grid pavements." Virginia Water Resources Center, Virginia Polytechnic and State University, Blacksburg, VA.

Dayton, E. A., and Basta, N. T. (2005). "A Method for Determining the Phosphorus Sorption Capacity and Amorphous Aluminum of Aluminum-Based Drinking Water Treatment Residuals." Journal of Environmental Quality, 34, 1112-1118.

Dietz, M. E. (2007). "Low Impact Development Practices: A Review of Current Research and Recommendations for Future Directions." Water, Air and Soil Pollution, 186(1-4), 351-363.

DiGeronimo Aggregates (2016). "Guide Specifications for Lightweight Geotechnical Applications." Independence, Ohio.

Drake, J., Bradford, A., and Marsalek, J. (2013). "Review of environmental performance of permeable pavement systems: state of the knowledge." *Water Quality Research Journal*, 48(3), 203-222.

Drake, J., Bradford, A., and Van Seters, T. (2014). "Stormwater quality of spring–summer-fall effluent from three partial-infiltration permeable pavement systems

and conventional asphalt pavement." Journal of Environmental Management, 139, 69-79.

Elliott, H. A., Liberati, M. R., and Huang, C. P. (1986). "Competitive Adsorption of Heavy Metals by Soils1." *Journal of Environmental Quality*, 15, 214-219.

Erickson, A. J., Gulliver, J. S., and Weiss, P. T. (2007). "Enhanced Sand Filtration for Storm Water Phosphorus Removal." Journal of Environmental Engineering, 133(5), 485-497.

Galloway, J. N., Likens, G. E., Keene, W. C., and Miller, J. M. (1982). "The composition of precipitation in remote areas of the world." *Journal of Geophysical Research: Oceans*, 87(C11), 8771-8786.

Gilbert, J. K., and Clausen, J. C. (2006). "Stormwater runoff quality and quantity from asphalt, paver, and crushed stone driveways in Connecticut." Water Research, 40(4), 826-832.

Goldberg, S., and Sposito, G. (1984). "A Chemical Model of Phosphate Adsorption by Soils: I. Reference Oxide Minerals1." *Soil Science Society of America Journal*, 48(4), 772.

Guppy, C. N., Menzies, N. W., Moody, P. W., and Blamey, F. P. C. (2005). "Competitive sorption reactions between phosphorus and organic matter in soil: a review." *Soil Research*, 43(2), 189-202.

Hatt, B. E., Fletcher, T. D., and Deletic, A. (2009). "Pollutant removal performance of field-scale stormwater biofiltration systems." *Water Science and Technology*, 59(8), 1567-1576.

Helsel, D. R. (2005). "More Than Obvious: Better Methods for Interpreting Nondetect

Data." *Environmental Science & Technology*, 39(20), 419A-423A.

Helsel, D.R. and Hirsch, R. M. (2002). Statistical Methods in Water Resources Techniques of Water Resources Investigations, Book 4, Chapter A3. U.S. Geological Survey. 522 pages.

Holtz, R. D., Kovacs, W. D., and Sheahan, T. C. (2011). An Introduction to Geotechnical Engineering, Pearson, Upper Saddle River, NJ.

Howarth, R. W., Sharpley, A., and Walker, D. (2002). "Sources of nutrient pollution to coastal waters in the United States: Implications for achieving coastal water quality goals." Estuaries, 25(4), 656-676.

Howe, K. J., Hand, D. W., Crittenden, J. C., Trussell, R. R., and Tchobanoglous, G. (2012). *Principles of water treatment*, John Wiley & Sons, Inc., Hoboken, New Jersey.

Huang, J., Valeo, C., He, J., and Chu, A. (2016). "Three Types of Permeable Pavements in Cold Climates: Hydraulic and Environmental Performance." *Journal of Environmental Engineering*, 142(6), 04016025.

Hunt, W. F. (2010). "Working with Regulators to Change Permeable Pavements Acceptance." Low Impact Development 2010, American Society of Civil Engineers, 1270-1280.

Ippolito, J. A., Barbarick, K. A., and Elliott, H. A. (2011). "Drinking Water Treatment Residuals: A Review of Recent Uses." Journal of Environmental Quality, 40(1).

Kaushal, S. S., Duan, S., Doody, T. R., Haq, S., Smith, R. M., Newcomer Johnson, T. A., Newcomb, K. D., Gorman, J., Bowman, N., Mayer, P. M., Wood, K. L., Belt, K. T., and Stack, W. P. (2017). "Human-accelerated weathering increases

salinization, major ions, and alkalinization in fresh water across land use." *Applied Geochemistry*, 83, 121-135.

Kaushal Sujay, S., Likens Gene, E., Pace Michael, L., Haq, S., Wood Kelsey, L., Galella Joseph, G., Morel, C., Doody Thomas, R., Wessel, B., Kortelainen, P., Räike, A., Skinner, V., Utz, R., and Jaworski, N. (2019). "Novel 'chemical cocktails' in inland waters are a consequence of the freshwater salinization syndrome." *Philosophical Transactions of the Royal Society B: Biological Sciences*, 374(1764), 20180017.

Kim, H., Seagren, E. A., and Davis, A. P. (2003). "Engineered Bioretention for Removal of Nitrate from Stormwater Runoff." *Water Environment Research*, 75(4), 355-367.

Kreeb, L. B. (2003). "Hydrologic Efficiency and Design Sensitivity of Bioretention Facilities.", University of Maryland, College Park, MD.

Komlos, J., Welker, A., Punzi, V., and Traver, R. (2013). "Feasibility Study of As-Received and Modified (Dried/Baked) Water Treatment Plant Residuals for Use in Storm-Water Control Measures." Journal of Environmental Engineering, 139(10), 1237-1245.

Legret, M., Colandini, V., and Le Marc, C. (1996). "Effects of a porous pavement with reservoir structure on the quality of runoff water and soil." Science of the Total Environment, 189–190, 335-340.

Legret, M., Nicollet, M., Miloda, P., Colandini, V., and Raimbault, G. (1999). "Simulation of heavy metal pollution from stormwater infiltration through a porous pavement with reservoir structure." Water Science and Technology, 39(2),

119.

LeFevre, G. H., Paus, K. H., Natarajan, P., Gulliver, J. S., Novak, P. J., and Hozalski, R. M. (2015). "Review of Dissolved Pollutants in Urban Storm Water and Their Removal and Fate in Bioretention Cells." *Journal of Environmental Engineering*, 141(1), 04014050.

Li, H., and Davis, A. P. (2008a). "Heavy Metal Capture and Accumulation in Bioretention Media." *Environmental Science & Technology*, 42(14), 5247-5253.

Li, H., and Davis A., P. (2008b). "Urban Particle Capture in Bioretention Media. I: Laboratory and Field Studies." *Journal of Environmental Engineering*, 134(6), 409-418.

Li, J., and Davis, A. P. (2016). "A unified look at phosphorus treatment using bioretention." Water Research, 90(14), 141-155.

Liu, J., and Davis, A. P. (2014). "Phosphorus Speciation and Treatment Using Enhanced Phosphorus Removal Bioretention." Environmental Science & Technology, 48(1), 607-614.

Lucas, W. C., and Greenway, M. (2008). "Nutrient Retention in Vegetated and Nonvegetated Bioretention Mesocosms." *Journal of Irrigation and Drainage Engineering*, 134(5), 613-623.

Lucas, W. C., and Greenway, M. (2011). "Phosphorus Retention by Bioretention Mesocosms Using Media Formulated for Phosphorus Sorption: Response to Accelerated Loads." Journal of Irrigation & Drainage Engineering, 137(3), 144-153.

McCuen, R. H. (2005). *Hydrologic analysis and design*, Pearson Prentice Hall, Upper

Saddle River, N.J.

McKeague, J. A., and Day, J. H. (1966). “Dithionite- and oxalate extractable Fe and Al as aids in differentiating various classes of soils.” Can. J. Soil Sci., 46(1), 13–22.

Mechleb, G. (2013). "The Effect of Expanded Shale Lightweight Aggregates on the Hydraulic Drainage Properties of Clays." Masters of Science in Engineering, University of Texas at Austin.

Nair, P. S., Logan, T. J., Sharpley, A. N., Sommers, L. E., Tabatabai, M. A., and Yuan, T. L. (1984). "Interlaboratory Comparison of a Standardized Phosphorus Adsorption Procedure." Journal of Environmental Quality, 13, 591-595.

National Center for Environmental Information (NCEI) (2018). "Climate Data Online." National Oceanic and Atmospheric Administration.

National Research Council (U.S.). Committee on Restoration of Aquatic Ecosystems-Science, Technology, and Public Policy (NRC) (1992). *Restoration of Aquatic Ecosystems: Science, Technology, and Public Policy*, National Academies Press, Washington, D.C.

National Research Council (U.S.). (2009). *Urban Stormwater Management in the United States*, The National Academies Press, Washington, DC.

Natural Resources Conservation Service (NRCS) (2004). National Engineering Handbook. Part 630 Hydrology. Chapter 10 Estimation of Direct Runoff from Storm Rainfall. United States Department of Agriculture. Washington, D.C.

Natural Resources Conservation Service (NRCS) (2009). National Engineering Handbook. Part 630 Hydrology. Chapter 7 Hydrologic Soil Groups. United States Department of Agriculture. Washington, D.C.

O'Neill, S. W., and Davis, A. P. (2012a). "Water Treatment Residual as a Bioretention Amendment for Phosphorus. I: Evaluation Studies." Journal of Environmental Engineering, 138(3), 318-327.

O'Neill, S. W., and Davis, A. P. (2012b). "Water Treatment Residual as a Bioretention Amendment for Phosphorus. II: Long-Term Column Studies." Journal of Environmental Engineering, 138(3), 328-336.

Papadopoulos, A. (2008). "Geotechnical Testing for Norlite Lightweight Aggregate." GEI Consultants, Inc., norliteagg.com, 88.

PaverGuide (2016). "PaverGuide." <http://www.paverguide.com>. (August 4, 2016).

Penn, C., Chagas, I., Klimeski, A., and Lyngsie, G. (2017). "A Review of Phosphorus Removal Structures: How to Assess and Compare Their Performance." *Water*, 9(8).

Pitt, R. (2011). "The National Stormwater Quality Database (NSDQ), Version 3.1 summary for EPA and CADMUS."

Pitt, R., Clark, S. E., Parmer, K., and Risk Reduction Engineering Laboratory. (1994). Potential groundwater contamination from intentional and nonintentional stormwater infiltration project summary, U.S. Environmental Protection Agency, Risk Reduction Engineering Laboratory, Office of Research and Development; Springfield, VA.

Pitt, R. E., and Maestre, A. (2005). "Stormwater quality as described in the National Stormwater Quality Database (NSQD)." 10th International Conference on Urban Drainage. Copenhagen, Denmark.

Pitt, R., Maestre, A., and Morquecho, R. (2004). "The national stormwater quality

2051 database (NSQD, version 1.1)." Department of Civil and Environmental
2052 Engineering, University of Alabama, Tuscaloosa, AL, 13-51.
2053 Roseen, R., Ballestero, T., Houle, J., Briggs, J., and Houle, K. (2012). "Water Quality and
2054 Hydrologic Performance of a Porous Asphalt Pavement as a Storm-Water
2055 Treatment Strategy in a Cold Climate." Journal of Environmental Engineering,
2056 138(1), 81-89.
2057 Saint-Gobain Weber, Ltd. (2016). "Moisture Content." Leca® UK Lightweight
2058 Aggregate, <http://www.weber.ie/lecar-uk-lightweight-aggregate/help-and-
2059 advice/technical-advice/technical-documents.html>. (August 12, 2016).
2060 Schindler, D. W. (1974). "Eutrophication and Recovery in Experimental Lakes:
2061 Implications for Lake Management." Science, 184(4139), 897-899.
2062 Schindler, D. W., Carpenter, S. R., Chapra, S. C., Hecky, R. E., and Orihel, D. M. (2016).
2063 "Reducing Phosphorus to Curb Lake Eutrophication is a Success." Environmental
2064 Science & Technology, 50(17), 8923-8929.
2065 Schueler, T., and Lane, C. (2015). "Recommendations of the Expert Panel to Define
2066 Removal Rates for Urban Stormwater Retrofit Projects." Chesapeake Stormwater
2067 Network, Annapolis, MD.
2068 Selbig, W. R. (2016). "Evaluation of leaf removal as a means to reduce nutrient
2069 concentrations and loads in urban stormwater." Science of the Total Environment,
2070 571, 124-133.
2071 Smith, D., and Hunt, W. (2010). "Structural/Hydrologic Design and Maintenance of
2072 Permeable Interlocking Concrete Pavement." Green Streets and Highways 2010,
2073 American Society of Civil Engineers, 360-377.

Snoeyink, V. L., and Jenkins, D. (1980). Water chemistry, Wiley, New York.

Stumm, W., and Morgan, J. J. (1996). *Aquatic chemistry: chemical equilibria and rates in natural waters*, Wiley, New York.

Tanada, S., Kabayama, M., Kawasaki, N., Sakiyama, T., Nakamura, T., Araki, M., and Tamura, T. (2003). "Removal of phosphate by aluminum oxide hydroxide." *Journal of Colloid and Interface Science*, 257(1), 135-140.

Thomle, J. N. (2010). "The declining pH of waters exposed to pervious concrete." Master's Thesis, Washington State University, 2010.

Tota-Maharaj, K., and Scholz, M. (2010). "Efficiency of permeable pavement systems for the removal of urban runoff pollutants under varying environmental conditions." *Environmental Progress & Sustainable Energy*, 29(3), 358-369.

United States Environmental Protection Agency (USEPA) (1983). "Results of the Nationwide Urban Runoff 809 Program: Volume 1 - Final Report." United States Environmental Protection Agency, Washington, D.C.

United States Environmental Protection Agency (USEPA) (1984). "Ambient Water Quality Criteria for Lead." United States Environmental Protection Agency, Office of Water, Washington, D.C.

United States Environmental Protection Agency (USEPA) (1986). "Quality Criteria for Water." United States Environmental Protection Agency, Office of Water, Washington, D.C.

United States Environmental Protection Agency (USEPA) (1988). "Ambient Water Quality Criteria for Aluminum." United States Environmental Protection Agency, Office of Water, Washington, D.C.

United States Environmental Protection Agency (USEPA) (1996). “Water Quality Criteria Documents for the Protection of Aquatic Life in Ambient Water." United States Environmental Protection Agency, Office of Water, Washington, D.C.

United States Environmental Protection Agency (USEPA) (2000). "Ambient Water Quality Criteria Recommendations." United States Environmental Protection Agency, Office of Water, Washington, D.C.

United States Environmental Protection Agency (USEPA) (2010). "Chesapeake Bay Total Maximum Daily Load for Nitrogen, Phosphorus and Sediment." United States Environmental Protection Agency Regions 2 and 3, Washington, D.C.

United States Environmental Protection Agency (USEPA) (2016). "Draft Aquatic Life Ambient Estuarine/Marine Water Quality Criteria for Copper." United States Environmental Protection Agency, Office of Water, Washington, D.C.

Virginia Department of Environmental Quality (VADEQ) (2013). "Virginia DEQ Stormwater Design Specification No. 7 Permeable Pavement. Version 2.0" Virginia Department of Environmental Quality, Richmond, VA.

Walsh, C. J., Roy, A. H., Feminella, J. W., Cottingham, P. D., Groffman, P. M., and Morgan, R. P. (2005). "The urban stream syndrome: current knowledge and the search for a cure." *Journal of the North American Benthological Society*, 24(3), 706-723.

Washington State Department of Ecology (WSDE) (2011). Technical Guidance Manual for Evaluating Emerging Stormwater Treatment Technologies. Technology Assessment Protocol – Ecology (TAPE), Washington State Department of Ecology, Olympia, WA. Publication no. 11-10-061.

Weber, W. J., McGinley, P. M., and Katz, L. E. (1991). "Sorption phenomena in subsurface systems: Concepts, models and effects on contaminant fate and transport." Water Research, 25(5), 499-528.

Weiss, P. T., Kayhanian, M., Gulliver, J. S., and Khazanovich, L. (2017). "Permeable pavement in northern North American urban areas: research review and knowledge gaps." *International Journal of Pavement Engineering*, 20(2), 143-162.

Winston, R. J., Davidson-Bennett, K. M., Buccier, K. M., and Hunt, W. F. (2016). "Seasonal Variability in Stormwater Quality Treatment of Permeable Pavements Situated Over Heavy Clay and in a Cold Climate." Water, Air, & Soil Pollution, 227(5), 140.

Wolf, A. M., and Baker, D. E. (1990). "Colorimetric method for phosphorus measurement in ammonium oxalate soil extracts." Communications in Soil Science and Plant Analysis, 21(19-20), 2257-2263.

Yan, Q., Davis, A., and James, B. (2016). "Enhanced Organic Phosphorus Sorption from Urban Stormwater Using Modified Bioretention Media: Batch Studies." Journal of Environmental Engineering, 142(4), 04016001.

Yan, Q., James, B. R., and Davis, A. P. (2018). "Bioretention Media for Enhanced Permeability and Phosphorus Sorption from Synthetic Urban Stormwater." Journal of Sustainable Water in the Built Environment.

Yang, Y., Zhao, Y. Q., Babatunde, A. O., Wang, L., Ren, Y. X., and Han, Y. (2006). "Characteristics and mechanisms of phosphate adsorption on dewatered alum sludge." Separation and Purification Technology, 51(2), 193-200.